

# Appendices

Blau Arenal Hotel Project

S. Bom

R.F. Vorderegger

P.J.P. Koot

E.A.F. Wendt

G.P. van Rinsum

October 2016

Delft University of Technology



**Cover image**

Aerial picture of Blau Arenal Hotel. [1]

# CONTENTS

<b>A</b>	<b>Site Visit Blau Arenal Hotel</b>	<b>1</b>
A.1	History Area . . . . .	1
A.2	Mangroves . . . . .	2
A.3	River . . . . .	3
A.4	Dunes . . . . .	3
A.5	Beach . . . . .	4
A.6	Visible problems . . . . .	6
<b>B</b>	<b>Google Earth Images</b>	<b>9</b>
B.1	Blau Arenal Hotel . . . . .	9
B.2	River mouth . . . . .	10
B.3	East of the hotel . . . . .	13
<b>C</b>	<b>Waste water and freshwater treatment plant</b>	<b>15</b>
C.1	Waste water treatment plant . . . . .	18
C.2	Freshwater treatment plant . . . . .	23
C.3	Water usage . . . . .	26
<b>D</b>	<b>Stakeholders</b>	<b>27</b>
D.1	Government of Cuba . . . . .	27
D.2	Others . . . . .	29
<b>E</b>	<b>Storm data</b>	<b>31</b>
E.1	Hurricanes . . . . .	31
E.2	Cold fronts . . . . .	32
<b>F</b>	<b>Wave Statistics ARGOSS</b>	<b>33</b>
F.1	Data . . . . .	33
F.2	Storm conditions . . . . .	36
<b>G</b>	<b>Sea level rise</b>	<b>41</b>
G.1	Global sea level rise . . . . .	41
G.2	Regional sea level rise . . . . .	42
<b>H</b>	<b>Morphology</b>	<b>43</b>
H.1	Sedimentology . . . . .	43
<b>I</b>	<b>Tidal inlet</b>	<b>45</b>
I.1	Type . . . . .	45
I.2	Escoffier curve . . . . .	47

<b>J</b>	<b>Hydrology</b>	<b>49</b>
J.1	Rational method . . . . .	49
J.2	Triangular unit hydrograph method . . . . .	51
J.3	Itabo catchment area . . . . .	52
J.4	Rain data . . . . .	55
J.5	Computation discharge . . . . .	59
<b>K</b>	<b>Consequences</b>	<b>65</b>
<b>L</b>	<b>Risk</b>	<b>67</b>
L.1	Fault trees . . . . .	67
L.2	Altitude data . . . . .	70
L.3	Vulnerability classification. . . . .	71
<b>M</b>	<b>Possible correlations</b>	<b>75</b>
<b>N</b>	<b>SWAN</b>	<b>77</b>
N.1	Input . . . . .	77
N.2	Results. . . . .	85
<b>O</b>	<b>Xbeach model set-up</b>	<b>89</b>
O.1	Input . . . . .	89
O.2	Output . . . . .	95
<b>P</b>	<b>Brainstorm solutions</b>	<b>97</b>
P.1	Flooding caused by waves . . . . .	97
P.2	Flooding caused by high river discharge . . . . .	98
P.3	Flooding caused by both waves and river discharge. . . . .	100
<b>Q</b>	<b>Wall structure design</b>	<b>103</b>
Q.1	Gravity wall . . . . .	103
Q.2	Embedded wall. . . . .	105
Q.3	Wall with slope . . . . .	111
Q.4	Sheetpile wall. . . . .	112
<b>R</b>	<b>Flood retention</b>	<b>113</b>
R.1	General principle. . . . .	113
R.2	Assumptions and limitations design . . . . .	114
R.3	Elevation flood retention area. . . . .	115
R.4	Inlet structure. . . . .	116
R.5	Two scenarios. . . . .	117
R.6	Reduction discharge . . . . .	118
R.7	Discussion . . . . .	122
<b>S</b>	<b>Solution: Mangrove forest extension</b>	<b>123</b>
S.1	Advantages . . . . .	123
S.2	Disadvantages . . . . .	124

---

S.3	Conclusion . . . . .	124
<b>T</b>	<b>Solution: Extra outflow point</b>	<b>125</b>
T.1	Advantages . . . . .	126
T.2	Conclusion . . . . .	127
<b>U</b>	<b>Multi Criteria Analysis</b>	<b>129</b>
U.1	Scores . . . . .	129
<b>V</b>	<b>Costs</b>	<b>135</b>
V.1	Primary Costs. . . . .	135
V.2	Secondary Costs . . . . .	136
V.3	Risk . . . . .	137
V.4	Costs estimation of each solution . . . . .	138
<b>W</b>	<b>Final solution</b>	<b>151</b>
W.1	Bearing capacity of the soil . . . . .	151
W.2	Calculation . . . . .	152
W.3	Piping . . . . .	153
W.4	Drainage of precipitation . . . . .	153
W.5	French drainage . . . . .	154
W.6	Accessibility. . . . .	155
<b>X</b>	<b>Construction method</b>	<b>157</b>
X.1	Stages . . . . .	157
X.2	Steps. . . . .	161
	<b>Bibliography</b>	<b>165</b>



# A

## SITE VISIT BLAU ARENAL HOTEL

On the 7<sup>th</sup> of September a visit was brought to the Blau Arenal Hotel. The main goal of this visit was to get a better insight into the study area and its development over the years.



Figure A.1: Entrance Blau Arenal Hotel, with drainage gutter, September 2016

### A.1. HISTORY AREA

Before the Blau Arenal Hotel was being built, the complete study area was covered by the delta of the river Itabo. This delta was largely covered by mangroves. The lagoon Itabo was also part of this delta. In the 80's a land reclamation was done in this delta in order to build a hotel. The Blau Arenal Hotel was opened in 1985 and changed the behaviour of the delta drastically. Mangroves were removed, and water was forced to flow around the land reclamation, causing larger flow velocities with, as a consequence, more losses of mangrove right next to the hotel.

A road that was built on the dune ridge was the cause of severe dune erosion. Waste water was collected and discharged to the lagoon Itabo. There the waste water was exposed to a treatment by nature itself. After that, the water flowed into the river Itabo, which transferred the treated water to the sea.

However, in 2008 the CITMA discovered the treated water did not comply with the national regulations. The concentration of pollution still present in the discharged water exceeded the norm, and the Ministry of Tourism, held responsible for the pollution, was forced to close the Blau Arenal Hotel. A water treatment plant was built, and in 2014 the hotel was opened again. Nowadays the hotel (figure A.1) has 149 rooms, with a total capacity of approximately 300 visitors. During high season 138 employees are working on a daily basis. The new waste water treatment plant works well, but the CITMA wants to ensure that the station will not suffer during extreme weather conditions, which can cause flooding of the lowlands the hotel is situated on.

## A.2. MANGROVES

As was shortly discussed above, the Itabo delta used to consist of mangroves. In figure A.2 these mangroves all around the hotel can be observed. The mangrove forest is very densely populated with trees, as can be seen in figure A.3. The water level in the mangrove forest is dictated by the discharge of the river Itabo. Because of the large variety in discharge of this river (see appendix J), the water level in the mangrove can vary a lot. The Blau Arenal Hotel is located on low grounds, resulting in the risk of flooding of the area due to a large river discharge.

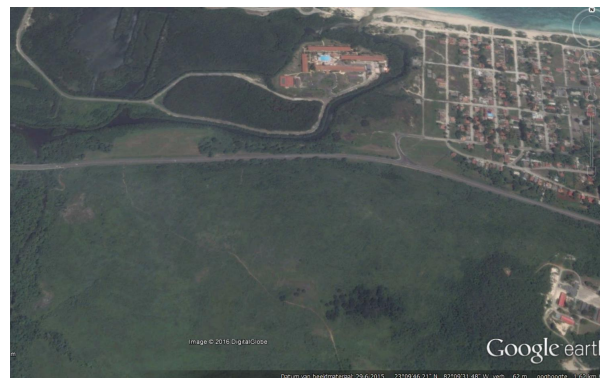


Figure A.2: Itabo Delta with its mangroves and Blau Arenal Hotel [2]



(a) Dense roots

(b) Mangrove

Figure A.3: Mangroves located around the Blau Arenal Hotel, September 2016

### A.3. RIVER

As mentioned previously, the river Itabo is concentrated along the land reclamation, resulting in larger flow velocities and the disappearance of mangroves next to the hotel. This can be observed in figure A.4. Both pictures are made on the walking bridge from the hotel to the sea. The left picture shows the landward view, while on the right picture the river mouth is shown. The water depth in figure A.4 is around 50 cm, while last January (dry season, figure A.5) parts of the area shown on these two pictures were dry.



(a) Landward view

(b) Seaside view

Figure A.4: View on the river mouth from the bridge, September 2016



(a) Landward view

(b) Seaside view

Figure A.5: View on the river mouth from the bridge, January 2016 [3]

### A.4. DUNES

During the closure of the hotel, in between 2011 and 2014 (see appendix B), the road over the dune ridges was closed. In figure A.6a the closed road and the roundabout can be seen, and when turning 180 degrees around, you see the road completely covered by sand (figure A.6b). In the background an old street light which used to be along the road can be seen. A big gap in the dunes is made for the tourists to get access to the beach, as can be seen in figure A.7



(a) Roundabout



(b) Closed road

Figure A.6: Closed road on top of the dunes, September 2016



Figure A.7: Gap in the dunes, September 2016

## A.5. BEACH

When walking eastwards from the entrance of the beach, a small scarp can be seen all over the alongshore direction till the river mouth (figure A.8).



(a) Scarp



(b) Scarp

Figure A.8: Scarp at the beach, September 2016

Walking some further, the river mouth is found. A large spit can be observed in figure A.9. This spit confirms the westward alongshore sediment transport. As Dr. ir. Córdova told us, this spit might be problematic when the water level of the river rises after heavy rainfall. The spit can prevent the water from being discharged into the sea.



Figure A.9: Spit at the river mouth, September 2016

The water behind the spit is brackish. One of the group members experienced this by first account. On the other side of the river mouth a hard sea defence can be observed. This indicates earlier erosion problems. In figure A.10 this sea defence is shown.



Figure A.10: Hard sea defence at the east side of the river mouth, September 2016

The piles of the removed bridge which used to cross the river mouth can still be observed (figure A.11). The place where the man is standing is clearly shallow. In January 2016 the water depth over there was around 1.5 m, according to Dr. ir. Córdova. As January is part of the dry season and the water level at the walking bridge was lower, this indicates the importance of the spit in front of the river mouth.



Figure A.11: Remaining piles of the former bridge, September 2016

When walking westwards from the entrance of the beach, another place can be found where the remaining of the former road on top of the dunes is clearly visible (figure A.12). As can be seen the (height of the) dune is clearly negatively affected by the presence of this road. Besides that, a big scarp can be seen in front of the remainings of the road. This also indicates the occurrence of erosion at this beach.



Figure A.12: Effect of the former road on the dunes, with a big scarp, September 2016

## A.6. VISIBLE PROBLEMS

Besides the problems with the former road (low dunes, dune gap) and the spit, some more problems became visible during the site visit. Although some gutters are present in the area (figure A.1), various spots covered with water were encountered (see figure A.13).



Figure A.13: Area covered with rain water, September 2016

This stresses out the importance of avoiding a severe flooding at the area. Although the site has been declared protected area by the CITMA, several spots with garbage were found in the area (figure A.14). This stresses out the importance of involving the employees (and maybe even the visitors) in the project to raise awareness about the project and the state of this area to preserve the unique ecosystem of mangrove forest.

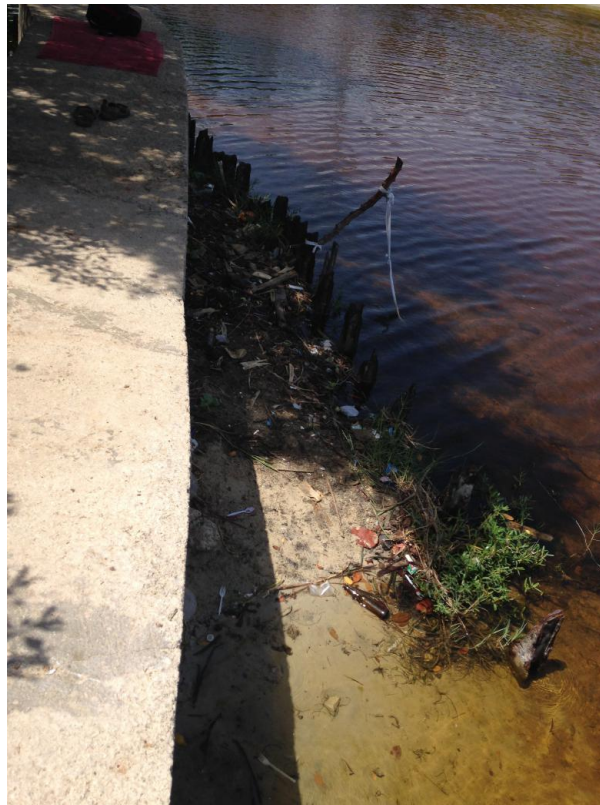


Figure A.14: Garbage present at several spots in the area, September 2016



# B

## GOOGLE EARTH IMAGES

In this appendix images, taken from Google Earth [2], are analysed. These images concern the surroundings of the study area around the Blau Arenal Hotel. The images used are from as early as 25-07-2002 and the most recent ones from 29-06-2015. They contain interesting information about changes in the area in the last fourteen years. Although a substantial length of time is taken, only one day per year of information is received. This means that the conclusions from this analysis do not comprehend a seasonal differentiation. Some changes could be the result of seasonal differences and not structural differences.

### B.1. BLAU ARENAL HOTEL



Figure B.1: Satellite image of the Blau Arenal Hotel (10-10-2002)



Figure B.2: Satellite image of Blau Arenal Hotel (29-06-2015)

Two images have been used to analyse the changes of the Blau Arenal Hotel, one from 10-10-2002 and the other one from 29-06-2015 (see figure B.1 and figure B.2). These images were chosen, because they have the largest timespan in between both and therefore contain the most changes.

Three major changes have taken place in the thirteen-year timespan of the two images. Highlighted in blue the waste water and freshwater treatment plants are located. In 2002, only the water tower and underground freshwater reservoir are visible, while in 2015 the newly constructed plants have been built. In appendix C a more detailed explanation about these new plants is given.

The yellow circle shows the construction of the water heating system. Nowadays Blau Arenal Hotel uses solar energy to heat the freshwater.

Lastly, in the red circle, it can be seen that a building has been built right next to the tennis courts. The purpose of this building is purely leisure, and houses a large quantity of tables and chairs.

## B.2. RIVER MOUTH



Figure B.3: Satellite image of the Itabo River mouth (10-10-2002)



Figure B.4: Satellite image of the Itabo River mouth (09-08-2004)



Figure B.5: Satellite image of the Itabo River mouth (02-10-2009)



Figure B.6: Satellite image of the Itabo River mouth (07-02-2014)



Figure B.7: Satellite image of the Itabo River mouth (29-06-2015)

For the analysis of the Itabo River mouth five images have been used stretching from 2002 to 2015 (see figures B.3 to B.7). A few sections have been highlighted to specify the different transformations of the area.

The yellow circle indicates the roundabout west of the river mouth. As can be seen in the oldest image, which is from 2002, the roundabout can still be completely used. As we progress in time it is clearly visible that sand from the dunes slowly overtakes the northern part of the roundabout. This is a clear indication that the dunes are moving landward.

The light green area shows the dynamical characteristic of the small lagoon to the West of the river mouth. As can be seen by the lighter colour in 2004, this section can fill up with large amounts of sediment. In other images such as 2009 the section looks similar to a river. The small lagoon is very dynamic and depending on the season or wave condition it will import or export sediment. This is further elaborated in section 2.5.

The blue circle is the location of the bridge. In 2002 the bridge is still in full operation. Looking at the second blue circle, which is in 2014, the bridge is completely removed. Only the foundation columns are visible.

The red area is placed over a hard structure at the east side of the river mouth. This structure has been placed when building the old bridge, from before 2014. The hard edge contains the flow of the river, so it cannot easily erode at the east side.

Finally, the river mouth itself, which has no colour indication, is very dynamic. Depending on a lot of factors like wave direction and river discharge, further explained in section 2.5, the mouth can travel straight, left, with a curve or even close completely. This can clearly be seen in all images, but no main direction can be extrapolated as it depends on too many factors.

## B.3. EAST OF THE HOTEL



Figure B.8: Satellite image of eastern section of Playas del Este (10-10-2002)

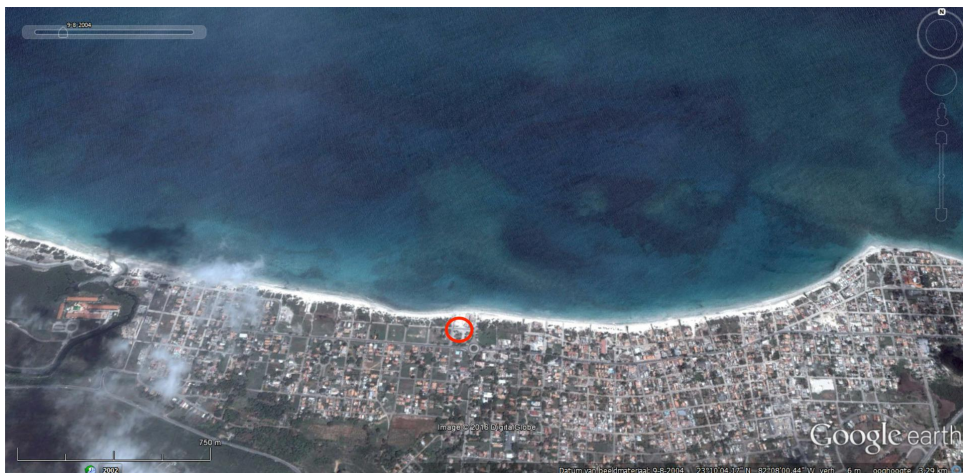


Figure B.9: Satellite image of eastern section of Playas del Este (09-08-2014)



Figure B.10: Satellite image of eastern section of Playas del Este (19-12-2014)

East of the hotel and study area, an image analysis has been done. For this analysis three images have been used (see figures [B.8](#) till [B.10](#)). The red dot is placed at the same building in each of the figures. This is done to analyse images better, as each one is from a different perspective.

As can be seen in the first two images from 2002 and 2004, a clear white beach is visible. The beach visible in those two images is wide and stretches over the entire area. When looking at the last image, from 2014, the beach is noticeably smaller. This could mean that the beach is eroding structurally.

# C

## WASTE WATER AND FRESHWATER TREATMENT PLANT

In figure C.1, the location of the waste water and freshwater treatment plant are highlighted inside the blue circle. In this appendix a detailed description of the functionality of these plants is given in combination with images taken during the site visit, which is described in appendix A. The knowledge about these plants is gained by interviews with David, who is the head of the UBI (Unidad Basica Inversiones) of Playas del Este, which is the investment office of the region and responsible for the plants. These interviews were recorded during the site visit and used to create this appendix.



Figure C.1: Aerial overview of the Blau Arenal Hotel and location of the new waste water treatment plant (blue circle) at 29-06-2015 [2]

In figure C.2 all the steps of the waste water and freshwater treatment plant have been visualised by pictograms. With the use of this figure the treatment plants are explained.



- 
- A – Receiving waste water and mixing
  - B – Pump
  - C – Sieve (filter)
  - D – Active sludge tank
  - E – Oxygen tank
  - F – Pump
  - G – Chlorine tank
  - H – Pump
  - I – Mixing tank and treated waste water reservoir
  - J – French drainage for filtration of the treated waste water into the soil and river
  - K – Pump
  - L – Basin for sludge to dry in the sun
  - M – Dried sludge is transported away for use as fertilizer
  - N – Pipes close to the sea to pump up seawater
  - O – Pump
  - P – Water tower (salt water reservoir)
  - Q – Desalination tank, which uses reverse osmosis
  - R – Pump
  - S – Valve to select the source of freshwater supply
  - T – Use of freshwater (Blau Arenal Hotel)
  - U – Supply of freshwater by trucks
  - V – Reservoir for freshwater
  - W – Pump
  - X – Valve to empty the desalination tank after cleaning
  - Y – Pump

In figure C.3 the blue circle of figure C.1 has been zoomed in and the locations of the major elements of the plants can be seen.

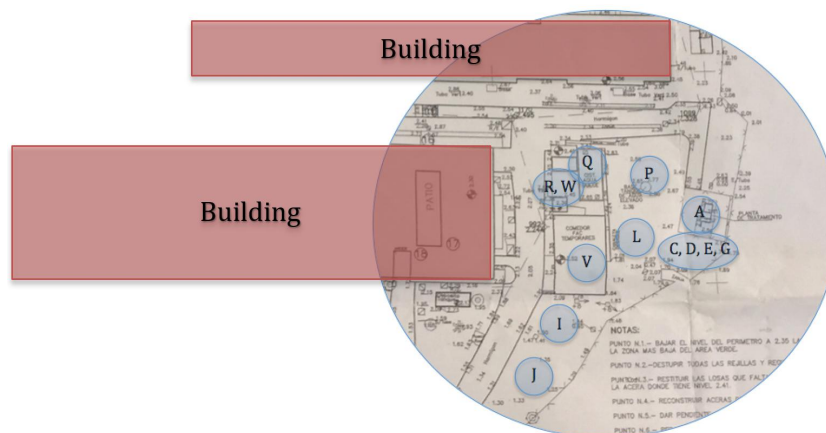


Figure C.3: Map of treatment plants with indicated locations in blue [4]

## C.1. WASTE WATER TREATMENT PLANT

### A - UNDERGROUND RESERVOIRS

The underground reservoirs are the location where the waste water enters the treatment plant from the hotel. The waste water is mixed and stored in the dark to minimise the risk of the growth of algae, who need sunlight to thrive. As can be seen in figure C.4, the mangrove forest is just behind the reservoirs. The water of the lagoon and river flows at the same location, as mangrove trees are almost always underwater. The water level is, taken from visual account, usually only 1 or 2 meters below the top of the reservoirs. These reservoirs contain untreated waste water, which can produce the highest contamination to the protected mangrove forest.



Figure C.4: Picture of underground reservoirs for untreated waste water, with direction of flow entry indicated

### B - PUMP

The untreated waste water is pumped to the highest section of the plant, from the reservoirs A to the filter C.

### C - SIEVE (FILTER)

The untreated waste water enters with a relative high velocity in the filter (see figure C.5). This filter blocks the largest solids and dilutes the waste water. The waste water flows directly from the filter in the large tanks, without any pumps in between.



Figure C.5: Picture of waste water treatment plant, section C highlighted in blue. The direction of flow is indicated

### D - ACTIVE SLUDGE TANKS

The waste water ends up in two large cylindrical tanks after passing through the filter (see figure C.6). These tanks are used to biologically treat the waste water with the addition of oxygen. Also, the separation between the sludge and the treated water takes place inside these tanks. The sludge will slowly sink to the bottom, while the treated water stays on top. The E. coli bacteria are killed using chlorine. The volume of added chlorine is precisely adjusted to the amount of bacteria present in the water.



Figure C.6: Picture of the two large cylindrical tanks

### E - OXYGEN TANK

The oxygen tank is just a tank filled with air. It supplies air to make the biological degradation of the waste water possible.

### F - PUMP

A pump provides the large cylindrical tank with air, and more specifically with oxygen. As can be seen in figure C.7a, the pump is only 30 centimeters above the ground. The pump is open, which means it is vulnerable for water damage. The area does have a roof, but has no flood protection. Without oxygen supply to the main tanks, the whole waste water treatment plant is out of order. If the biological process would not function it leads to leading to untreated effluent of waste water.



(a) Picture of the aeration pump (highlighted in blue)



(b) Picture of the chlorine tank

Figure C.7

### G - CHLORINE TANK

The chlorine tank, as can be seen in figure C.7b, is used to store the chlorine before it will be used in the waste water. Chlorine is used as a disinfectant and kills almost all the E. coli bacteria. The number of E. coli bacteria is, as mentioned earlier, used to determine how clean the water is.

### H - PUMP

Exact doses of chlorine are pumped in the cylindrical tanks. The doses have to be as exact as possible, because chlorine is a hazardous substance that will harm the environment. If the amount of chlorine is too high, it will not entirely be used to kill the E. coli bacteria and the remaining chlorine will stay in the water and be released in the area, destroying the flora and fauna. If the quantity is not enough the E. coli bacteria will still be alive and also harm the surrounding flora and fauna.

### I - RESERVOIR

The treated waste water from the large cylindrical tanks is temporarily stored in a large reservoir, as can be seen in figure C.8, before it is released in the surrounding area. When the desalination tank, which will be described later, gets cleaned, hazardous cleaning material has to be used. This cleaning has to be done to prevent the desalination tank from getting clogged. The cleaning material together with some freshwater is also pumped to the large reservoir and is mixed with the treated waste water to lower the content of harmful substances.



Figure C.8: Picture of the water reservoir for treated waste water

### J - FRENCH DRAINAGE

A drainage pipe is used to return the treated waste water back into nature. This pipe uses small holes as a filter, so the water slowly pours into the soil. Around the pipe a geotextile layer and gravel has been placed to make sure the pipe will not clog with sand or clay. In figure C.9 the mangrove forest is just to the left of the pipe. Therefore, the river is only at a distance of approximately 15 meters from the pipe. During a flood, the waste water will not be able to flow out of the pipe. The water level outside the pipe will give too much pressure against the effluent trying to exit the pipe. This cannot be countered, since the system works with a natural head difference and no mechanical intervention takes place.



Figure C.9: Picture of the water reservoir for treated waste water

### K - PUMP

The sludge that sinks to the bottom of the cylindrical tanks is pumped to drying basins. The pump is placed low (see figure C.10), because the sludge in the tank is a lot heavier than the treated water and therefore sinks to the bottom, where it can be removed easily.



Figure C.10: Picture of the sludge pump, with direction of flow indicated

### L - DRYING BASINS

The sludge is deposited in three relatively large basins (see figure C.11). The sludge consists of about 90% water. All this water is naturally evaporated in these basins by the sun. Three basins are used, because it takes a long time for the sludge to dry. In that time a new basin can be filled to keep the process going.



Figure C.11: Picture of the basins, where sludge naturally dries

### M - TRUCK TRANSPORT

The remaining dry sludge is taken away by trucks. This dry sludge is recycled as fertilizer, because of the high nutrient content.

## C.2. FRESHWATER TREATMENT PLANT

### N - PIPES

Pipes are placed in the dunes, which have holes for water to enter. The water that is entering these pipes is salty seawater, because the dunes are relatively narrow and the extraction point is close to the sea.

### O - PUMP

The seawater from the dunes is sucked up by a pump. The pump also transports the salty water from the dunes to the water tower.

### P - WATER TOWER

A water tower is used to temporarily store untreated salt water (see figure C.12). The water tower is about 20 meters high. This height is used to deliver water pressure for the use of the desalination tank.



Figure C.12: Picture of the water tower

### Q - DESALINATION TANK

To make the desalination possible, reverse osmosis is utilised. The salt water enters the tank under pressure from the water tower and flows through a membrane. This membrane functions as a filter and traps the salt, but not the water. The effluent of the desalination tank is freshwater.



Figure C.13: Picture of the desalination tank, highlighted in blue

### R - PUMP

The distribution of the freshwater from the desalination tank to the hotel is done by pumps. Multiple pumps are used to generate enough pressure to deliver water in both low- and peak usage.



Figure C.14: Picture of the pumps for distribution of the freshwater to Blau Arenal Hotel

### S - VALVE

To switch between two different sources of freshwater, a valve is used.

### T - USER

The freshwater is used for multiple purposes such as showers, toilets, water taps and more.

### U - TRUCK TRANSPORT

If the desalination tank is out of order, freshwater still needs to be supplied to the hotel. The delivery of freshwater by trucks is the back-up system of Blau Arenal Hotel.

### V - FRESHWATER RESERVOIR

An underground reservoir is used as storage of freshwater, which is delivered by the trucks (see figure C.15). The freshwater will be used as water source for the hotel, if the desalination tank is not functioning.



Figure C.15: Picture of the underground freshwater reservoir, indicated in blue

### W - PUMP

The water in the underground reservoir is distributed in the Blau Arenal Hotel by pumps. Again, just as in figure C.14, multiple pumps are used for the same reason.

### X - VALVE

A valve will be used to drain the water from the desalination tank into the final waste water reservoir in figure C.8. The desalination tank can get clogged, so periodically it has to be cleaned. The materials used to clean the tank are hazardous, so have to be mixed and drained away with the treated waste water.

### Y - PUMP

A pump transports the cleaning materials from the desalination tank to the final mixing reservoir of the treated waste water. This pump is only used after the desalination tank has been cleaned.

### C.3. WATER USAGE

The data of the water usage of the Blau Arenal Hotel and its tourist is obtained by an interview during the site visit of the project group [5]. The monthly water usage of four months in 2016 is presented in table C.1. An average water usage per month of 3,385 m<sup>3</sup> is determined. As can be seen in the table, January is the month with the maximum water usage. However, the highest average water usage per day is in February (counting 29 days, as 2016 is a leap year). The difference in water usage with July and August can be explained by the time of the year. Both January and February are in the high season, with lots of tourists visiting the Blau Arenal Hotel. Whereas July and August are months in the low season.

Table C.1: The water usage per month and per day in in m<sup>3</sup>

Month	Water usage per month [m <sup>3</sup> ]	Water usage per day [m <sup>3</sup> ]
January	4,028	130
February	3,835	132
July	2,139	69
August	3,537	114

From table C.1 the average water usage of 132 m<sup>3</sup> per day (February) will be used for the calculation of the capacity of the French drainage. To be conservative the month with the highest average water usage per day is chosen.

It should be taken into account that the maximum water usage per day can differ significantly with the average water usage per day. Several factors can play a role, like the weather (hot or cold days). Besides, the water usage is different for every individual. Due to the variation in water usage per day, a standard deviation of 20 m<sup>3</sup>/day is assumed. Assuming a normal distribution and using a confidence interval of 95%, a maximum water usage per day of 165 m<sup>3</sup> is obtained.

The amount of waste water is estimated to be 90% of the water used at the Blau Arenal Hotel daily. This value is obtained by considering the fact that not all the water will go to the waste water treatment plant, like drinking water and water used for gardening. This leads to a maximum waste water production of 148.5 m<sup>3</sup>/day.

# D

## STAKEHOLDERS

### D.1. GOVERNMENT OF CUBA

#### D.1.1. MINISTRY OF SCIENCE, TECHNOLOGY AND ENVIRONMENT (CITMA)

CITMA is responsible for the environment of Cuba. Therefore, they need to deal with the rehabilitation and protection of the coast of Cuba. CITMA is the only party that is concerned with the environment, as there are no other Cuban environmental organisations.

In 2008, the mangrove forest that surrounds Blau Arenal Hotel, is officially stated as protected area due to its unique ecosystem. CITMA wants to conserve this ecosystem. They have the power to close the Blau Arenal Hotel if they are not fulfilling the requirements of waste water treatment. Therefore, the hotel was closed from 2008 to 2012 when the Itabo River was contaminated due to malfunctioning of the lagoon as retention basin to treat the waste water.

CITMA demands the MoT to solve the waste water treatment problems, because the MoT is responsible for the areas with tourism. CITMA wants that the waste water treatment functions in such a way that it fulfills the requirements and that, no damage to the mangrove ecosystem is caused by the contaminated waste water in case of flooding.

#### D.1.2. MINISTRY OF TOURISM (MoT)

As mentioned above, the Ministry of Tourism deals with all touristic activities in Cuba. With state enterprises, like Cubanacan, the MoT has partial ownership of several hotels. Because Playas del Este has white sandy beaches and azure blue seawater it provides a major source of income due to the attractiveness of the area for tourists. Therefore, the MoT will choose to do what CITMA demands and solve the flooding and waste water problem. In this way, they will satisfy CITMA by protecting the unique ecosystem at Blau Arenal Hotel and they will use this ecosystem to attract tourists.

The MoT has made a contract with the Ministry of Higher Education to get information about the project. The Cuban enterprises, that are part of the Ministry of Construction, need to make an offer to choose their company for the execution of the project.

In case that part of the solution consists of rehabilitating the beaches, the MoT can make CITMA pay for this part as they are responsible for the beaches in Cuba. Gamma, the organisation of CITMA that does investigation at the Cuban coast, will have to deal with the execution of this solution. After that, Gamma, and not the MoT, needs to go to the MoC for the construction of the solution. They can also choose to go to international contractors for external expertise.

### **D.1.3. CUBANACAN**

Cubanacan is the state enterprise of the MoT where Blau Arenal Hotel is being part of. For that reason, it has the same interests as the MoT. They are willing to invest in the project to please CITMA and to keep this attractive area open for tourists.

### **D.1.4. BLAU ARENAL HOTEL**

Blau Arenal Hotel is one of the hotels of Cubanacan and is located at Playas del Este in the middle of the lagoon Itabo surrounded by mangrove forest. The hotel should focus on giving the tourist a pleasant stay and not on dealing with flooding and contamination. They do not want to close the hotel again, so they will be delighted if the project is executed. Blau Arenal Hotel will value an aesthetic solution to attract tourists to their hotel, but more important is reducing the flood risk of the residences of the tourists and to improve the waste water treatment system.

### **D.1.5. MINISTRY OF CONSTRUCTION (MOC)**

The Ministry of Construction has the task to make sure the construction of projects, including hydraulic structures, bridges, buildings and more, are satisfactorily realised. They have several state enterprises that can fulfill the role as contractor of the project.

### **D.1.6. CUBAN CONTRACTORS**

Several Cuban enterprises have specialists in the field of coastal flood protection. For the execution of the project they have to make an offer in such a way that they are chosen to carry out the project.

### **D.1.7. MINISTRY OF HIGHER EDUCATION (MOHE)**

The Ministry of Higher Education is involved with the higher education of Cuba, like the quality and the development of the education at the universities.

They have a contract with the MoT to provide information about the project. Universities, like the CUJAE, are working for them to get this information.

### **D.1.8. CUJAE INCLUDING CIH**

The Instituto Superior Politécnico José Antonio Echeverría (CUJAE) is the university of technology of Havana and is part of the MoHE. They are contacted by the MoHE to provide them with information about the project. The hydraulic research center of the CUJAE University is called CIH and is concerned with the research of, amongst others, the protection of the Cuban coast against flooding.

This new project is relevant for the CIH, because they enlarge their data about the Cuban coast and gain more knowledge about the area, that will help with the execution of the project. They will provide information to the MoHE from previous studies and the data gathered during the new research. In case of lacking data resources, they can use their connections with other organisations to complete this.

## **D.2. OTHERS**

### **D.2.1. TOURISTS**

Playas del Este, with its astonishing beaches, is a perfect location for tourists to spend their holidays, as described above. This area however, will only attract tourists when the safety against flooding and contamination is guaranteed. The availability of good tourist facilities will probably become even more important, because an increase of American tourists visiting Cuba is expected due to the possibility of commercial flights between the United States and Cuba since the 31st of August 2016. The solution considered should be both safe and aesthetic, because tourists will keep visiting only if the beauty of the area stays intact.

### **D.2.2. LOCAL RESIDENTS**

The local residents are living in Playas del Este and most of them are working in the tourist business. Their houses and work area should be a safe and healthy environment and without the danger of flooding or contamination. They need to be reassured that the measures against these problems will guarantee a safe living and business area for the coming decades. This insurance is important for the locals, because, with this in mind, they will complain less about the hindrance and nuisance during the construction of the project.

### **D.2.3. INTERNATIONAL CONTRACTORS**

Normally, international contractors will not work on the project. They are solely hired for their expertise when the resources of the Cuban contractors are insufficient. When information, equipment or facilities are lacking, the international contractors can be asked for help to realise the project.

Since the embargo between Cuba and other countries is loosened, international contractors are interested in working in Cuba. Working on one of the first projects in Cuba as an international contractor could be a step to improve the relationship with the Cuban government. In this way, more projects in the future could be executed by the company and their market share will increase.



# E

## STORM DATA

The data provided by the Meteorological Institute is shown in this appendix. Table E.1 shows the hurricanes and tropical storms, measured by the Casablanca measuring station. Table E.2 shows the cold fronts.

### E.1. HURRICANES

Table E.1: Hurricanes and tropical storms [6]

Date	Meteorological situation	Wind direction	Wind speed [m/s]	$H_s$ [m]	$T_p$ [s]
25-09-1975	Hurricane Eloise	-	-	5.4	8.2
28-10-1985	Hurricane Juan	-	-	5.8	8.9
19-11-1985	Hurricane Kate	NNE	18.2	5	10.7
12-10-1987	Hurricane Floyd	NW	20.5	5.2	9.43
14-11-1994	Tropical storm Gordon	NNW	18.2	3.5	8.06
04-10-1995	Hurricane Opal	-	-	3.3	6.3
25-09-1998	Hurricane Georges	N	22.7	3.9	11.16
15-10-1999	Hurricane Irene	NW	13.6	3.7	9.43
17-09-2000	Tropical storm Gordon	N	11.4	3.5	7.69
04-11-2001	Hurricane Michelle	NE	25.0	4.5	11.75
26-08-2005	Hurricane Katrina	N	18.2	5.3	10.7
20-09-2005	Hurricane Rita	N	13.6	3.7	11.09
24-10-2005	Hurricane Wilma	NW	22.7	5.8	11.34

## E.2. COLD FRONTS

Table E.2: Cold fronts and subtropical storms [6]

Date	Meteorological situation	Wind direction	Wind speed [m/s]	$H_s$ [m]	$T_p$ [s]
03-02-1970	Strong cold front	NW	18.2	5.8	10
19-01-1977	Strong cold front	NW	20.5	5.5	9.64
03-01-1979	Strong cold front	NNW	15.9	5.7	10.3
02-03-1980	Strong cold front	NW	13.6	4.2	7.69
05-11-1982	Strong cold front	NNE	9.1	2.5	6.22
17-03-1983	Subtropical storm	-	-	5.6	8.4
28-02-1984	Moderate cold front	NW	13.6	4.3	7.69
29-03-1984	Moderate cold front	NW	13.6	3.6	7.69
23-11-1984	Moderate cold front	N	11.4	3.1	6.98
04-01-1985	Moderate cold front	NNW	13.6	3.7	7.69
12-02-1985	Moderate cold front	NW	9.1	3.4	6.8
05-01-1987	Subtropical storm	NW	13.6	5.1	8.3
23-01-1987	Moderate cold front	NW	13.6	3.9	7.69
25-01-1988	Moderate cold front	NNW	11.4	3.5	6.98
12-04-1988	Subtropical storm	NW	13.6	4.5	7.69
15-02-1991	Moderate cold front	NW	13.6	4	7.69
06-02-1992	Subtropical storm	NW	13.6	5.3	9.2
13-03-1993	Subtropical storm	NW	13.6	5.3	9.2
03-03-1994	Subtropical storm	NW	13.6	4.6	7.69
23-12-1994	Subtropical storm	NW	11.4	3.8	8.3
08-01-1996	Moderate cold front	NW	13.6	3.6	7.69
04-02-1996	Moderate cold front	NNW	13.6	3.6	7.69
08-03-1996	Strong cold front	NNW	15.9	3.4	8.37
20-03-1996	Moderate cold front	NW	11.4	3.8	8.3
14-12-1997	Weak cold front	NW	13.6	3.6	7.69
27-12-1997	Weak cold front	NW	11.4	3.4	6.22
04-02-1998	Subtropical storm	WNW	15.9	4.6	8.7
15-03-1999	Moderate cold front	NW	13.6	3.7	7.69
24-01-2000	Moderate cold front	NW	13.6	3.4	7.69
20-03-2001	Subtropical storm	NW	13.6	3.7	7.69
23-02-2002	Moderate cold front	NW	13.6	4.7	9.2
24-11-2005	Moderate cold front	NW	9.1	3.5	7.69

# F

## WAVE STATISTICS ARGOSS

### F.1. DATA

From the website of BMT ARGOSS, wave- and wind data at an offshore location north of the Playas del Este, where Boca Ciega beach is located (24°00'N, 82°30'W), are downloaded [7]. The area of the measurements is 100 x 100 km<sup>2</sup>. Figure E1a shows the area from [www.waveclimate.com](http://www.waveclimate.com) and figure E1b shows the location compared to Boca Ciega beach. A series of observations of the waves starting at 01-01-1992 and ending at 31-12-2014 is available. The time step in this series of observations is three hours. These 23 years of data consists of 67208 observations.

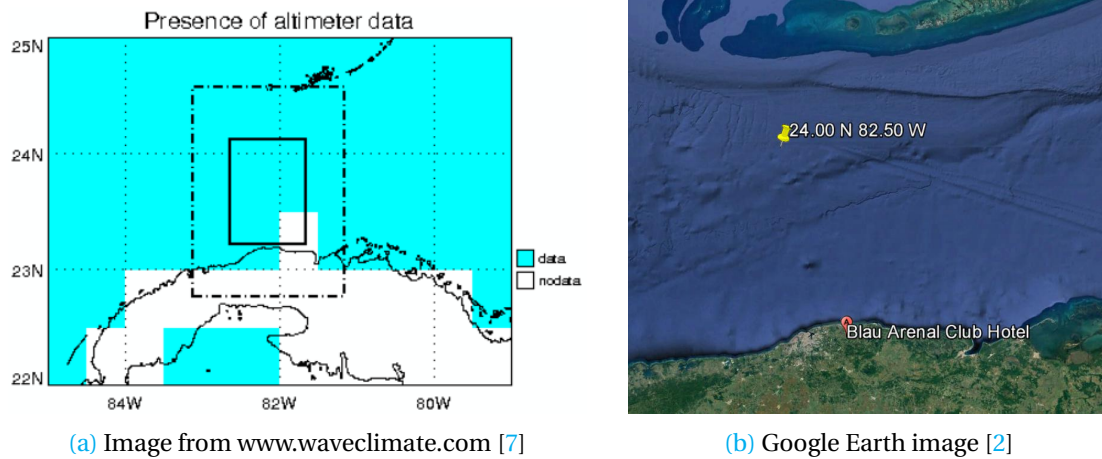


Figure E1: Overview of the location of the wave data

In table E1 the wave observations are divided into bins. For each bin, the number of waves and the cumulative value are shown. The probability of a wave height  $H'_s$  being equal or less than a given value  $H_s$  is given by equation E1 and the opposite by equation E2 [8]:

$$P = P(H'_s \leq H_s) \quad (\text{E.1})$$

$$Q = Q(H'_s \geq H_s) = 1 - P \quad (\text{E.2})$$

Table F.1: Wave data from the Argos database [7]

Wave height class $H_s$ (m)		Number of observations		P	Q
		per bin	cumulative		
0.00	0.25	3922	3922	5.8356E-02	9.4164E-01
0.25	0.50	16782	20704	3.0806E-01	6.9194E-01
0.50	0.75	16145	36849	5.4828E-01	4.5172E-01
0.75	1.00	11167	48016	7.1444E-01	2.8556E-01
1.00	1.25	7662	55678	8.2844E-01	1.7156E-01
1.25	1.50	4955	60633	9.0217E-01	9.7831E-02
1.50	1.75	3077	63710	9.4795E-01	5.2047E-02
1.75	2.00	1683	65393	9.7299E-01	2.7006E-02
2.00	2.25	830	66223	9.8534E-01	1.4656E-02
2.25	2.50	476	66699	9.9243E-01	7.5735E-03
2.50	2.75	224	66923	9.9576E-01	4.2406E-03
2.75	3.00	112	67035	9.9743E-01	2.5741E-03
3.00	3.25	59	67094	9.9830E-01	1.6962E-03
3.25	3.50	48	67142	9.9902E-01	9.8203E-04
3.50	3.75	18	67160	9.9929E-01	7.1420E-04
3.75	4.00	16	67176	9.9952E-01	4.7613E-04
4.00	4.25	7	67183	9.9963E-01	3.7198E-04
4.25	4.50	5	67188	9.9970E-01	2.9758E-04
4.50	4.75	4	67192	9.9976E-01	2.3807E-04
4.75	5.00	1	67193	9.9978E-01	2.2319E-04
5.00	5.25	2	67195	9.9981E-01	1.9343E-04
5.25	5.50	3	67198	9.9985E-01	1.4879E-04
5.50	5.75	1	67199	9.9987E-01	1.3391E-04
5.75	6.00	1	67200	9.9988E-01	1.1903E-04
6.00	6.25	0	67200	9.9988E-01	1.1903E-04
6.25	6.50	0	67200	9.9988E-01	1.1903E-04
6.50	6.75	2	67202	9.9991E-01	8.9275E-05
6.75	7.00	1	67203	9.9993E-01	7.4396E-05
7.00	7.25	0	67203	9.9993E-01	7.4396E-05
7.25	7.50	0	67203	9.9993E-01	7.4396E-05
7.50	7.75	1	67204	9.9994E-01	5.9517E-05
7.75	8.00	0	67204	9.9994E-01	5.9517E-05
8.00	8.25	1	67205	9.9996E-01	4.4638E-05
8.25	8.50	1	67206	9.9997E-01	2.9758E-05
8.50	8.75	0	67206	9.9997E-01	2.9758E-05
8.75	9.00	0	67206	9.9997E-01	2.9758E-05
9.00	9.25	0	67206	9.9997E-01	2.9758E-05
9.25	9.50	0	67206	9.9997E-01	2.9758E-05
9.50	9.75	1	67207	9.9999E-01	1.4879E-05
9.75	10.00	1	67208	1	0

### F.1.1. WAVE DIRECTIONS

As shown previously, the wave data are obtained from a large area north of Boca Ciega beach. The data contains waves from all directions. Of course, not all these waves will reach the shore. Therefore, a part of the dataset has to be excluded. In order to do this, the full range of directions is divided in eight sections. Each section contains 45°. Waves from the northern direction will reach the shore, because they already move straight towards it. This are waves with directions between 337.5° and 22.5°, because in the nautical convention, North is 0°. Waves from northeastern- and northwestern direction are assumed to reach the shore as well. Due to refraction the direction of these waves will change. The full range of waves that are taken into account is between 292.2° and 67.5°. Table F.2 shows the resulting dataset. Now the dataset contains 22360 observations.

Table F.2: Wave data from the Argos database [7], waves only coming from directions between 292.2° and 67.5°.

Wave height class $H_s$ (m)		Number of observations		P	Q
		per bin	cumulative		
0.00	0.25	1513	1513	6.7665E-02	9.3233E-01
0.25	0.50	5030	6543	2.9262E-01	7.0738E-01
0.50	0.75	4516	11059	4.9459E-01	5.0541E-01
0.75	1.00	3526	14585	6.5228E-01	3.4772E-01
1.00	1.25	2552	17137	7.6641E-01	2.3359E-01
1.25	1.50	1960	19097	8.5407E-01	1.4593E-01
1.50	1.75	1380	20477	9.1579E-01	8.4213E-02
1.75	2.00	840	21317	9.5335E-01	4.6646E-02
2.00	2.25	484	21801	9.7500E-01	2.5000E-02
2.25	2.50	290	22091	9.8797E-01	1.2030E-02
2.50	2.75	126	22217	9.9360E-01	6.3953E-03
2.75	3.00	70	22287	9.9674E-01	3.2648E-03
3.00	3.25	28	22315	9.9799E-01	2.0125E-03
3.25	3.50	29	22344	9.9928E-01	7.1556E-04
3.50	3.75	6	22350	9.9955E-01	4.4723E-04
3.75	4.00	7	22357	9.9987E-01	1.3417E-04
4.00	4.25	1	22358	9.9991E-01	8.9445E-05
4.25	4.50	1	22359	9.9996E-01	4.4723E-05
4.50	4.75	0	22359	9.9996E-01	4.4723E-05
4.75	5.00	0	22359	9.9996E-01	4.4723E-05
5.00	5.25	0	22359	9.9996E-01	4.4723E-05
5.25	5.50	1	22360	1	0

## F.2. STORM CONDITIONS

### F.2.1. PEAK OVER THRESHOLD METHOD

For calculation of the wave height in a design storm at Boca Ciega beach, the significant wave height of the individual waves have to be transformed into storms. The Peak over Threshold method is used for this. Waves are assumed to be part of a storm if the wave height exceeds 2.0 m. This is done to get rid of the influence of the small waves during calm conditions on the significant wave height during storm conditions. Also, if multiple consecutive wave observations exceed 2.0 m, they are assumed to be part of the same storm. The results of these assumptions are shown in table F3. The directions of the origin of the waves in these storms are shown in figure F2a and wind in figure F2b.

**Table F3:** Wave data from the Argos database [7], waves only coming from directions between 292.2° and 67.5°, only waves with wave height exceeding 2.0 m

Wave height class $H_s$ (m)		Number of storms		P	Q	Reduced Weibull
		per bin	cumulative			
2.00	2.25	55	55	3.6424E-01	6.3576E-01	0.372
2.25	2.50	44	99	6.5563E-01	3.4437E-01	1.083
2.50	2.75	25	124	8.2119E-01	1.7881E-01	1.972
2.75	3.00	14	138	9.1391E-01	8.6093E-02	3.069
3.00	3.25	4	142	9.4040E-01	5.9603E-02	3.654
3.25	3.50	4	146	9.6689E-01	3.3113E-02	4.630
3.50	3.75	2	148	9.8013E-01	1.9868E-02	5.513
3.75	4.00	1	149	9.8675E-01	1.3245E-02	6.236
4.00	4.25	1	150	9.9338E-01	6.6225E-03	7.509
4.25	4.50	0	150	9.9338E-01	6.6225E-03	7.509
4.50	4.75	0	150	9.9338E-01	6.6225E-03	7.509
4.75	5.00	0	150	9.9338E-01	6.6225E-03	7.509
5.00	5.25	0	150	9.9338E-01	6.6225E-03	7.509
5.25	5.50	1	151	1	0	-

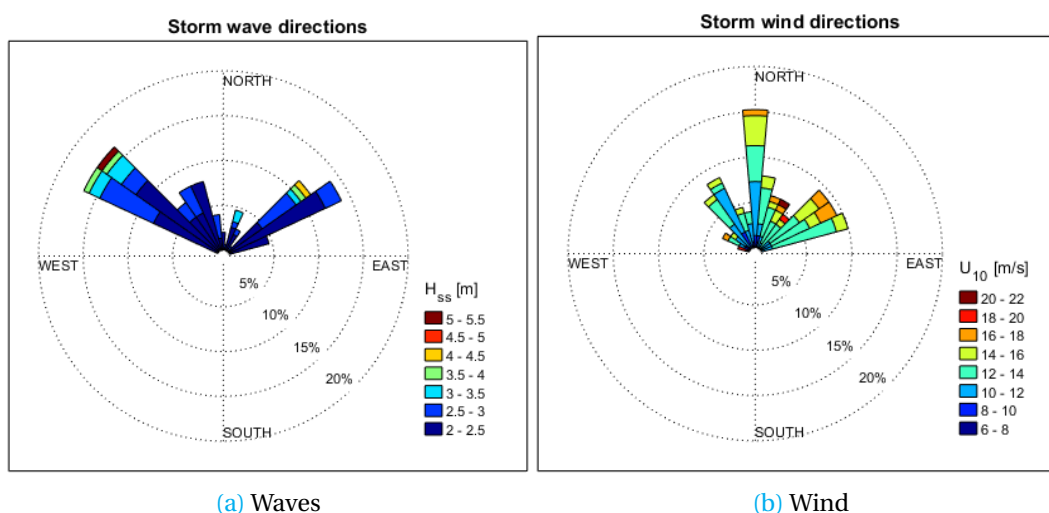


**Figure E2:** Graphs showing directions during a storm

In 23 years of data, 151 storms are found with a minimum wave height of 2.0 m. This is equal to 6.6 storms per year. To calculate the design storm height, a Weibull-, Gumbel- or exponential distribution will be used. Afterwards they will be compared and the best option will be chosen.

### WEIBULL

The Weibull distribution is given by equation E3.

$$P(H_{ss}) = Q = \exp \left[ - \left( \frac{H_{ss} - \gamma}{\beta} \right)^\alpha \right] \quad (E3)$$

In order to determine the variables  $\alpha$ ,  $\beta$  and  $\gamma$ , equation E3 is reduced to a linear equation [8]:

$$(-\ln(Q))^{1/\alpha} = \frac{H_{ss} - \gamma}{\beta}$$

$$W = \frac{1}{\beta} H_{ss} - \frac{\gamma}{\beta}$$

$$H_{ss} = \beta \cdot W + \gamma \quad \text{with } W = -(\ln Q)^{1/\alpha} \quad (E4)$$

- Where:
- $H_{ss}$  = design storm wave height [m]
  - $Q$  = probability of exceedance [-]
  - $W$  = Weibull reduced variable [m]
  - $\alpha, \beta, \gamma$  = Weibull variables [-], [-], [m]

The variables in equation E4 can be determined when the reduced Weibull variable ( $W$ ) is plotted against the storm wave height. To do this, a value for  $\alpha$  has to be assumed. The first attempt is with an  $\alpha$ -value of 1.0. The data points that can be calculated with the values from table E3 are plotted as dots. A linear trend line is drawn in the plot, which has certain values for  $\beta$  and  $\gamma$ . It also has a correlation coefficient ( $R^2$ ), which should be as close to 1 as possible. When trying multiple  $\alpha$ -values, the trend line for  $\alpha = 0.80$  has the highest value of the correlation coefficient and is the straightest line, so therefore this value is chosen [8]. The result is shown in figure E3.

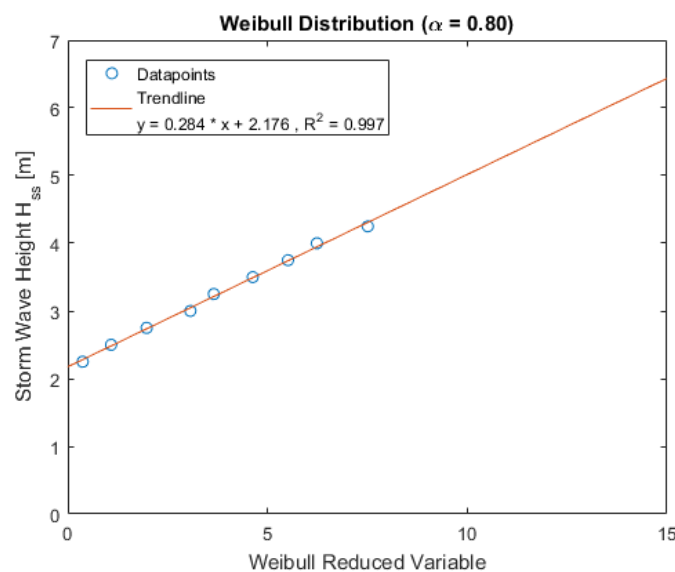


Figure E3: Exceedance graph for measurements of storms with a Weibull distribution

From the graph is deduced that  $\beta = 0.284$  and  $\gamma = 2.176$ . Making use of equation E4, the chosen return period (225 years) and the calculated number of storms per year ( $N_s = 6.6$ ), an estimate of the design wave height is calculated. The probability of exceedance of a storm in a year ( $Q_s = 1/\text{return period}$ ) is equal to:

$$Q_s = N_s \cdot Q \quad (\text{E5})$$

Using equations E4 and E5 follows:

$$H_{ss} = \beta \cdot \left( \ln \left( \frac{Q_s}{N_s} \right) \right)^{1/\alpha} + \gamma \quad (\text{E6})$$

### GUMBEL

The Gumbel distribution is given by equation E7.

$$P(H \leq H_{ss}) = \exp \left[ -\exp \left( -\frac{H_{ss} - \gamma}{\beta} \right) \right] \quad (\text{E7})$$

In order to determine the variables  $\beta$  and  $\gamma$ , equation E7 is reduced to a linear equation [8]:

$$-\ln(-\ln(P)) = \frac{H_{ss} - \gamma}{\beta}$$

$$G = \frac{1}{\beta} H_{ss} - \frac{\gamma}{\beta}$$

$$H_{ss} = \beta \cdot G + \gamma \quad \text{with } G = -\ln \left( \ln \left( \frac{1}{P} \right) \right) \quad (\text{E8})$$

Where:  $H_{ss}$  = design storm wave height [m]  
 $P$  = probability of non-exceedance [-]  
 $G$  = Gumbel reduced variable [m]  
 $\beta, \gamma$  = Gumbel variables [-], [m]

The variables in equation E8 are determined in the same way as for the Weibull distribution. The result is shown in figure E4

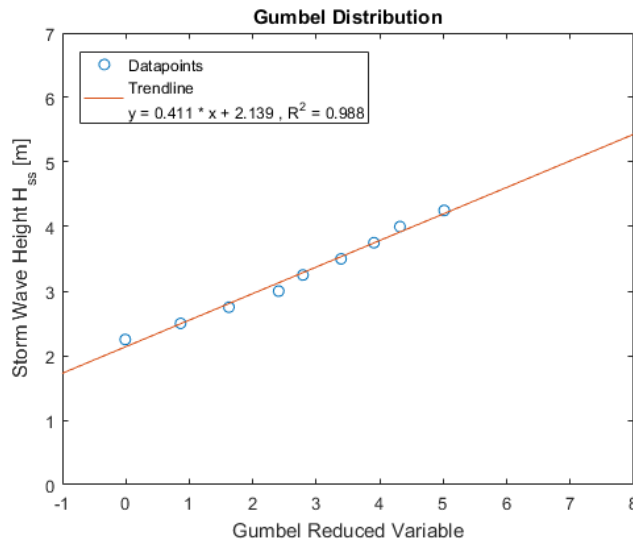


Figure E4: Exceedance graph for measurements of storms with a Gumbel distribution

From the graph is deduced that  $\beta = 0.411$  and  $\gamma = 2.139$ . Using equations F.8, F.1 and F.5 follows:

$$H_{ss} = \beta \cdot -\ln\left(\ln\left(\frac{N_s}{N_s - Q_s}\right)\right) + \gamma \quad (\text{E.9})$$

### EXPONENTIAL

The exponential distribution is given by equation F.10.

$$P(H_{ss}) = Q = \exp\left(-\frac{H_{ss} - \gamma}{\beta}\right) \quad (\text{E.10})$$

This can be rewritten to:

$$H_{ss} = -\beta \cdot \ln(Q) + \gamma \quad (\text{E.11})$$

Where:  $H_{ss}$  = design storm wave height [m]  
 $Q$  = probability of exceedance [-]  
 $\beta, \gamma$  = variables [-], [m]

In order to determine the variables  $\beta$  and  $\gamma$ , the data is plotted on an axis with a logarithmic scale and a trendline is created. This can be seen in figure F.5.

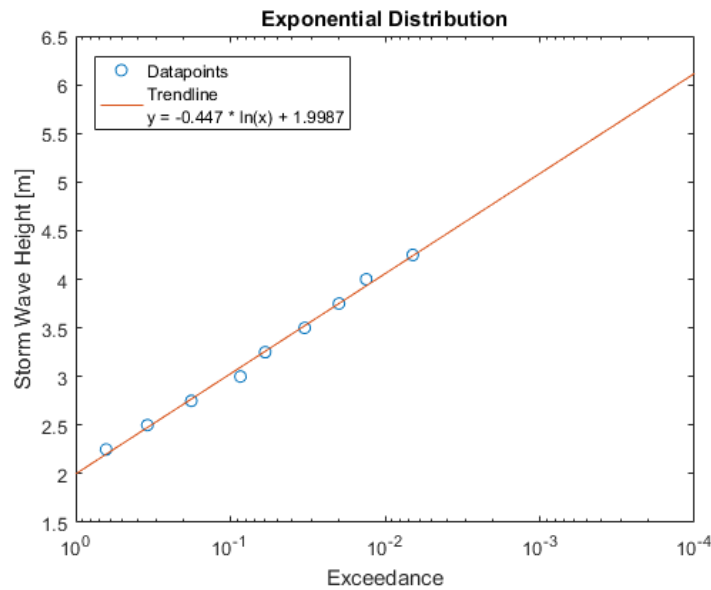


Figure F.5: Exceedance graph for measurements of storms with an exponential distribution

From the graph is deduced that  $\beta = 0.447$  and  $\gamma = 1.9987$ . Using equations F.11 and F.5 follows:

$$H_{ss} = -\beta \cdot \ln\left(\frac{Q_s}{N_s}\right) + \gamma \quad (\text{F.12})$$

### F.2.2. COMPARISON AND CONCLUSION

In order to compare the three different distributions, they are plotted all together in one figure. The x-axis contains the return period in years and the y-axis contains the wave height. The plot can be seen in figure E6.

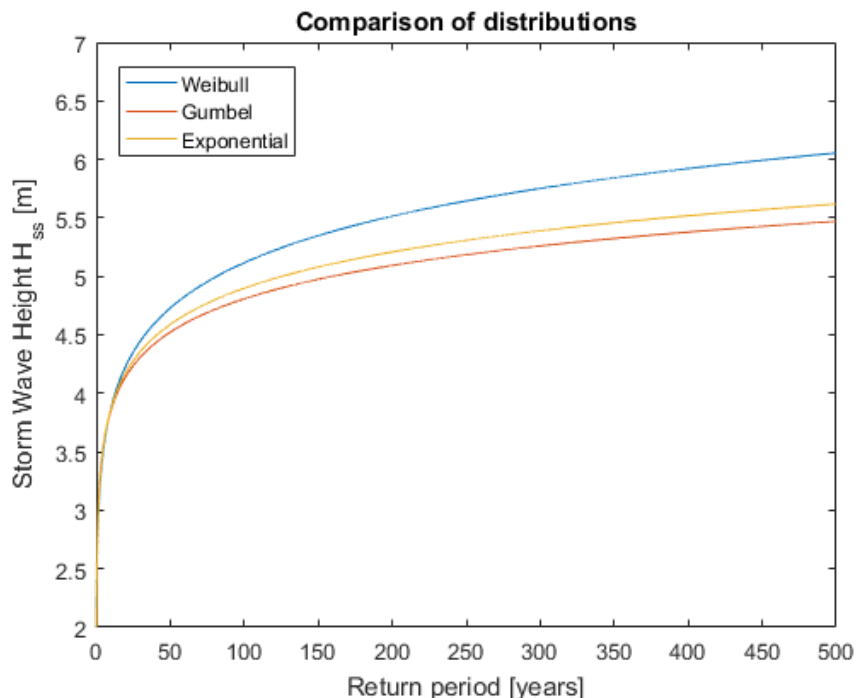


Figure E6: Comparison of the different distributions

From the graph can be deduced that the different distributions are close to each other. Therefore, it is not clear which of them is the best.

### CONCLUSION

The Weibull distribution is a good example of an extreme value distribution and it has the highest value of the significant wave height. To get a safe value for the significant wave height, Weibull is chosen as the final distribution. Now, the other characteristics of the design storm are being determined.

The corresponding direction of the storm is the average direction of all storms in figure E2a, which results in  $354^\circ$ . The mean wind direction is determined in the same way as the wave direction, resulting in  $12^\circ$ . The wind speed is calculated using the average of the wind speed of all the storms:  $U_{10} = 12.8$  m/s.

# G

## SEA LEVEL RISE

### G.1. GLOBAL SEA LEVEL RISE

The projections from process-based models of five scenarios with their likely ranges and median values for the GMSL rise from 1986-2005 to 2081-2100 can be seen in figure G.1. Their median values are within a range of 0.05 m. The least GMSL rise is 0.40 m with a range of 0.26 to 0.55 m in scenario RCP2.6 and the most in scenario RCP8.5 with 0.63 m and a range of 0.45 to 0.82 m. The main contribution of the GMSL rise is thermal expansion (red), followed by the melting of glaciers (lightblue) (see figure G.1) [9].

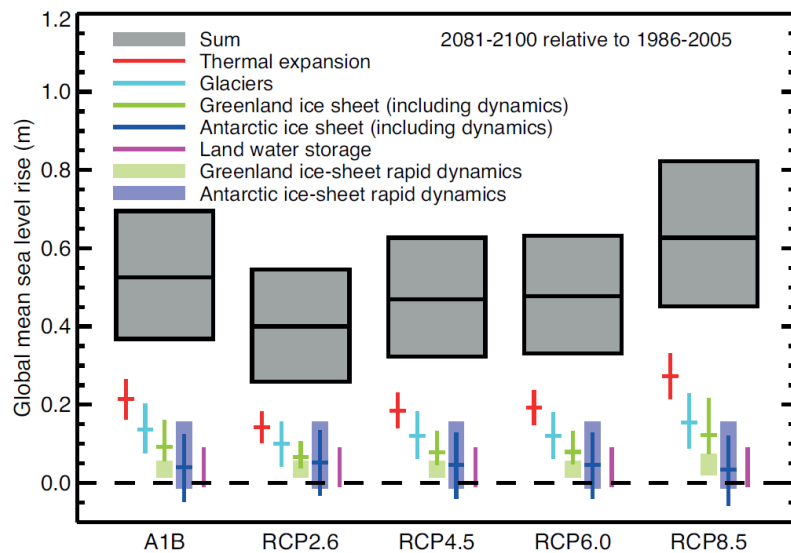


Figure G.1: Projections of five scenarios with likely ranges and median values for the GMSL rise and its contributions in 2081-2100 relative to 1986-2005 used in the AR4 [9]

## **G.2. REGIONAL SEA LEVEL RISE**

The regional sea level rise can differ from the GMSL rise due to complex spatial patterns caused by dynamical processes of the ocean, movements of the sea floor and gravitational changes due to water mass redistribution. Furthermore, the regional sea level variations are dependent on processes like changes in winds and air pressure, air-sea heat, freshwater fluxes and ocean currents [9]. The Cuban Institute of Meteorology (INSMET) estimated a mean sea level rise of 0.29 m for the next century [10].

# H

## MORPHOLOGY

### H.1. SEDIMENTOLOGY

#### H.1.1. COMPOSITION

The distribution of the sediment composition in Boca Ciega at maximum erosion and accumulation in the period of the measurements between 2007 and 2008 can be seen as a pie chart in figure H.1. The sediment is abundant with algae, followed by foraminifers and mollusks [11]. Algae (mainly Halimeda seaweed, consisting of 89% of carbonate) and foraminifers are both vegetable organisms. Mollusks are non-vegetable, carbonic organisms. Therefore, it can be said that the project area consists of biogenic carbonated sand. When comparing the sediment composition of maximum erosion with that of maximum accumulation, the content of algae and inorganic material decreases and that of the other types increases in case of erosion. The low content of inorganic material, like minerals, at Boca Ciega beach can be explained by the low amount of sediment deposits from the river Itabo.

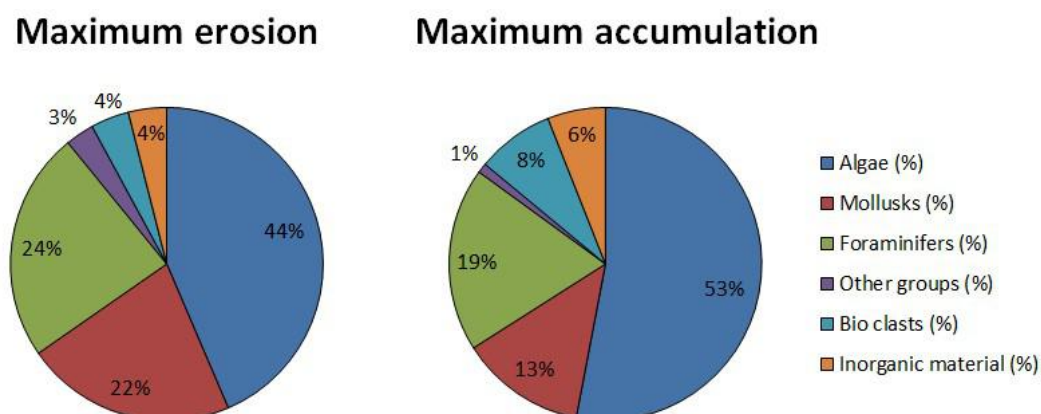


Figure H.1: Pie chart of the sediment composition at Boca Ciega Beach in period 2007-2008 [11]

### **H.1.2. LIGHTNESS**

Boca Ciega beach has a lightness of 66.11 on a scale of -16 (pure black) to 100 (pure white) when comparing the sediment colour. This value is just a little higher than the mean of 63.01 of the 93 researched beaches in Cuba [12].

### **H.1.3. CAUSES OF EROSION**

The erosion of the beach can be due to natural or anthropological causes [13]. Alongshore sediment transport due to oblique incident waves is a natural cause of erosion. Another cause of erosion by nature is cross-shore sediment transport due to extreme weather conditions, like hurricanes, cold fronts and severe storms. Finally, the sea level rise due to climate change will also make the coastline of the beaches retreat more and more every year [14].

Anthropological interferences leading to erosion of the beaches are the buildings and roads on, or behind, the dunes. Also, the large sand extraction for the building industry caused erosion in the past due to the disturbance of the slope of the beach profile. These human actions lead to a decrease in the natural function of the dune-beach environment to protect the hinterland against flooding.

# I

## TIDAL INLET

### I.1. TYPE

A tidal inlet is a dynamic entity, governed by important factors such as tidal currents, storms, the tidal prism and littoral sediment transport. The analysis of the stability of this specific inlet is based upon the Bruun inlet stability criterion  $r$ . The criterion is an indicator for the type of bypassing of the sediment. To calculate this criterion the tidal prism  $P$  and annual alongshore transport or littoral drift  $M$  are needed [15]. In figure I.1, a scheme is shown about the classification for stability of different inlet types.

Inlet Type	$r = P/M$	Bruun Classification
Type 1	> 150	Good
	100 - 150	Fair
	50 - 100	Fair to Poor
	20 - 50	Poor
Type 2	10 - 20	Unstable (open and migrating)
Type 2/3	5 - 10	Unstable (migrating or intermittently closing)
Type 3	0 - 5	Unstable (intermittently closing)

Figure I.1: Bruun classification for different inlet types [16]

To identify, which type the inlet at Boca Ciega beach is, the tidal prism has to be calculated. This is calculated with equation I.1. This equation can be used, as the basin is a short basin (the length of the basin is less than twenty times as small as the tidal wave length). Also the mean river discharge is relatively low, which allows for the equation to be applicable [17].

$$P = A_b \cdot \Delta h \quad (\text{I.1})$$

Where:  $P$  = Tidal prism [m<sup>3</sup>]  
 $A_b$  = Area of the tidal basin [m<sup>2</sup>]  
 $\Delta h$  = Mean tidal range [m]

In figure I.2, the area of the tidal basin or lagoon is visualised. Measured by computer, from different satellite images like the one above, the surface area of the lagoon is about 327,000 m<sup>2</sup>.



Figure I.2: Bruun classification for different inlet types [16]

Furthermore the average tidal range for this region has been analysed in section 2.3.2. The same has been done with the annual sediment transport in section 2.4.2. These values have been taken for the further calculations (see table I.1, with values and results).

Table I.1: Values and results that are used for further calculations of the tidal inlet stability

Parameter	Value
$A_b$	327.000 m <sup>2</sup>
$h$	0.312 m
$P$	102,024 m <sup>3</sup>
$M$	50,000 m <sup>3</sup> /year
$r$	2.04

As can be seen in table I.1 the result of the Bruun inlet stability criterion  $r$  is low, which means that the inlet is of type 3. Type 3 is an unstable inlet that closes at irregular or seasonal intervals, but is locationally stable. This  $r$  value has a lot of uncertainty as the annual alongshore transport is closer to the net value than to the gross. The gross value of the alongshore transport is always higher than the net, which will result in an even lower value for  $r$ . A lower value will always result in a type 3 inlet, so the estimation is correct.

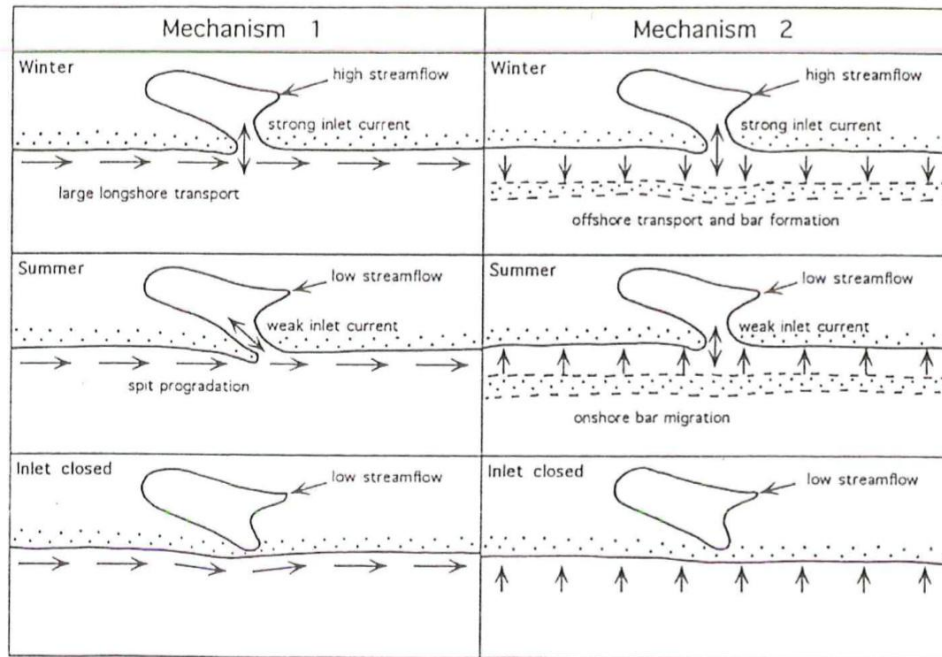


Figure I.3: Concept of the seasonal inlet closure mechanisms [18]

In figure I.3, a modelled visualisation of the different phases of the study area is shown. As can be seen, there are two mechanisms that can cause the closure of the inlet. Closure may occur due to alongshore sediment transport (mechanism 1) or due to onshore migration and welding of sandbars (mechanism 2) [16]. Also, a combination of both mechanisms can cause the closure of such an inlet. The time of closure can also be derived from the figure. In late summer (Northern Hemisphere) or fall, the chance of a closed inlet is much higher than in other periods. During the site visit, which took place in September, a confirmation of this process was seen. The inlet was closed, as can be seen in appendix A. During a site visit in January, done by Cuban researchers, amongst which Dr. ir. L.F. Córdova López, the exact opposite was seen and the inlet was open [3]. These occurrences do not always happen at the same time each year; the factor of river discharge also plays a major role in the opening and closing of the river mouth. Especially when the raining season starts in summer and ends in fall.

## I.2. ESCOFFIER CURVE

A different method to analyse the stability of an inlet is with the use of an Escoffier diagram [19]. This is an hydraulic stability curve, where the maximum flow velocity in the inlet channel is plotted against the cross-sectional flow area. If a sinusoidal tidal motion is assumed, equation I.2 for the maximum channel velocity can be used [17].

$$u_e = \frac{\pi \cdot P}{A_e \cdot T} \quad (I.2)$$

Where:  $u_e$  = Channel flow velocity [m/s]  
 $P$  = Tidal prism [m<sup>3</sup>]  
 $A_e$  = Cross-sectional channel area [m<sup>2</sup>]

$T$  = Tidal period [s]

The tidal prism has already been calculated and the tidal period can be taken out of the tide predictions from NOAA [20]. Together, an Escoffier curve can be constructed, because the cross-sectional channel area is the x-axis input. The Escoffier curve can be seen in figure I.4.

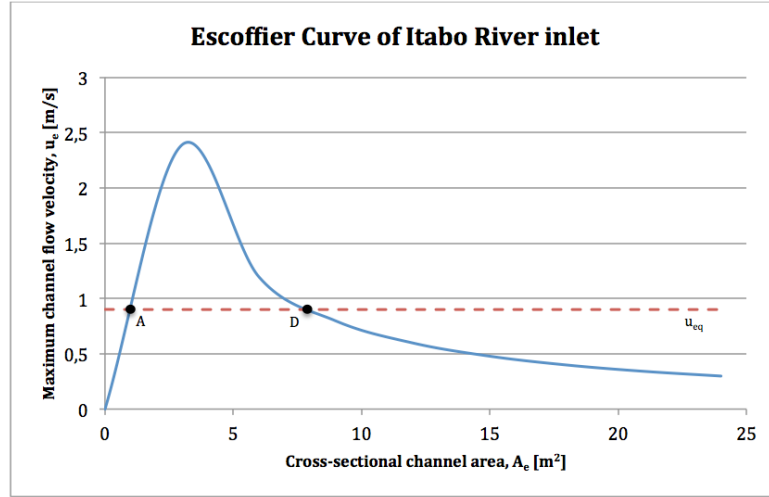


Figure I.4: Escoffier diagram of Itabo River inlet

The red line in figure I.4 is the equilibrium maximum velocity  $u_{eq}$ . This critical velocity is introduced as a line. Below the line the velocity in the entrance channel is too low to erode sediment and keep the entrance channel open. The constant critical velocity intersects the graph at two locations  $A$  and  $D$ . Location  $A$  is an unstable point and the inlet will always diverge from this point, while location  $D$  is a stable point. The  $u_{eq}$  is calculated with the equation I.3 [17].

$$u_{eq} = \pi \cdot A_e^{1/q} \cdot C^{-1/q} \cdot T^{-1} \quad (I.3)$$

Where:  $u_{eq}$  = Equilibrium maximum channel flow velocity [m/s]  
 $A_e$  = Cross-sectional channel area [m<sup>2</sup>]  
 $T$  = Tidal period [s]  
 $C, q$  = Coefficients [m<sup>2-3q</sup>], [-]

The coefficients are empirical parameters and can only be obtained by observational data. For the study area no such observational data is available, so estimations have to be made. According to several researchers, the coefficient  $q$  is in order of magnitude one and  $C$  in the range of  $10^{-5}$  to  $10^{-4}$  [15] [21]. With these estimations the value of the equilibrium maximum channel velocity will result into 0.9 m/s, as can be seen in figure I.4. The curve can be used to confirm the dynamic transformation of the tidal inlet in different seasons and different wave and river conditions.

# J

## HYDROLOGY

### J.1. RATIONAL METHOD

The rational method is applicable for small catchment areas, but a lot of uncertainty will come with this method. The uncertainty will increase for bigger catchment areas, because of the higher variability of the soil, precipitation and evaporation. The formula is given below in equation J.1 [22]:

$$Q_p = C \cdot i \cdot A \quad (\text{J.1})$$

Where:  $Q_p$  = Peak river discharge [m<sup>3</sup>/s]  
 $C$  = Runoff coefficient [-]  
 $i$  = Rainfall intensity [m/s]  
 $A$  = Catchment area [m<sup>2</sup>]

The rational method method assumes a uniformly and stationary distributed precipitation over the entire catchment area during the concentration time. The concentration time is: “the time required for the farthest point of the catchment to contribute to runoff” [22]. There are several methods to calculate this concentration time, which is a catchment characteristic. For the Itabo catchment area the most widely applied Kirpich formula [22] is used, based on an interview with *Prof. dr. Norberto Marrero de León* from CUJAE on *Thursday 8 September 2016*. He said that this method is best applicable to this area. The formula is given below in equation J.2:

$$t_c = 0.015 \cdot \left( \frac{L}{\sqrt{S}} \right)^{0.8} \quad (\text{J.2})$$

Where:  $t_c$  = Concentration time [min]  
 $L$  = Maximum length of the catchment [m]  
 $S$  = Slope of the catchment over the distance L [-]

The total amount of rain in the area is given by the multiplication of the catchment area by the intensity. However, not all the water will contribute to the direct runoff. The 'losses' are for example due to evaporation and infiltration in the ground. The amount of 'losses' is highly dependent on the area characteristics and is accounted for by the runoff coefficient  $C$ . The variability of the factor is shown in figure J.1 [22]. This runoff coefficient is therefore the most important contribution in the uncertainty of the method. There are many factors that determine this value, such as the amount of evaporation, the soil conditions, the amount of moisture in the soil etc.

Type of drainage area	Runoff coefficient
Sandy soil	0.05-0.20
Heavy soil	0.13-0.35
Business	0.50-0.95
Residential	0.25-0.75
Industrial	0.50-0.90
Streets	0.75-0.95
Roofs	0.75-0.95
Forests	0.10-0.60
Pastures	0.10-0.60
Arable land	0.30-0.80

Figure J.1: Runoff coefficients different areas [22]

According to this method, the peak discharge will occur when the duration of the rain is equal to the concentration time, because at that moment the whole catchment area contributes to the runoff. This peak discharge will continue until the precipitation stops, but with the same rain intensity it can not increase, as can be seen in figure J.2 [23].

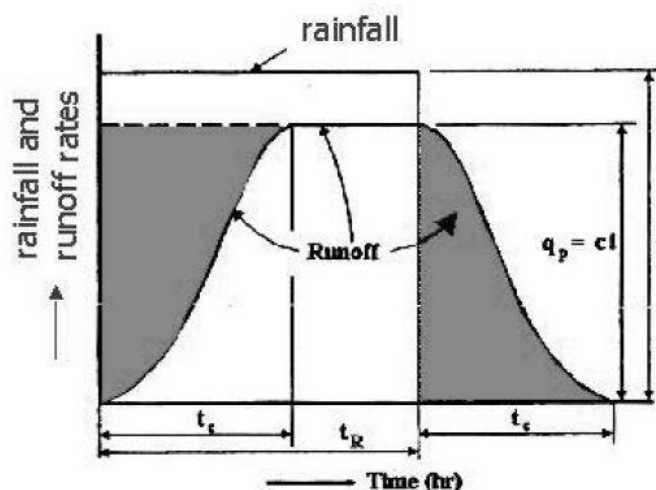


Figure J.2: Rainfall and runoff: rational method [23]

In order to come to the discharge of the river given a certain return period, the duration of the precipitation should be taken as the concentration time. For this area Intensity Duration Frequency curves (IDF) are available. The intensity can be selected from the graphs in correspondence with the duration equal to the concentration time  $t_c$  [22].

## J.2. TRIANGULAR UNIT HYDROGRAPH METHOD

The triangular unit hydrograph method is a method to calculate the unit hydrograph for a given amount of precipitation (mm) in the catchment area during a rain shower. The hydrograph has a triangular shape, see figure J.3. The total amount of effective precipitation is given by the box on the left side. The rain is assumed to be constant during the time  $t_r$  (duration of precipitation) and uniform over the whole catchment area. The discharge is zero at the start of the precipitation. The peak discharge occurs after time  $\frac{t_r}{2} + t_p$ . The discharge is zero again at time equal to  $t_b$ . The unit

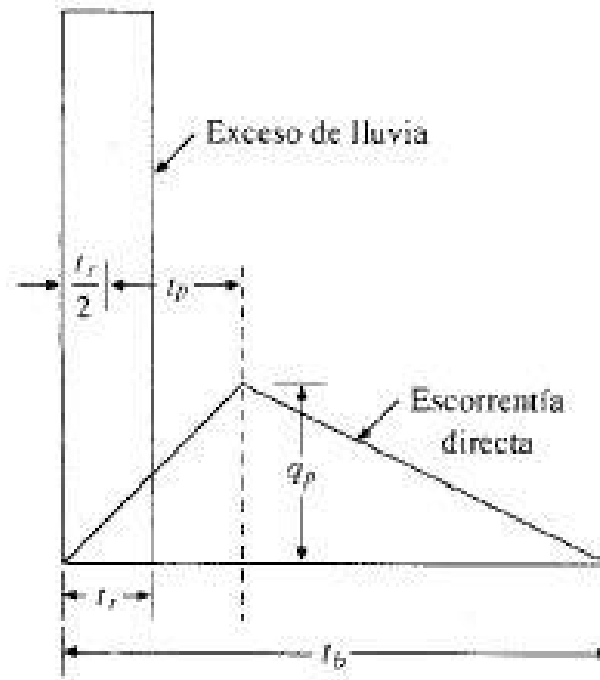


Figure J.3: Rainfall and runoff: rational method [24]

hydrograph can be scaled to the total amount of precipitation. This triangular shape is the hydrograph for one bin of the total rain histogram. All bins of the rain histogram have a triangular shaped hydrograph. All triangles are added together, which results in the total hydrograph. The dimensions of the triangles are calculated based on formula J.3, J.4 and J.5 [25]:

$$t_p = \sqrt{t_c} + 0.6 \cdot t_c \quad (\text{J.3})$$

$$t_b = 2.67 \cdot t_p \quad (\text{J.4})$$

$$Q_p = 0.5555 \cdot \frac{A \cdot h_p}{t_b} \quad (\text{J.5})$$

Where:	$t_p$	=	Peak time	[hours]
	$t_c$	=	Concentration time, see equation J.2	[hours]
	$t_b$	=	Base time	[hours]
	$Q_p$	=	Peak discharge	[m <sup>3</sup> /s]
	$A$	=	Catchment area	[km <sup>2</sup> ]
	$hp$	=	Effective precipitation	[mm]

The input for this method is the so called synthetic histogram, a histogram of the rain based on the Intensity Duration Frequency curve. This method is explained in paragraph J.4 of this appendix.

### J.3. ITABO CATCHMENT AREA

The Itabo River is the river that flows through the Blau Arenal Hotel area. The catchment area of the river is shown in figure 2.14, in the main report. The information on the exact location of the Itabo river catchment area is very limited, but it can be retrieved based on a comparison between Google Earth images (from 2010) [2] and the low resolution map from a study [26] about the Itabo catchment. The two lakes on the map do have the same shape as on the Google Earth images. There are no other lakes with this shape in the area, see figure J.4. Based on this information the length of the catchment area is approximated using the measuring tool of Google Earth. The length and height profile can be seen in figure J.5. The length of the catchment area is approximately 10 km and the maximum elevation is 75 m, this elevation is in accordance with the article about the Itabo catchment area [26]. The elevation and catchment length are used to calculate de slope of the catchment over the distance L, which is 0.0075%. The total size of the catchment area is equal to 35.6 km<sup>2</sup> [26].

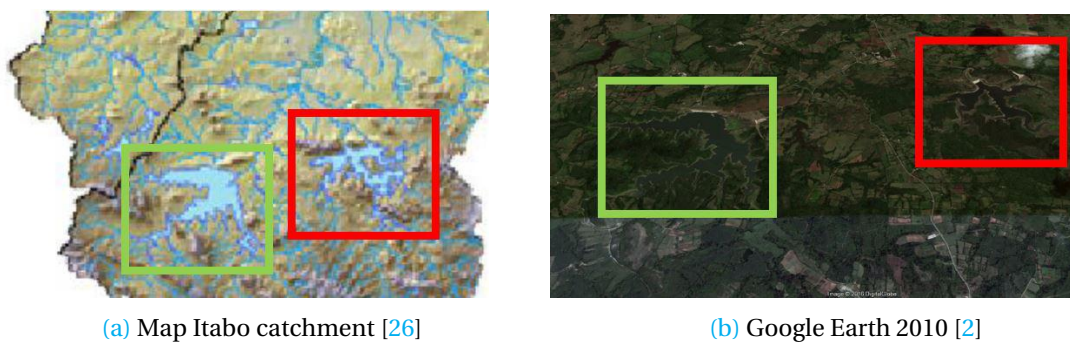


Figure J.4: Comparison map and Google Earth images



Figure J.5: Length and height profile Itabo catchment area Google Earth 2010 [2]

### J.3.1. INFILTRATION COEFFICIENT C

The runoff coefficient in the rational method formula is highly variable in the rational method formula. The values to be used in Cuba are specified in the Hydrologia Superficial [27]. The values are given in figure J.6.

Type of vegetation Tipo de vegetación	Steepness terrain Pendiente del terreno (%)	Soil texture Textura del suelo		
		Sandy Arenosa	Muddy-clay Limo-arcillosa	Clay Arcillosa
Forrest Forestal	0 - 5	0.10	0.30	0.40
	5 - 10	0.25	0.35	0.50
	10 - 30	0.30	0.50	0.60
Grasslands Praderas	0 - 5	0.10	0.30	0.40
	5 - 10	0.15	0.35	0.55
	10 - 30	0.20	0.40	0.60
Cultivated terrain Terrenos cultivados	0 - 5	0.30	0.50	0.60
	5 - 10	0.40	0.60	0.70
	10 - 30	0.50	0.70	0.80

Figure J.6: Infiltration coefficient (C) values. Translated from Hydrologia Superficial [27]

The steepness of the terrain is 65.4% according to a study in the Itabo catchment area [13]. This value seems to be very high, but this is the only value that is available. Based on this steepness, the highest steepness class is chosen: [10 - 30]. This is the most conservative approach, since this will result in higher discharges. According to an interview with *Prof. dra. Ing. Yakelin Rodríguez López* from CUJAE on Tuesday 6 September 2016, the soil conditions in the area are between muddy-clay and clay. The type of vegetation is analysed based on Google Earth images. The Google Earth images are shown in figure J.7. The left figure shows the total catchment area and the figures on the right are enlargements of parts of the area. The figure shows all three types of vegetation namely: forests, grasslands and cultivated terrain. However, grasslands and cultivated terrain are the main parts of the area, based on review of the images. This information gives still quite a range in C-values, between 0.4 and 0.8. A higher value of C means smaller 'losses' and hence a higher discharge.

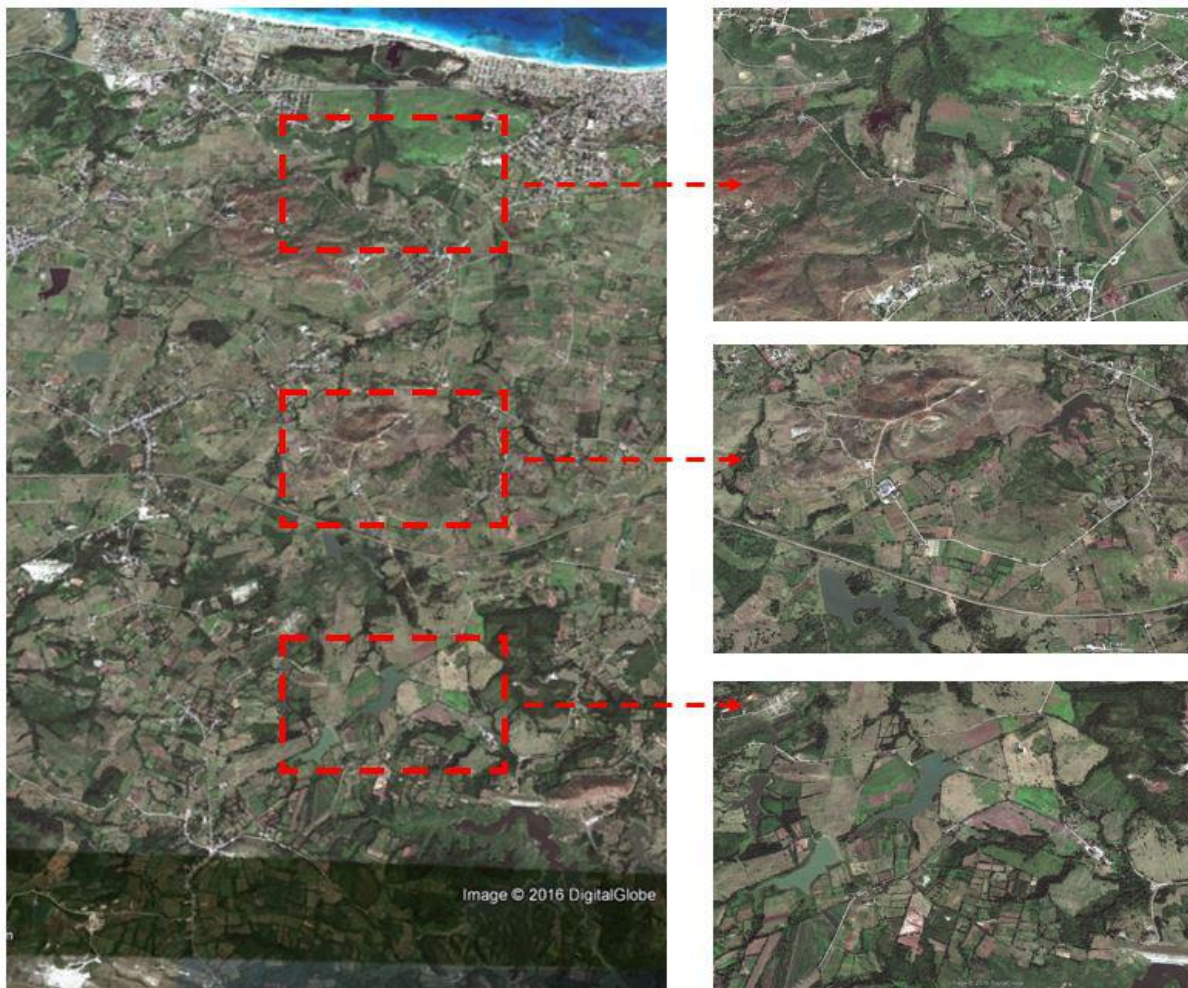


Figure J.7: Google Earth images terrain catchment area [2]

## J.4. RAIN DATA

### J.4.1. YEARLY AND MONTHLY AVERAGED VALUES

The yearly averaged values from 1970 till 2006 can be found in figure J.8a and the monthly averages of the same period can be found in figure J.8b [26].

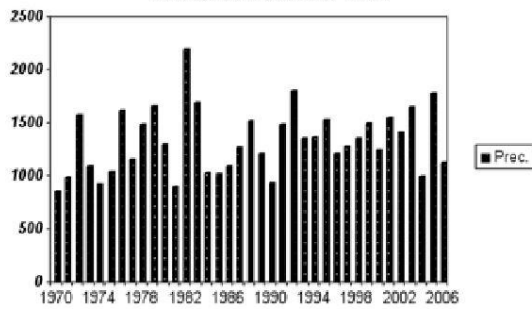
**CUADRO 1**  
VALORES DE LA PRECIPITACIÓN MEDIA ANUAL DE LAS ESTACIONES PLUVIOMÉTRICAS DE AMBAS CUENCAS EN EL PERÍODO 1970-2006

Año	Prec. Media Anual	Año	Prec. Media Anual	Año	Prec. Media Anual
1970	841.4	1983	1683.1	1996	1204.8
1971	972.5	1984	1016.8	1997	1269.7
1972	1564.9	1985	1001.6	1998	1343.0
1973	1085.2	1986	1080.4	1999	1485.7
1974	914.5	1987	1253.1	2000	1237.0
1975	1027.4	1988	1503.8	2001	1542.4
1976	1598.8	1989	1206.3	2002	1402.9
1977	1151.5	1990	918.0	2003	1632.3
1978	1473.7	1991	1477.3	2004	989.5
1979	1641.4	1992	1787.9	2005	1766.3
1980	1293.3	1993	1339.9	2006	1118.1
1981	883.0	1994	1351.4		
1982	2177.5	1995	1518.9		

**CUADRO 2**  
PRECIPITACIÓN MEDIA MENSUAL PARA AMBAS CUENCAS. PERÍODO 1970-2006.

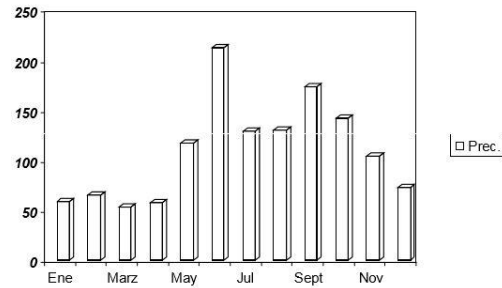
Ene	Feb	Marz	Abr	May	Jun	Jul	Agos	Sept	Oct	Nov	Dic	Total
58	65	53	57	117	212	129	130	173	142	104	72	1317

**FIGURA 11**  
PRECIPITACIÓN ANUAL PARA LAS CUENCAS GUANABO E ITABO. PERÍODO 1970 - 2006.



(a) Yearly averaged values

**FIGURA 12**  
DISTRIBUCIÓN INTRA-ANUAL DE LA PRECIPITACIÓN MEDIA MENSUAL. PERÍODO 1970-2006.



(b) Monthly averaged values

Figure J.8: Rain data [26]

### J.4.2. INTENSITY DURATION FREQUENCY DATA

The Intensity Duration Frequency (IDF) data used in this analysis is from station CH-345, La Habana del Este. The location of the station can be seen in figure J.9. The location of the rain station is in the catchment area, hence the rain data is representative for this analysis.

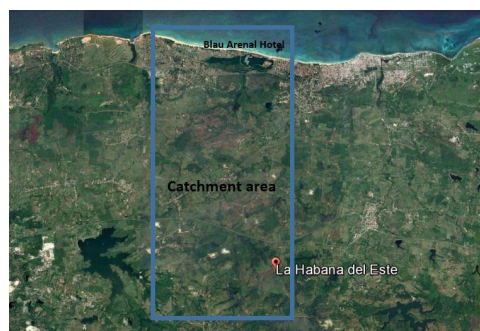


Figure J.9: Location rain station CH-345 [2]

The IDF-curve is expressed in formula J.6:

$$I_{tr} = \frac{A}{(t + B)^n} \quad (J.6)$$

Where:  $I_{tr}$  = Rain intensity by return period [mm/h]  
 $t$  = Duration [min]  
 $A$  = Station coefficient 1 [-]  
 $B$  = Station coefficient 2 [-]  
 $n$  = Station coefficient 3 [-]

The coefficients for station CH-345 are listed in table J.1.

Table J.1: IDF characteristics station CH-345 [27]

Return period [year]	A	B	n
2	6389.16	43.0	1.01
5	6142.79	45.0	0.96
10	6173.63	46.0	0.94
25	6313.46	47.0	0.92
50	6358.41	47.0	0.90
100	6874.91	49.0	0.90
1000	7884.52	52.5	0.88

The resulting graph is shown in figure J.10, with on the vertical axis the rain intensity in mm/h and on the horizontal axis the duration of the rain in minutes. The different curves represent the different return periods.

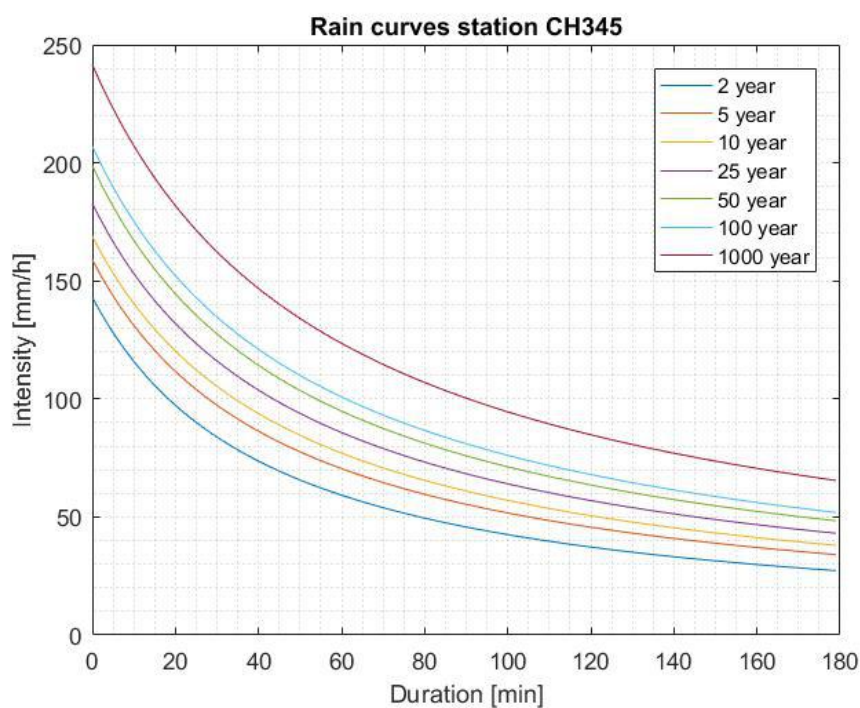


Figure J.10: Intensity Duration Frequency curve station CH345

### SYNTHETIC HISTOGRAM

The input for the triangular unit hydrograph method is the synthetic rain histograms, which are calculated based on the Intensity Frequency Duration curves from station CH-345. The method to obtain the synthetic histogram is described in Hidrologia Aplicada [24] and is summarised below:

- The method is explained based on a duration interval of 10 minutes. See figure J.11.
- The intensity given the specific duration (10, 20, ..., 120 min) is calculated based on the IDF curve. The duration is given in column 1 and the resulting intensity in column 2.
- The total amount of precipitation is calculated by multiplying the duration with the intensity, see column 3.
- The increase of precipitation is calculated in column 4 for example by subtracting the 10 minute precipitation from the 20 minute rain. This is done for all durations from column 1 except for the first one.
- The bins of the synthetic histogram is given in column 5. The bin width is 10 minutes.
- The increase of precipitation from column 4 is placed in column 6 in a different order. The maximum precipitation (line 1, column 4) is placed in the middle of the histogram. The other values are ordered from low at 10 and 120 minutes to high at the middle.

For this specific situation a time step of 0.5 hour and a duration of 24 hours is used. The intensity of each bin is retrieved from the IDF-curve.

Columna:	1	2	3	4	5	6
	Duración	Intensidad	Profundidad acumulada	Profundidad incremental	Tiempo	Precipitación
	(min)	(pulg/h)	(pulg)	(pulg)	(min)	(pulg)
	10	4.158	0.693	0.693	0-10	0.024
	20	3.002	1.001	0.308	10-20	0.033
	30	2.357	1.178	0.178	20-30	0.050
	40	1.943	1.296	0.117	30-40	0.084
	50	1.655	1.379	0.084	40-50	0.178
	60	1.443	1.443	0.063	50-60	0.693
	70	1.279	1.492	0.050	60-70	0.308
	80	1.149	1.533	0.040	70-80	0.117
	90	1.044	1.566	0.033	80-90	0.063
	100	0.956	1.594	0.028	90-100	0.040
	110	0.883	1.618	0.024	100-110	0.028
	120	0.820	1.639	0.021	110-120	0.021

Figure J.11: Synthetic histogram calculation [24]

The synthetic histogram is computed for all the return periods, this result is used in the triangular unit hydrograph. The histogram for the 100 year return period rain can be seen in figure J.12 the 1000 year return period can be seen in figure J.13. The cumulative precipitation is 230 and 305 mm during respectively the 100 and 1000 year return period.

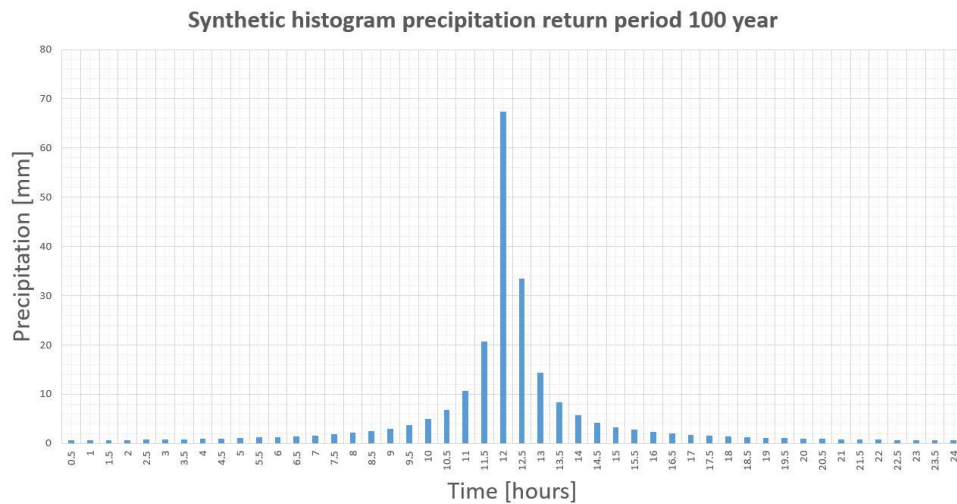


Figure J.12: 100 year return period rain data

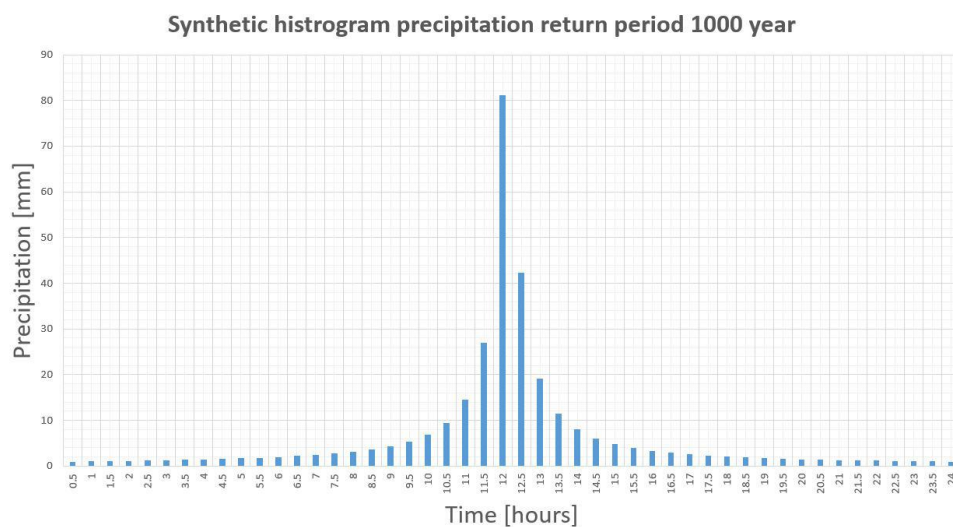


Figure J.13: 1000 year return period rain data

### J.4.3. RAIN DATA 1982 EVENT

During the tropical system, called Albertico, in 1982 a lot of precipitation was observed. The total amount of precipitation was approximately 700 mm in 24 hours. [13]. A distribution of the rain is calculated by *Prof. dr. Yoel Martinez* from *Instituto Superior de Tecnologias Ciencias Aplicadas InSTEC* using the 'Curvas de masa dimensionales del SCS-24 h de duracion', type III. This method is described in *Hidrologia Aplicada* [24]. This results in a distribution of the rain during that day, this distribution can be seen in figure J.14.

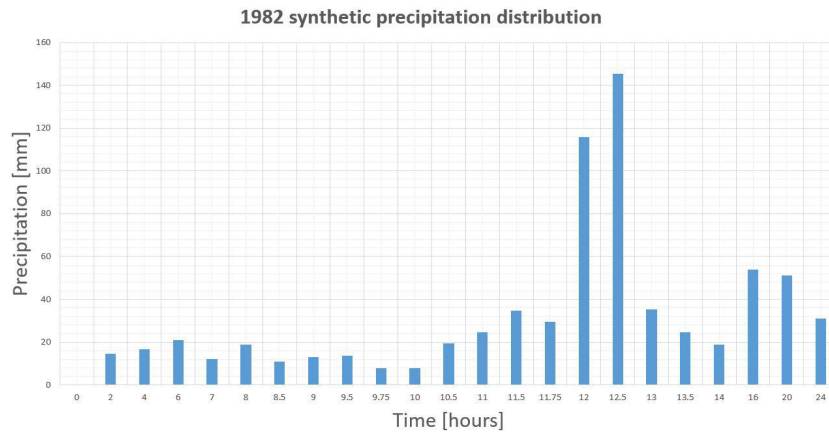


Figure J.14: 1982 rain data

The time steps of this rain data is not equally distributed. This data is interpolated in order to make the calculation of the discharge easier. The interpolated data is also provided by *Prof. dr. Yoel Martinez* [28], the time step used is approximately 0.7 hours.

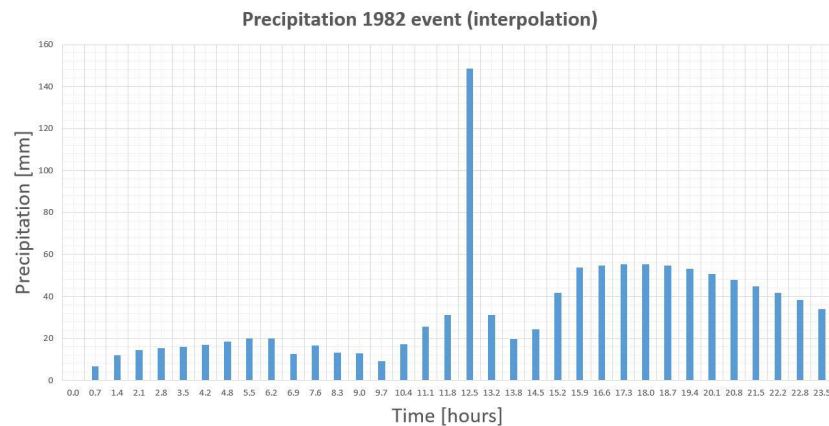


Figure J.15: Synthetic histogram calculation

## J.5. COMPUTATION DISCHARGE

### J.5.1. RATIONAL METHOD - INPUT PARAMETERS

The peak river discharge is calculated based on the following input parameters:

- Catchment area of 35.6 km<sup>2</sup>
- Runoff coefficient  $C$  range between 0.4 and 0.8
- Rain intensity for the seven different return periods corresponding with the duration of the rain equal to the concentration time of the catchment area. The concentration time is calculated with equation J.2 with input parameters:
  - Maximum catchment area length  $L = 10,000$  m
  - Catchment area slope  $S = 0.75$  %

This results in a concentration time of 168.3 minutes, equal to 2.8 hours.

## J.5.2. RATIONAL METHOD - RESULT

### PEAK RIVER DISCHARGE

The resulting river discharge for the different return periods is shown in figure J.16.

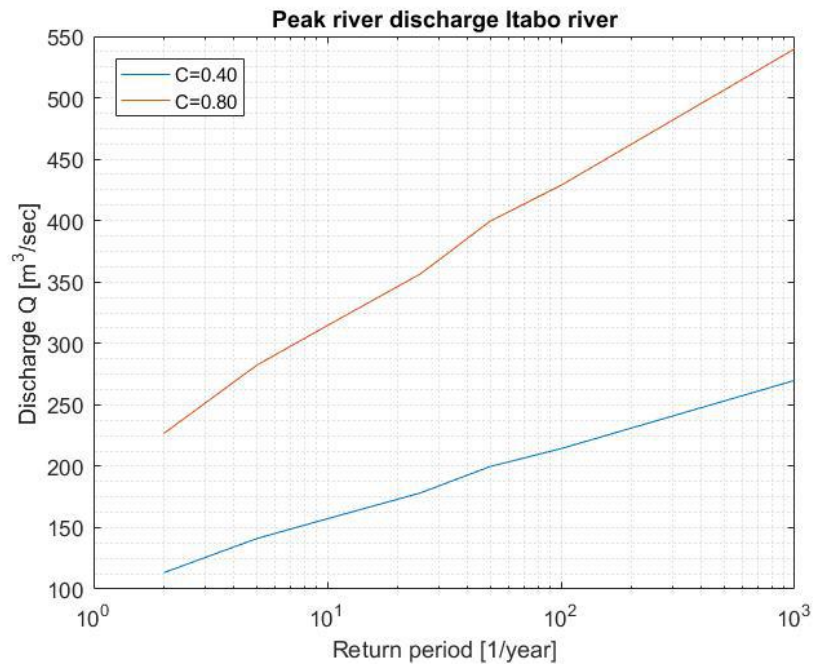


Figure J.16: Peak river discharge Itabo river  $C = 0.4$  and  $C = 0.8$

### MEAN RIVER DISCHARGE

The mean river discharge is calculated based on monthly and yearly averaged rain data [26], see paragraph J.4.

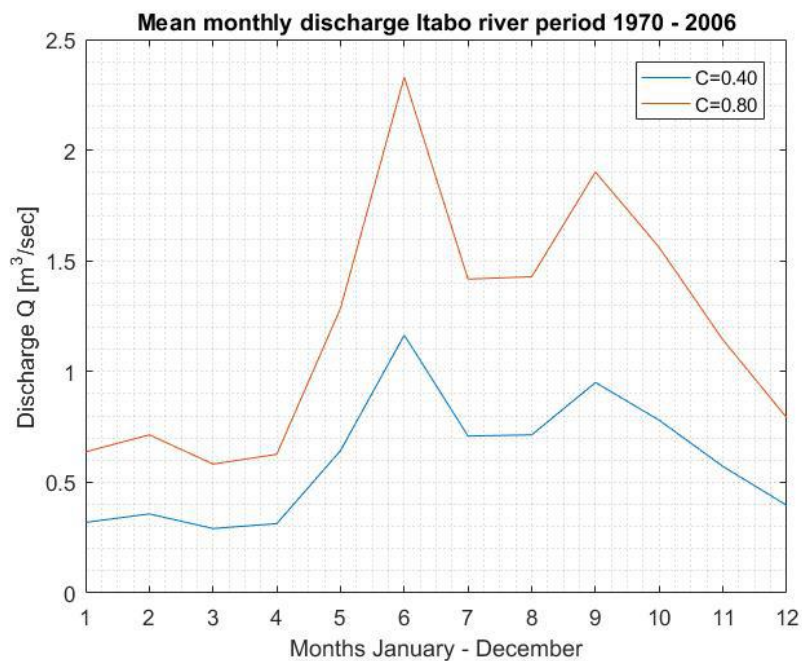


Figure J.17: Mean monthly discharge Itabo river  $C = 0.4$  and  $C = 0.8$

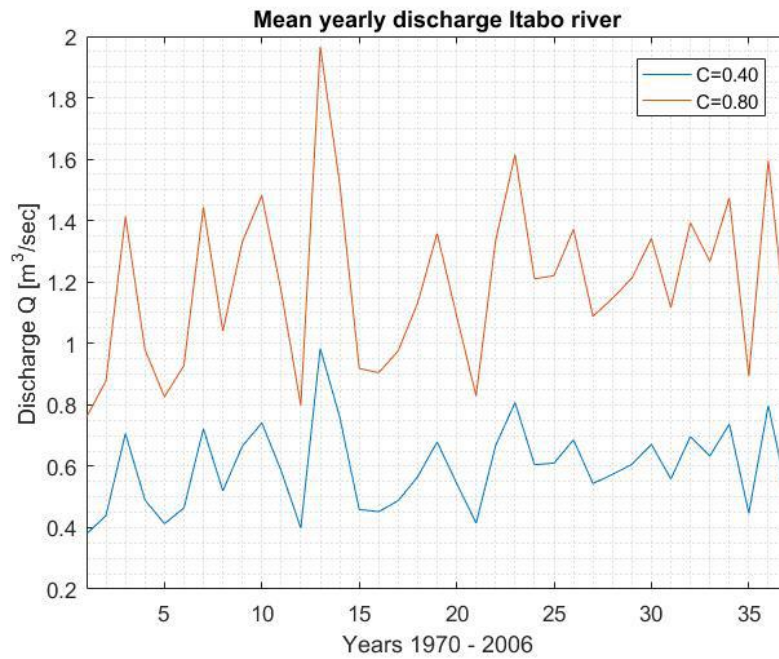


Figure J.18: Mean yearly discharge Itabo river C = 0.4 and C = 0.8

### J.5.3. TRIANGULAR UNIT HYDROGRAPH METHOD - INPUT PARAMETERS

The peak river discharge is calculated based on the following input parameters:

- Catchment area of 35.6 km<sup>2</sup>
- Reduction factor rain equal to zero.
- Concentration time of 168.3 minutes, 2.8 hours. Calculation equal to rational method.
- Peak time of 3.36 hours.
- Base time of 8.97 hours
- Synthetic histogram based on IDF-curve station CH345.

### J.5.4. TRIANGULAR UNIT HYDROGRAPH METHOD - RESULT

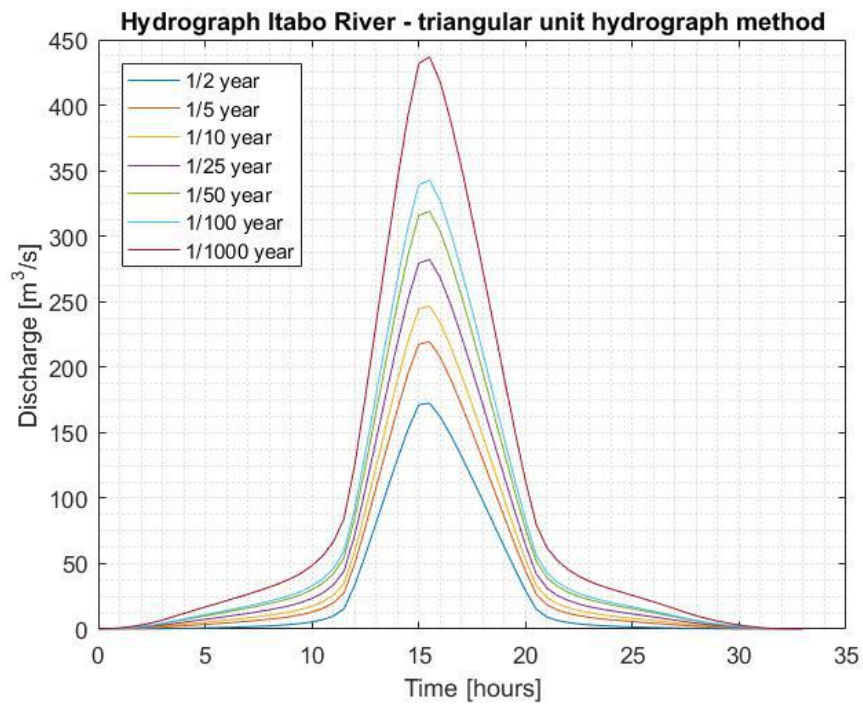


Figure J.19: Triangular unit hydrograph method per return period

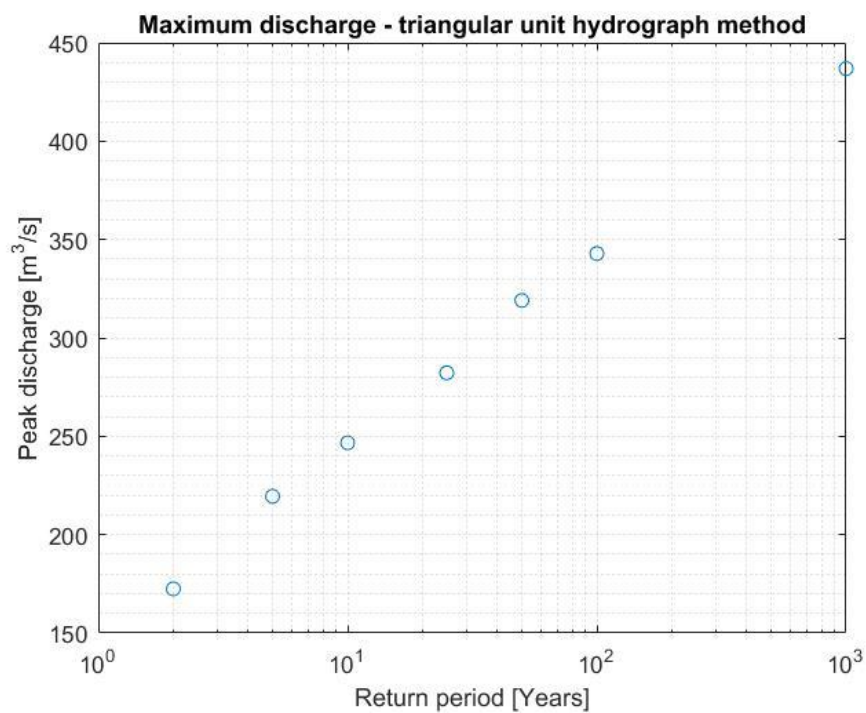


Figure J.20: Peak discharge triangular unit hydrograph method

### J.5.5. 1982 EVENT, TRIANGULAR UNIT HYDROGRAPH METHOD - RESULT

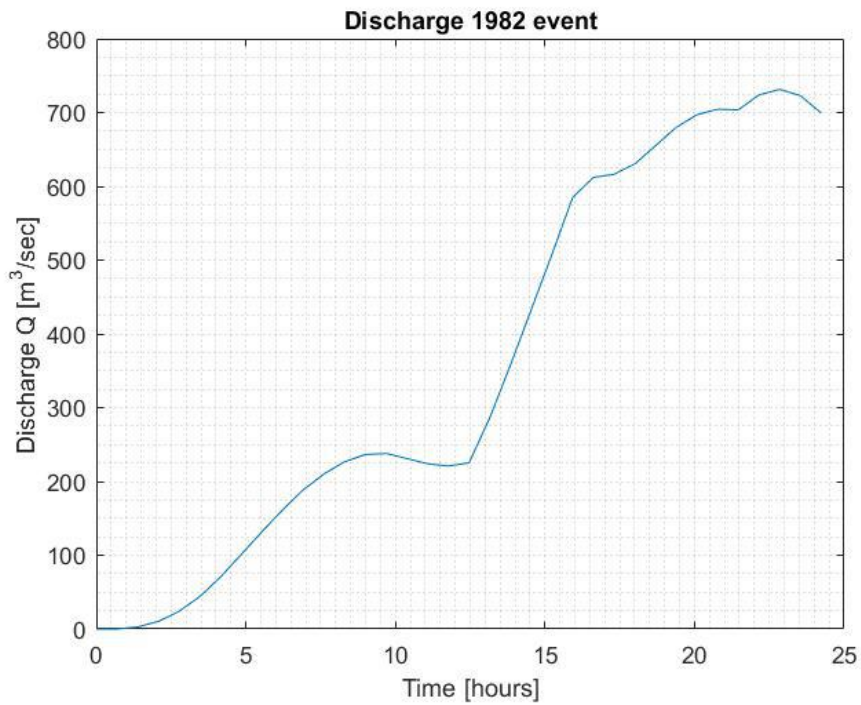


Figure J.21: Discharge 1982 storm event

### J.5.6. SENSITIVITY ANALYSIS

In figure J.22 the sensitivity of the resulting discharge with respect to the different  $C$  values is presented.

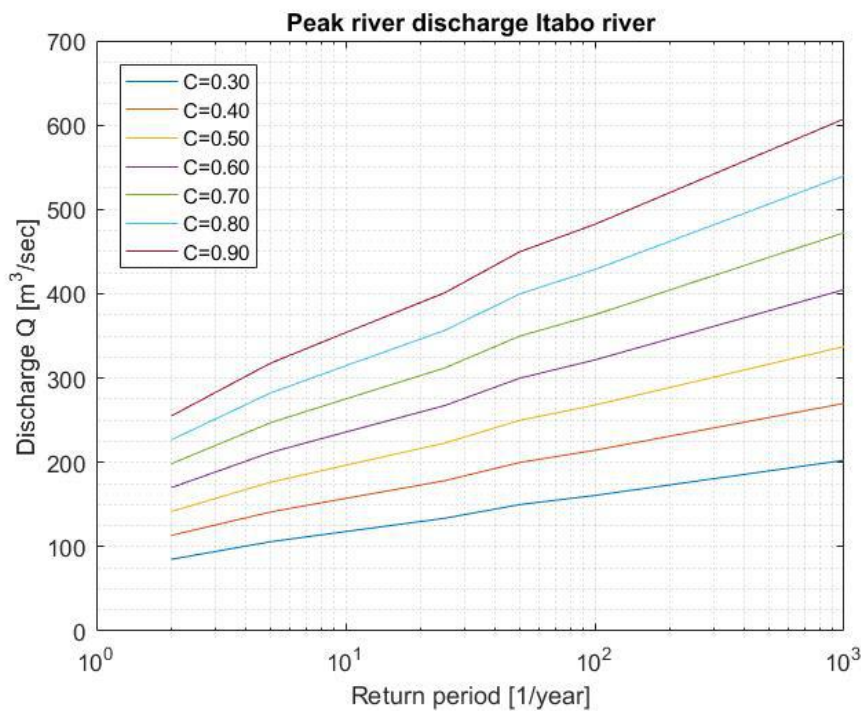


Figure J.22: Sensitivity peak river discharge C value



# K

## CONSEQUENCES

The eight consequences from section 2.8 are worked out here.

### **1. Damage waste water treatment plant**

Flooding of the area can lead to damage to the waste water treatment plant. The total value of the waste water treatment plant is \$ 300,000 US dollar [5]. Damage to the treatment plant might result in pollution in the area. For example, flooding can damage the pumps, with as a consequence that the waste water treatment plant will not work anymore, but the environment is not at risk. The damage can be expressed in terms of costs depending on the amount of damage.

### **2. Damage hotel facility**

Flooding of the hotel area will damage the hotel facilities. The total amount of damage and costs are a function of the inundation depth.

### **3. Evacuation and rescue operation**

Based on storm and discharge prediction, an evacuation can be done to bring tourists and hotel staff to safe ground. Evacuation can be done after flooding has occurred. This can be expressed in terms of costs depending on the number of tourists and staff in the area.

### **4. Clean up and reconstruction costs**

After flooding has occurred, clean up and reconstruction will take place. Clean up of the area is especially needed when the waste water treatment plant is flooded. Reconstruction costs are dependent on the total damage.

### **5. Decrease tourism revenues**

Damage to the hotel and the environment will have an impact on the tourism in the area. These decrease in tourism revenues will harm the (local) economy. These are indirect costs. The total costs are difficult to predict in advance.

## 6. Fatalities and injuries

The maximum capacity of the hotel is approximately 300 tourists and the total staff consists of 200 persons at most [5]. So, at most there are 500 persons at risk. The likelihood of the maximum occupancy during an extreme event is not very high, but it is the upper boundary for the total amount of people in the area. The total amount of people in the area is not equal to the total estimation of loss of life during a flood. The total estimation of loss of life is expressed by equation K.1 [29].

$$N_{loss} = F_d \cdot (1 - F_E) \cdot N_{par} \quad (\text{K.1})$$

Where:  $N_{loss}$  = Loss of life estimate  
 $F_d$  = Mortality fraction  
 $F_E$  = Evacuation fraction  
 $N_{par}$  = Number of people at risk

The total number of fatalities is expressed by the total number of people in the area, reduced by the amount of people that are evacuated. This total amount of people at risk is multiplied by the mortality fraction. This mortality fraction is a function of the flood characteristics. A flood with a large inundation depth and a flood that rises quick will have a large mortality fraction. For the Blau Arenal Hotel the evacuation fraction is assumed to be high, because the total amount of people to be evacuated is relatively small. The mortality fraction can be assumed based on the model results. The important parameters are the total inundation depth of the hotel area and the rising time.

## 7. Environmental losses

As described in section 2.1, the area is a protected environment. Flooding of the waste water treatment plant will damage the protected mangrove forest. This intangible consequence is difficult to express in terms of costs.

## 8. Damage to reputation Ministry of Tourism

The Ministry of Tourism is responsible for the Blau Arenal Hotel. Quantifying this costs is difficult.

# L

## RISK

### L.1. FAULT TREES

#### L.1.1. EXPLANATION

A fault tree is used to provide insight in mechanisms of system failure and the associated failure probabilities. These insights can be used to optimise system design and management, because so-called 'weak links' can quickly be obtained.

Fault trees give a logical succession of all events that lead to one undesired 'top event' at the top of the tree [30]. To analyse parallel and series systems, different gates are used. These gates and other symbols used in the fault trees are explained below.

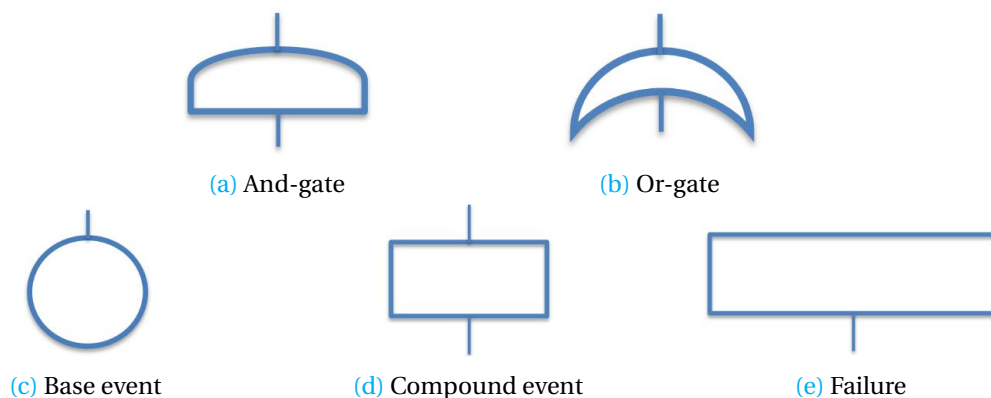


Figure L.1: Components of a fault tree

#### AND-GATE

The and-gate is used for parallel systems, when all the underlying events have to take place for the top event to occur.

### OR-GATE

The or-gate is used for series systems, when at least one of the underlying events have to take place to pass the gate in the fault tree.

### BASE EVENT

A base event is an initial event, which is situated at the base of the fault tree. Such an event usually concerns the failure of a system component.

### COMPOUND EVENT

A compound event is a consequential event that occurs if the condition defined in the underlying gate is met.

### FAILURE

Failure is the event that has to be avoided. With the formulae of each gate and probabilities of each compound the probability of failure of the final top event can be calculated.

## L.1.2. FAILURE OF THE HOTEL

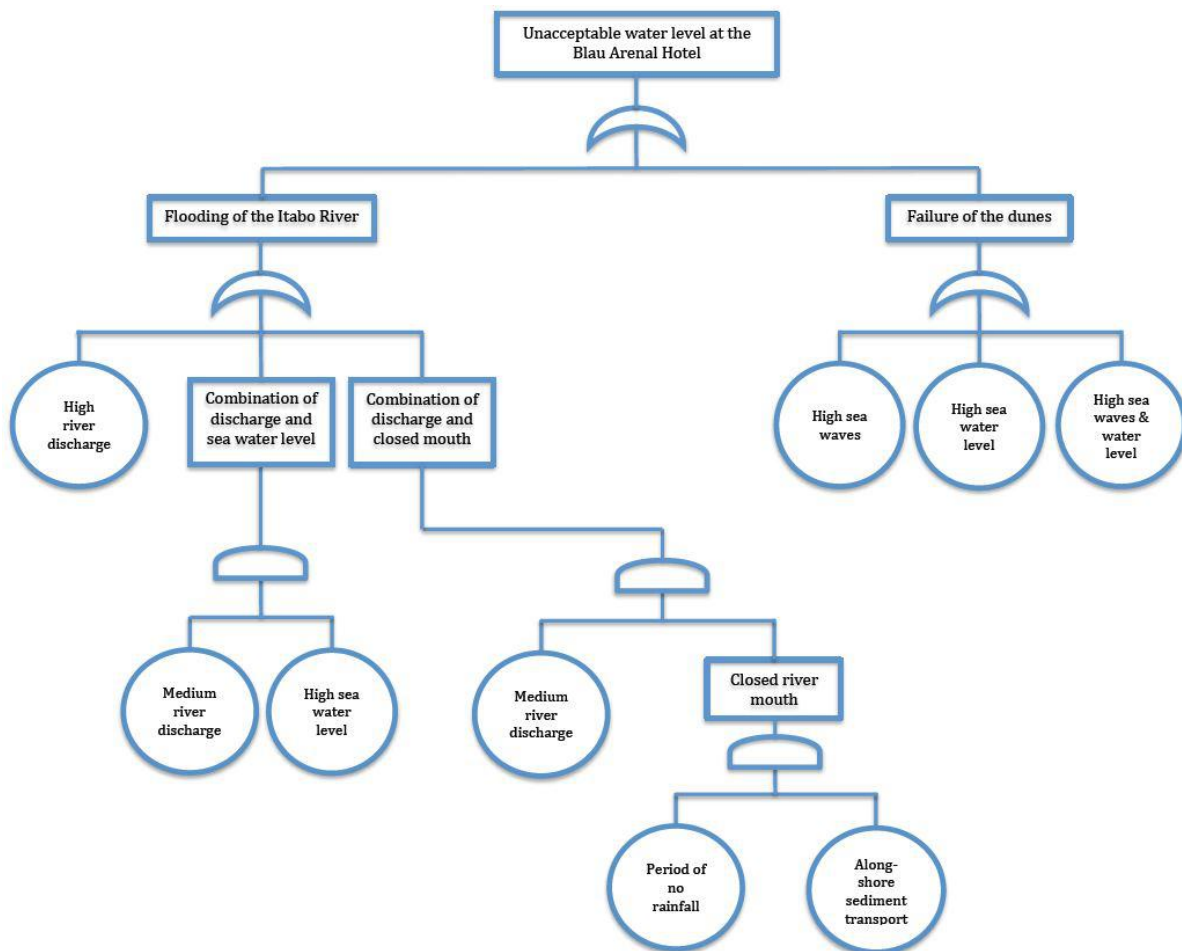


Figure L.2: Fault tree of the unacceptable water level at the Blau Arenal Hotel

### L.1.3. FAILURE OF THE WASTE WATER TREATMENT PLANT

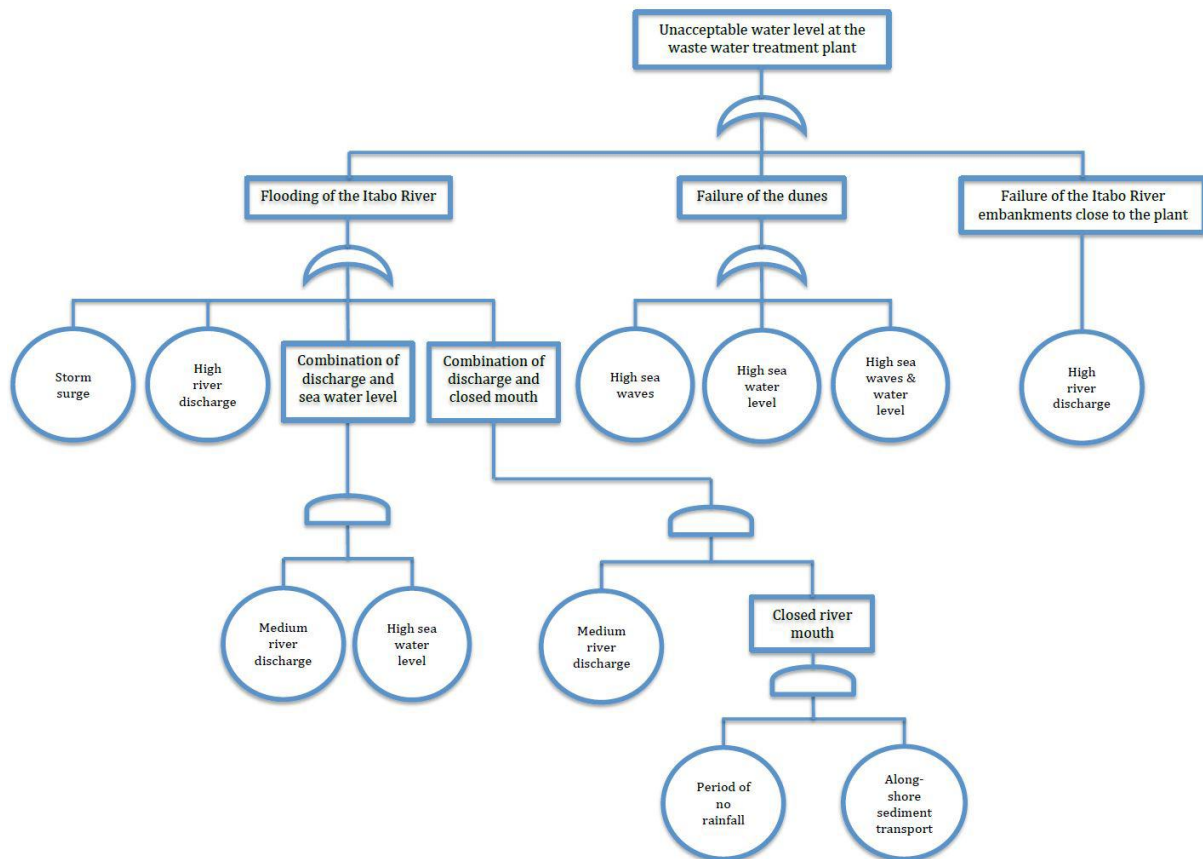


Figure L.3: Fault tree of the unacceptable water level at the waste water treatment plant

As can be seen in figure L.3, the waste water treatment plant could also fail due to instability of the embankments of the river and lagoon. This failure is not considered in this report, because of lacking information about the stability of the embankments. The assumption is done that the present mangroves, growing at the embankments, will provide sufficient stability.

## L.2. ALTITUDE DATA

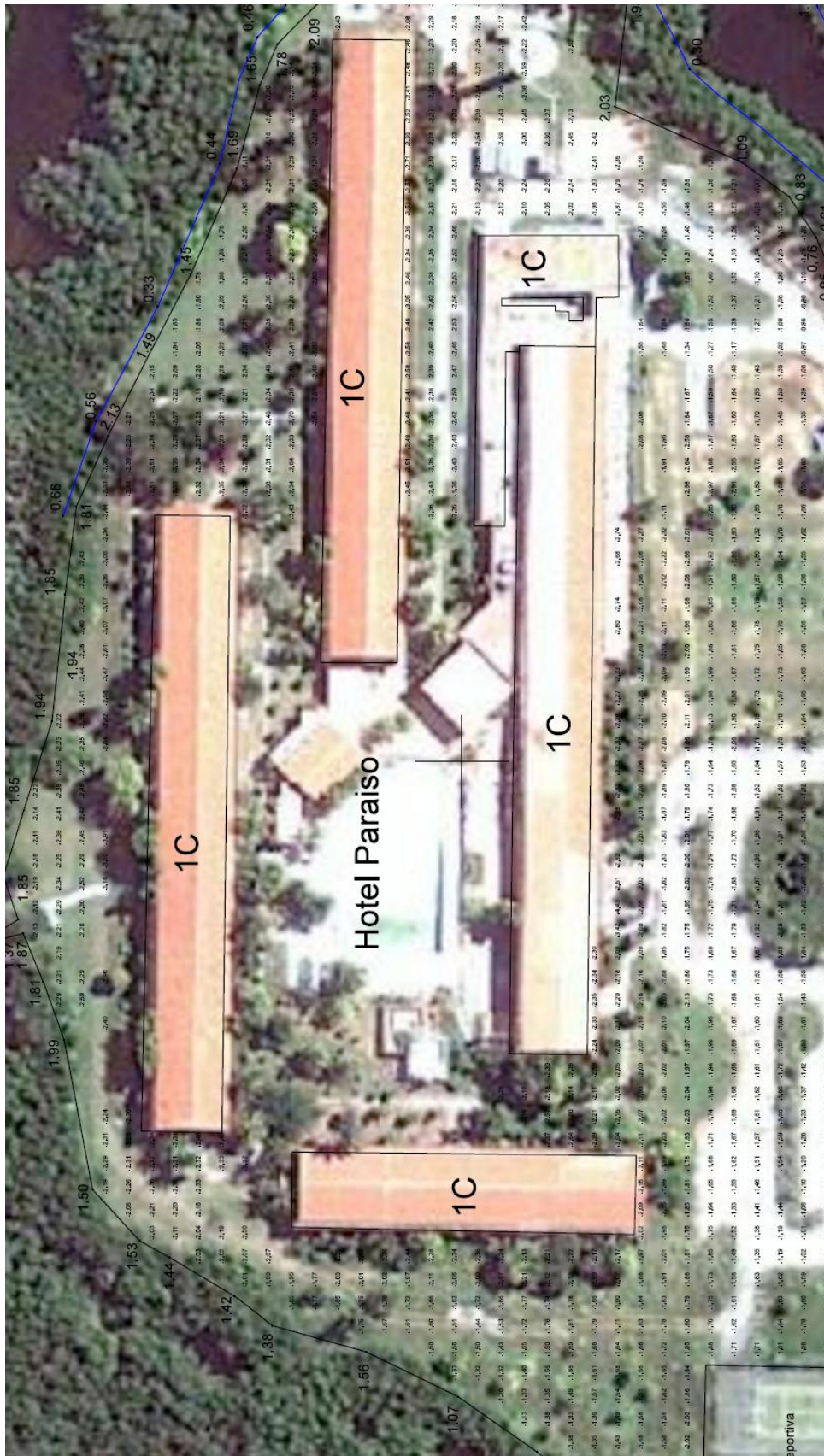


Figure L.4: Aerial view of Blau Arenal Hotel with altitude data [31]

### L.3. VULNERABILITY CLASSIFICATION

This section contains values related to the vulnerability of the study area for both flooding by waves or river discharge. These values have been carefully chosen with the use of the Cuban handbook with methodologies for the determination of the risks of disasters for territorial areas [32]. This handbook uses a clear system of grading for each different value. If all values are counted a total number of vulnerability will be the result. This number has a range of 1 to 100, where 100 is very vulnerable and 1 is resilient.

The tables in this appendix are similar to the ones in the Cuban handbook, only the chosen values for the specific area of interest are added. Every table has its own topic, which will be presented in the caption of the table.

#### L.3.1. VULNERABILITY OF FLOODING CAUSED BY RIVER DISCHARGE

Table L.1: Structural, values for vulnerability of flooding caused by river discharge [32]

	Maximum value	Chosen value
Soil permeability	1.0	0.5
Steepness	1.0	0.5
Terrain	1.0	0.5
Potential danger to structures	17.0	6.0
<b>Total</b>	<b>20.0</b>	<b>7.5</b>

Table L.2: Non structural, values for vulnerability of flooding caused by river discharge [32]

	Maximum value	Chosen value
State of drainage	5.0	2.5
Obstruction of roads	3.0	1.5
Damage to vital lines	2.0	1.0
<b>Total</b>	<b>10.0</b>	<b>5.0</b>

Table L.3: Functional, values for vulnerability of flooding caused by river discharge [32]

	Maximum value	Chosen value
Availability of emergency group	4.0	0.0
Preparation of the system	4.0	0.0
Evacuation capacity	4.0	0.0
Access to isolated zones	4.0	2.0
Reserve supplies	4.0	0.0
<b>Total</b>	<b>20.0</b>	<b>2.0</b>

Table L.4: Social, values for vulnerability of flooding caused by river discharge [32]

	Maximum value	Chosen value
Affected population	10.0	5.0
Perception of danger	3.0	1.5
Presence of weak and poor people	2.0	0.0
Preparation of population	3.0	1.5
Presence of rubbish	2.0	0.0
<b>Total</b>	<b>20.0</b>	<b>8.0</b>

Table L.5: Ecology, values for vulnerability of flooding caused by river discharge [32]

	Maximum value	Chosen value
Fragile ecosystem	5.0	5.0
Presence of protected nature	5.0	5.0
<b>Total</b>	<b>10.0</b>	<b>10.0</b>

Table L.6: Economy, values for vulnerability of flooding caused by river discharge [32]

	Maximum value	Chosen value
Budget for risk reduction	4.0	1.0
Industrial zone	4.0	0.0
Cost of response	4.0	3.0
Cultivated zone	4.0	1.0
Presence of animals	4.0	1.0
<b>Total</b>	<b>20.0</b>	<b>6.0</b>

The total vulnerability of flooding caused by river discharge is 38.5. This value is characterised as medium (between 34 and 66 points) in the Cuban handbook.

### L.3.2. VULNERABILITY OF FLOODING CAUSED BY WAVES

Table L.7: Structural, values for vulnerability of flooding caused by waves [32]

	Maximum value	Chosen value
Soil permeability	1.0	0.5
Steepness	1.0	0.5
Terrain	1.0	0.5
Potential danger to structures	17.0	6.0
<b>Total</b>	<b>20.0</b>	<b>7.5</b>

Table L.8: Non structural, values for vulnerability of flooding caused by waves [32]

	Maximum value	Chosen value
Affect to infrastructure	3.0	1.5
Affect to aquaducts	2.0	0.0
Affect to sewer	3.0	1.5
Affect to vital lines	2.0	0.0
<b>Total</b>	<b>10.0</b>	<b>3.0</b>

Table L.9: Functional, values for vulnerability of flooding caused by waves [32]

	Maximum value	Chosen value
Availability of emergency group	4.0	0.0
Preparation of the system	4.0	0.0
Evacuation capacity	4.0	0.0
Access to isolated zones	4.0	2.0
Reserve supplies	4.0	0.0
<b>Total</b>	<b>20.0</b>	<b>2.0</b>

Table L.10: Social, values for vulnerability of flooding caused by waves [32]

	Maximum value	Chosen value
Affected population	10.0	2.5
Perception of danger	3.0	1.5
Preparation of population	3.0	1.5
Presence of weak and poor people	2.0	0.0
Presence of rubbish	2.0	0.0
<b>Total</b>	<b>20.0</b>	<b>5.5</b>

Table L.11: Ecology, values for vulnerability of flooding caused by waves [32]

	Maximum value	Chosen value
Fragile ecosystem	5.0	5.0
Presence of protected nature	5.0	5.0
<b>Total</b>	<b>10.0</b>	<b>10.0</b>

Table L.12: Economy, values for vulnerability of flooding caused by waves [32]

	Maximum value	Chosen value
Budget for risk reduction	4.0	1.0
Industrial zone	4.0	0.0
Cost of response	4.0	3.0
Cultivated zone	4.0	1.0
Presence of animals	4.0	1.0
<b>Total</b>	<b>20.0</b>	<b>10.0</b>

The total vulnerability of flooding caused by waves is 33.5 points. This value is between the low (between 0 and 33 points) and medium (between 34 and 66 points) vulnerability in the Cuban handbook.

# M

## POSSIBLE CORRELATIONS

- **Fully dependent**

The two events do always happen at the same time when one event takes place, in case of full dependency. This means that the total probability of simultaneous occurrence is equal to the highest individual probability. The correlation coefficient is equal to 1 in this case.

- **Independent**

If the precipitation and waves are independent, it means that the two events are unrelated. They occur randomly with respect to each other, but they can occur at the same time. The correlation coefficient is equal to 0 in case of independence.

- **Mutually exclusive**

Mutually exclusive events can not happen at the same time. In this case it is not possible that high river discharge and high waves occur simultaneously. The correlation coefficient is equal to -1 for mutually exclusive events.

- **Partly correlated**

Full dependency, independency and events that are mutually exclusive are the boundaries of the possible relation between the high river discharge and the occurrence of high sea waves. However, a fourth option is partly correlation. The correlation coefficient is between 0 and 1. This value expresses the likelihood of simultaneous occurrence of the two events. The correlation coefficient can be calculated based on data.



# N

## SWAN

This model description is based on information from Waves in Oceanic and Coastal Waters [33] and from the SWAN user manual [34]. The SWAN model [35], which stands for Simulating Waves Nearshore, is a freely available, open source third-generation wave model. This implies the implementation of quadruplet wave-wave interactions, which are computed explicitly. SWAN is used to compute the wave transformation from deep water conditions to shallow water conditions, based on a wave action balance. The model does not solve for individual waves, but it transforms an offshore wave spectrum to a wave spectrum nearshore. In a third-generation wave model this wave spectrum is free to develop without any shape imposed a priori, because of the energy redistribution of the quadruplet wave-wave interactions. Besides a spectral shape this wave spectrum is defined by a significant wave height, different frequencies with one of them defined as the peak frequency. These properties vary in every direction in a 2D shore model, as is the case in our project. Next to the quadruplet wave-wave interactions other physical phenomena included in SWAN are white capping, triad wave-wave interactions, friction, depth-induced wave breaking and wave-setup.

### N.1. INPUT

The computational grid, the spectral grid and grid of other parameters are all input for the SWAN model, together with preferences on physical processes and on numerics. Also the type of output should be specified in the input file. In the following subsections the considerations on these different input aspects will be mentioned.

#### N.1.1. GENERAL

The water level for summer and winter conditions is set to Mean Sea Level (MSL), as no storm conditions are simulated during these conditions and waves are not expected to be governing for such conditions. As the tidal range is very small (at most 50 cm, see section 2.3.2), this tide is not included for these calm conditions, where the significant wave height ( $H_s$ ) offshore is only 1.1 m.

The output for XBeach is at a depth of around 10 m, so excluding this tidal amplitude of at most 25 cm will not affect the wave spectrum at this depth. This can be seen by a rough wave breaking estimation. This is done by equation N.1 [17].

$$H_{max} = \gamma \cdot (d + \bar{\eta}) \quad (\text{N.1})$$

Where:	$H_{max}$	=	Max wave height	[m]
	$\gamma$	=	Breaker parameter	[-]
	$d$	=	Average water depth	[m]
	$\bar{\eta}$	=	Fluctuating water depth	[m]

A depth of two meters would still allow waves with a significant height of 1.1 meter to propagate without breaking. For an explanation on the parameter  $\gamma$ , see section N.1.5. For severe and extreme conditions, the significant wave height can be 7.7 m or even more (see appendix F). In this case the water depth nearshore matters. The tide (0.25 m) is included, as well as a storm surge of 0.4 m (see section 2.3.5). Also a sea level rise during 50 years is accounted for (0.25 m, see section 2.3.6), because this is the lifetime of the structure. This results in a total water level of MSL +0.9 m.

The wave field is a stationary one, in two dimensions. As can be found in section 2.4.3, all depth files are transformed from WGS84 to a Cartesian coordinate system with a (0,0) point located in the lower left corner of the data set.

### N.1.2. COMPUTATIONAL GRID

The characteristic spatial scales of wind waves propagating from deep to shallow waters change. The spatial scale in oceanic waters can be in the order of 10-100 km, while these scales reduce to 100-1000 m at the breaker zone. These small scale processes require a refined computational grid to deal accurately with these smaller scales. On the northern boundary of the domain, around 25 km from the coast, the depth of the Gulf of Mexico is 1500 meters and deep water conditions are present. At this boundary a significant wave height ( $H_s$ ) and a peak period ( $T_p$ ), both for deep water conditions, are required as an input, together with a spectrum shape. The deep water conditions derived in appendix F are used over here. This input is discussed in section N.1.4 However, one should also impose boundary conditions on the two open boundaries east and west of the domain. As no boundaries are known close to the coast, often in engineering practice the deep water conditions are imposed here as well. This results in deep water waves propagating into the domain at shallow water zones, with errors as a consequence. A so called 'shadow zone' occurs on both sides of the computational domain, in which boundary effects influence the results. To get adequate results, the domain of interest should be out of the shadow zones. These shadow zones propagate from the northeast corner and the northwest corner of the grid towards the coast with an angle of at most 45°. The coast is 25 km away from the northern boundary, this means that a shadow zone of 25 km develops on both sides. The domain of the study area is from 90.0 km to 93.5 km. Adding some more than 25 km on both sides results in the following domain: [58900; 133900] (in meters).

### TRIANGULAR GRID

A special wish of the employer was to look at the propagation of waves into the river mouth. An unstructured grid would be useful to compute these very small spatial scales in an efficient way. A flexible mesh can have less grid points than a structured (nested) grid, resulting in faster computations. Because of the shadow zones introduced in the previous section, a relatively large grid is needed to ensure no boundary effects in the area of interest. This shadow zones do not need the same precision as the area of interest. Therefore a much coarser grid can be used in these shadow zones. However, to make sure that the waves propagating into the area of interest are solved precisely enough, the grid cells should be smaller around the boundaries of the area of interest to adequately solve for the bathymetry over there. These requirements can lead to the usage of two or three nested grids. If three grids are used, with step sizes of respectively 1 km, 100 m and 20 m, this results in more than 70,000 grid points for this problem scale. The created flexible mesh contains 27,876 points, which is significantly less.

The final result, made using Triangle [36] and BatTri 11.11.03 [37], can be seen in figure N.1a.

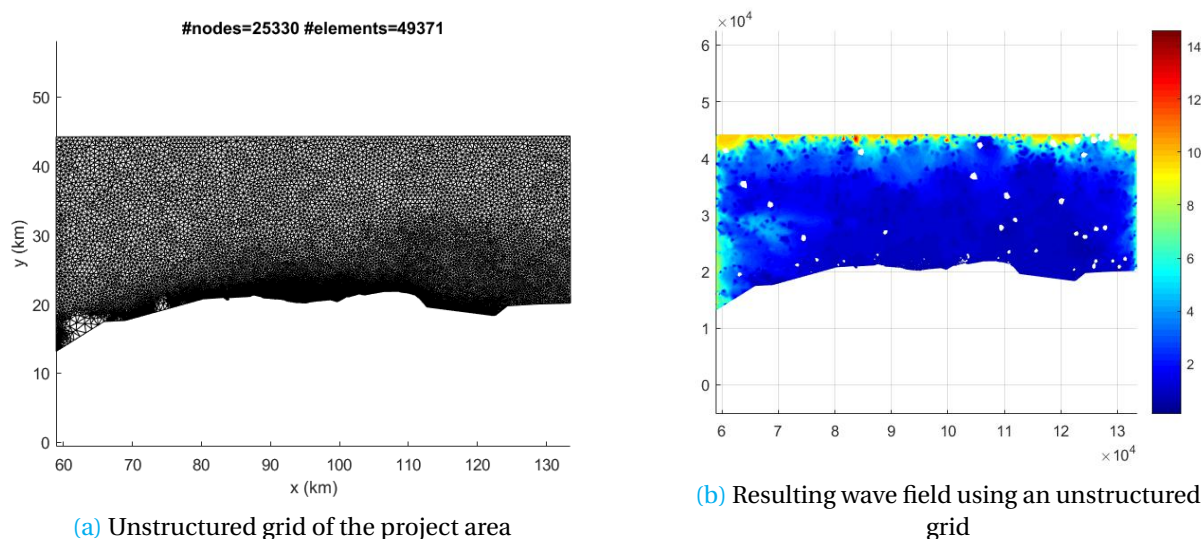


Figure N.1: Grid and wave field resulting from Triangle and BatTri

The results in SWAN can be seen in figure N.1b. As can be seen a lot of energy dissipation is happening close to the boundary, resulting in unrealistic low wave heights throughout the wave field.

As this issue could not be solved easily, the choice was made to use a nested structured grid, with a structured bottom depth file.

## STRUCTURED GRID

This nested approach consists of three grids:

- 1 Coarse grid, covering the whole area:  $x$  (58901.04, 133901.04) and  $y$  (11441.88, 44941.88) with a grid size of 500 x 500 m
- 2 Nest 1, covering 10 x 10 km around the project area:  $x$  (87300, 97300) and  $y$  (19740, 29740) with a grid size of 100 x 100 m
- 3 Nest 2, covering 4.62 x 4 km around the project area:  $x$  (90000, 94620) and  $y$  (19740, 23740) with a grid size of 20 x 20 m

The coarsest grid with the total gridded bathymetry can be seen in figure N.2.

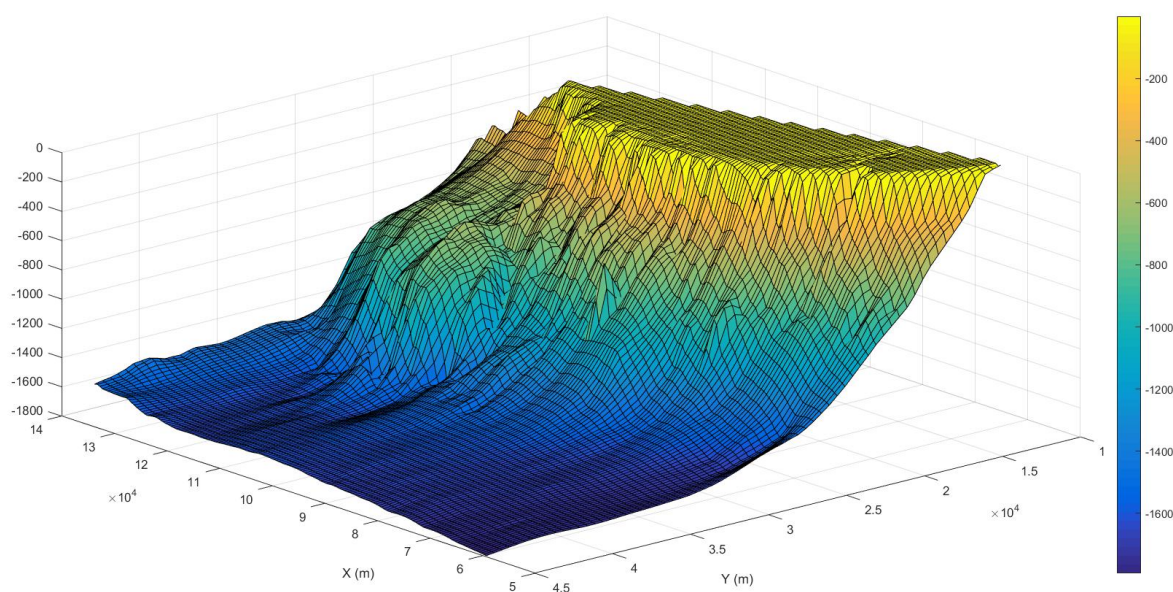


Figure N.2: Bathymetry of the coarse grid

### N.1.3. WIND

Wind parameters are obtained from section 2.11, in table 2.16.

### N.1.4. WAVE SPECTRUM

For the shape of the wave spectrum the JONSWAP shape is chosen. This spectrum shape is useful for young sea states, and “the JONSWAP spectrum has been shown to be rather universal, not only for idealised fetch-limited conditions but also for arbitrary wind conditions in deep water, including storms and hurricanes. The reason for this is that, for sufficiently steep waves, the quadruplet wave-wave interactions tend to stabilise the shape of the spectrum into the JONSWAP shape” [33]. Since the fetch of the Gulf of Mexico is in the same order as the North Sea (100 km) and wind waves will be present, this spectrum shape will indeed occur. Also, a part of the study will be on storm conditions (section 2.11). From Waves in Oceanic and Coastal Waters [33] average values for the JONSWAP spectrum can be deduced, which gives a  $\gamma = 3.3$ . This  $\gamma$  stands for the peak enhancement parameter of the JONSWAP spectrum. The wave spectrum should be imposed on the western, the

northern and the eastern boundary. The  $H_s$ ,  $T_p$  and direction of the waves can be deduced from section 2.11, in table 2.16.

### N.1.5. PHYSICS

Quadruplet wave-wave interactions are included by choosing the *Generation 3 Komen* model. Whitecapping, triad wave-wave interactions and setup are included with default parameters. The default value for the JONSWAP bottom friction is  $0.067 \text{ m}^2\text{s}^{-3}$ . However, for a typical sandy bottom the recommended value is  $0.038 \text{ m}^2\text{s}^{-3}$ . For a smooth seafloor, like the Gulf of Mexico, a lower value of  $0.019 \text{ m}^2\text{s}^{-3}$  is advised [34]. So this latter value will be used for this project.

Also depth-induced breaking of waves is included. According to Waves in Oceanic and Coastal Waters [33], several researches have shown that  $\gamma$  in the simple wave breaking equation N.1 depends on the slope. When examining the bathymetry of the breaker zone, the steepness from MSL -13.5 m to 0 m has an average value of 1:90. This is a mild slope, which implies waves will break earlier and a lower breaker parameter should be used. Equation N.2 [38] is only one of the empirical formulas which back up this idea. This equation can be used from gentle slopes (1:500) up to slopes with a steepness of 1:10.

$$\gamma = 0.56 \cdot e^{3.5m} \quad (\text{N.2})$$

For a slope of 1:90 this formula gives a breaker parameter of 0.58. However, since a lot of uncertainty is present in this parameter, the default value of 0.73 is used. This is a conservative approach, resulting in larger waves at the shore.

### N.1.6. OUTPUT

The output of the largest two grids consists of a grid of points with wave spectrum input for the following (nested) grid.

The output of the smallest and finest grid consists of five output points exactly at the boundaries of the XBeach model. Three points on the northern boundary, and one point on the east and west boundary are given as output.

The SWAN input files for severe storm conditions can be found below.

## Coarse grid input file for SWAN

```
1 $*****Heading*****
2 PROJ 'Cuba' '3'
3
4 $1=Summer Conditions
5 $2=Winter Conditions
6 $3=Severe Conditions
7 $4=Extreme Conditions
8 $*****Model Input*****
9 SET 0.9 NAUTICAL
10
11 MODE STATIONARY TWODIMENSIONAL
12
13 COORDINATES CARTESIAN
14
15 CGRID 58901.04 11441.88 0. 75000 33500 150 67 CIRCLE 36 0.03 1. 31
16
17 INPGRID BOTTOM 58901.04 11441.88 0. 150 67 500. 500.
18 READINP BOTTOM 1. 'swancoarse.bot' 3 0 FREE
19
20 WIND 14.6 12
21
22 BOUND SHAPESPEC JON 3.3 PEAK DSPR DEGREES
23
24 BOUNDSPEC SIDE N CCW CON PAR 7.7 11.3 354 30
25 BOUNDSPEC SIDE W CCW CON PAR 7.7 11.3 354 30
26 BOUNDSPEC SIDE E CCW CON PAR 7.7 11.3 354 30
27
28 $*****Physics*****
29 GEN3 KOMEN
30 WCAP
31 QUADRUPL
32 BREAKING
33 FRICTION JONSWAP 0.019
34 TRIADS
35 SETUP
36
37 $*****Numerics*****
38 NUM STOPC STAT 100
39
40 $*****Output*****
41 BLOCK 'COMPGRID' NOHEADER '3_coarsegrid.mat' LAY 3 XP YP DEP HS BOTLEV RTP DIR
42                                                                 PDIR SETUP
43 NGRID 'INPUT1' 87300 19740 0 10000 10000 100 100
44 NESTOUT 'INPUT1' '3_inputnest1.spc'
45
46 COMPUTE
47 STOP
```

## First nested grid input file for SWAN

```
1 $*****Heading*****
2 PROJ 'Cuba' '3'
3
4 $*****Model Input*****
5 SET 0.9 NAUTICAL
6
7 MODE STATIONARY TWODIMENSIONAL
8
9 COORDINATES CARTESIAN
10
11 CGRID 87300 19740 0. 10000 10000 100 100 CIRCLE 36 0.03 1. 31
12
13 INPGRID BOTTOM 87300 19740 0. 100 100 100. 100.
14 READINP BOTTOM 1. 'swanfine.bot' 3 0 FREE
15
16 WIND 14.6 12
17
18 BOUNDNEST1 NEST '3_inputnest1.spc' CLOSED
19
20 $*****Physics*****
21 GEN3 KOMEN
22 WCAP
23 QUADRUPL
24 BREAKING
25 FRICTION JONSWAP 0.019
26 TRIADS
27 SETUP
28
29 $*****Numerics*****
30 NUM STOPC STAT 100
31
32 $*****Output*****
33 BLOCK 'COMPGRID' NOHEADER '3_nest1.mat' LAY 3 XP YP DEP HS BOTLEV RTP DIR PDIR
34                                         SETUP
35 NGRID 'INPUT2' 90000 19740 0 4620 4000 231 200
36 NESTOUT 'INPUT2' '3_inputnest2.spc'
37 COMPUTE
38 STOP
```

## Second nested grid input file for SWAN

```
1 $*****Heading*****
2 PROJ 'Cuba' '3'
3
4 $*****Model Input*****
5 SET 0.9 NAUTICAL
6
7 MODE STATIONARY TWODIMENSIONAL
8
9 COORDINATES CARTESIAN
10
11 CGRID 90000 19740 0. 4620 4000 231 200 CIRCLE 36 0.03 1. 31
12
13 INPGRID BOTTOM 90000 19740 0. 231 200 20. 20.
14 READINP BOTTOM 1. 'swanfinest.bot' 3 0 FREE
15
16 WIND 14.6 12
17
18 BOUNDNEST1 NEST '3_inputnest2.spc' CLOSED
19
20 $*****Physics*****
21 GEN3 KOMEN
22 WCAP
23 QUADRUPL
24 BREAKING
25 FRICTION JONSWAP 0.019
26 TRIADS
27 SETUP
28
29 $*****Numerics*****
30 NUM STOPC STAT 100
31
32 $*****Output*****
33 BLOCK 'COMPGRID' NOHEADER '3_nest2.mat' LAY 3 XP YP DEP HS BOTLEV RTP DIR PDIR
34                                         SETUP
35 POINT '3N92000' 92000 20840
36 POINT '3N92300' 92300 20840
37 POINT '3N92600' 92600 20840
38 POINT '3W20600' 92000 20600
39 POINT '3E20560' 92600 20560
40
41 SPECOUT '3N92000' '3N92000.sp2'
42 SPECOUT '3N92300' '3N92300.sp2'
43 SPECOUT '3N92600' '3N92600.sp2'
44 SPECOUT '3W20600' '3W20600.sp2'
45 SPECOUT '3E20560' '3E20560.sp2'
46
47 COMPUTE
48 STOP
```

## N.2. RESULTS

For the severe storm the wave fields of the coarse grid, the first nested grid and the second nested grid are shown respectively in figure N.3, figure N.4 and figure N.5. In the coarse grid the influence of the shadow zones can clearly be observed. In the first nested grid the influence of the shadow zones is already decreased a lot. The resolution gets larger for the smaller grids, resulting in more details in the wave field.

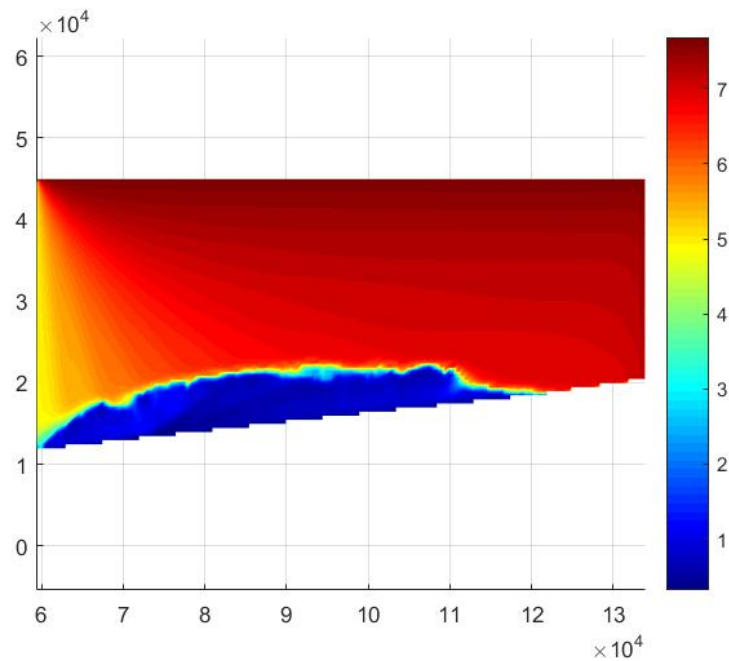


Figure N.3: Coarse grid with wave field during severe conditions (scale is in meters)

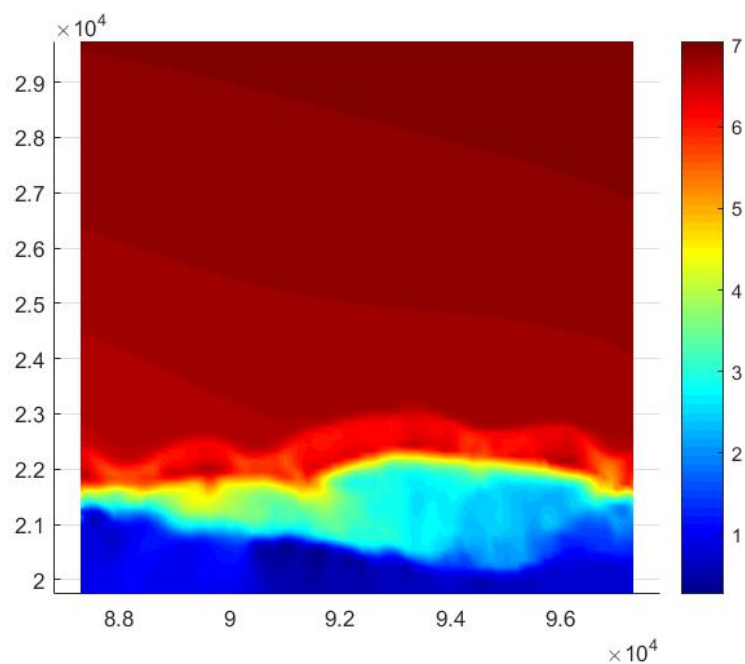


Figure N.4: First nested grid with wave field during severe conditions (scale is in meters)

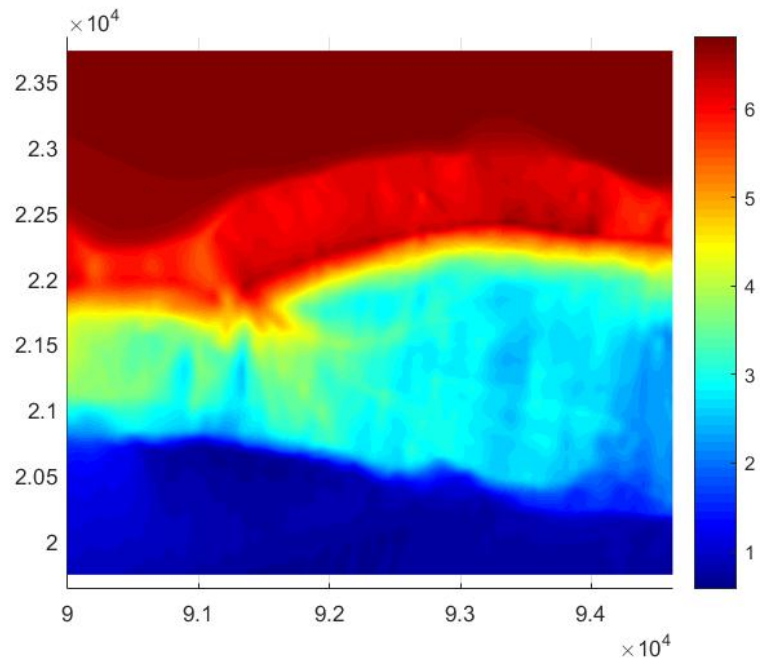


Figure N.5: Second nested grid with wave field during severe conditions (scale is in meters)

The wave fields of the smallest grid with summer conditions, winter conditions and extreme conditions are shown in figure N.6, figure N.7 and figure N.8.

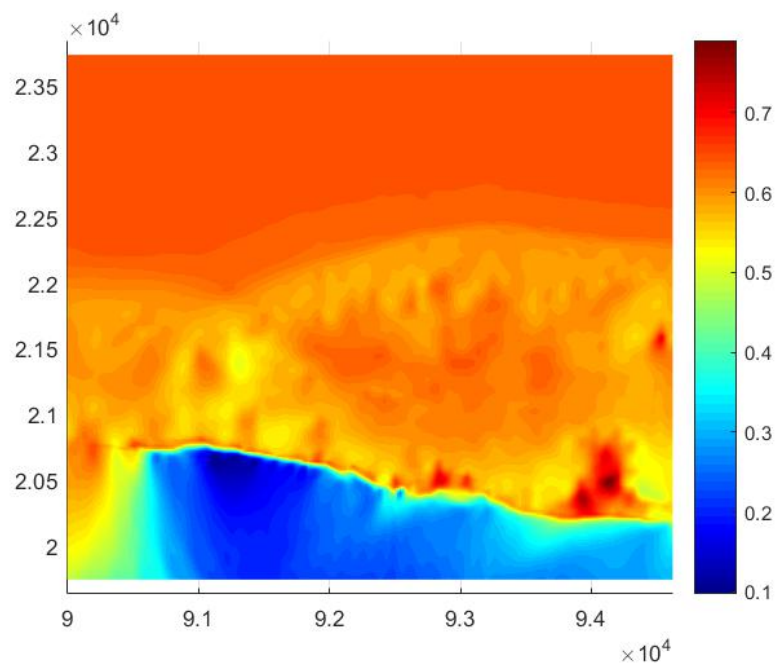


Figure N.6: Second nested grid with wave field during summer conditions (scale is in meters)

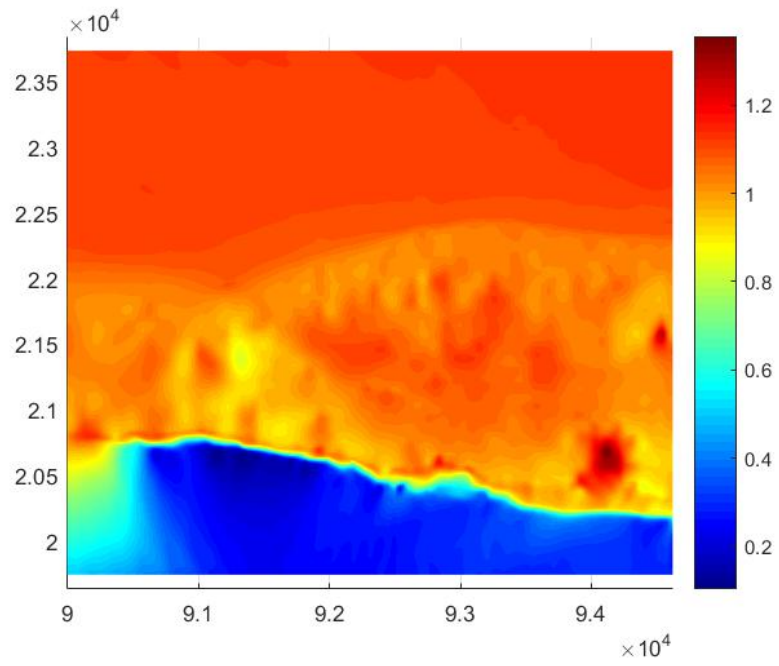


Figure N.7: Second nested grid with wave field during winter conditions (scale is in meters)

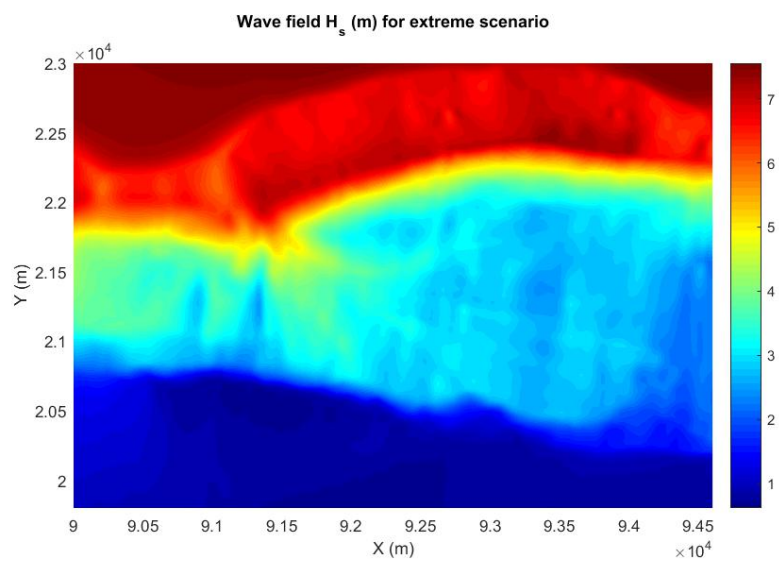


Figure N.8: Second nested grid with wave field during extreme conditions (scale is in meters)



# O

## XBEACH MODEL SET-UP

XBeach is a numerical model, developed by Deltares, UNESCO-IHE, University of Technology Delft and the University of Miami. According to the *XBeach User Manual* [39], it is originally intended to simulate hydrodynamic and morphodynamic processes on a spatial scale of kilometers and a temporal scale of hours to days. The processes included in XBeach are: hydrodynamic processes of short wave transformation (refraction, shoaling and breaking), long wave (infragravity wave) transformation (generation, propagation and dissipation), wave-induced setup and unsteady currents, as well as overwash and inundation. The morphodynamic processes include bed load and suspended sediment transport, dune face avalanching, bed update and breaching. Besides that, effects of vegetation, hard structures and discharge input can be simulated [39].

In this project, XBeach is used to simulate the possible flooding due to extreme rain- and storm events. The entire study area is put into the model, together with the river, dunes and mangrove forest.

### 0.1. INPUT

In this section the XBeach input is described.

#### 0.1.1. PARAMS INPUT FILE

When running an XBeach model, the executable reads the *params.txt* file. This file contains all the information that is needed to run the model. Parameters about the grid, bathymetry, tide, waves, discharge, bed friction, morphology, time and output are described in the *params.txt* file. They are described using a *keyword = value* layout. All keywords have their own line. The input file that is used for this project is shown below. For further explanation of keywords, the *XBeach User Manual* [39] is recommended.

*Params.txt* input file for XBeach runs

```
1  %%% Flow boundary condition parameters %%%%%%%%%%%%%%%%%%%%%%%%%%%%%%%%%%%%%%%%%%%%%%%%%%%%%%%%%%%%%%%%%%%%%%%%%%
2
3  front      = abs_2d
4  back       = abs_2d
5
6  %%% Grid parameters %%%%%%%%%%%%%%%%%%%%%%%%%%%%%%%%%%%%%%%%%%%%%%%%%%%%%%%%%%%%%%%%%%%%%%%%%%
7
8  depfile    = Xbeach_183x214_new.dep
9  posdwn     = -1
10 vardx      = 1
11 thetamin   = 202.5
12 thetamax   = 337.5
13 dtheta     = 15
14 thetanut   = 1
15 gridform   = delft3d
16 xyfile     = Xbeach_183x214.grd
17
18 %%% Model time %%%%%%%%%%%%%%%%%%%%%%%%%%%%%%%%%%%%%%%%%%%%%%%%%%%%%%%%%%%%%%%%%%%%%%%%%%
19
20 tstop      = 16200
21
22 %%% Morphology parameters %%%%%%%%%%%%%%%%%%%%%%%%%%%%%%%%%%%%%%%%%%%%%%%%%%%%%%%%%%%%%%%%%%%%%%%%%%
23
24 morfac     = 10
25 morstart   = 0
26 struct     = 1
27 ne_layer   = bedlayers.dep
28 D50        = 0.00041
29
30 %%% Tide boundary conditions %%%%%%%%%%%%%%%%%%%%%%%%%%%%%%%%%%%%%%%%%%%%%%%%%%%%%%%%%%%%%%%%%%%%%%%%%%
31
32 zs0        = 1.71
33 tideloc    = 1
34 tidelen    = 16
35 zs0file    = tide_new.txt
36
37 %%% Wave boundary condition parameters %%%%%%%%%%%%%%%%%%%%%%%%%%%%%%%%%%%%%%%%%%%%%%%%%%%%%%%%%%%%%%%%%%%%%%%%%%
38
39 instat     = swan
40
41 %%% Wave-spectrum boundary condition parameters %%%%%%%%%%%%%%%%%%%%%%%%%%%%%%%%%%%%%%%%%%%%%%%%%%%%%%%%%%%%%%%%%%%%%%%%%%
42
43 wbcversion = 3
44 nspectrumloc= 5
45 bcfile     = spectra.txt
46 random     = 0
47 rt         = 16200
48 dtbc      = 1
49
```

```
50  %% Discharge parameters %%%%%%%%%%%%%%%%%%%%%%%%%%%%%%%%%%%%%%%%%%%%%%%%%%%%%%%%%%%%%%%%%%%%%%%%%%
51
52  ndischarge   = 1
53  ntdischarge  = 67
54  disch_loc_file = river_loc.txt
55  disch_timeseries_file = rain_100years_72.txt
56
57  %% Friction parameters %%%%%%%%%%%%%%%%%%%%%%%%%%%%%%%%%%%%%%%%%%%%%%%%%%%%%%%%%%%%%%%%%%%%%%%%%%
58
59  bedfriction   = chezy
60  bedfricfile   = bedfriction_chezy.dep
61
62  %% Output variables %%%%%%%%%%%%%%%%%%%%%%%%%%%%%%%%%%%%%%%%%%%%%%%%%%%%%%%%%%%%%%%%%%%%%%%%%%
63
64  outputformat = netcdf
65  tintm        = 10800
66  tintp        = 30
67  tintg        = 120
68  tstart       = 0
69
70  nglobalvar   = 10
71  zb
72  zs
73  u
74  ue
75  v
76  ve
77  Susg
78  Svsg
79  sedero
80  H
81
82  nmeanvar     = 5
83  zs
84  u
85  ue
86  v
87  ve
88
89  npointvar    = 6
90  zs
91  zb
92  u
93  ue
94  v
95  ve
96
97  npoints      = 3
98  92489  20110  %% Waste water
99  92287  20088  %% Hotel
100  92386  20000  %% River
```

### 0.1.2. GRID

The computational grid is an important part of the model. The grid defines the area and the resolution of the simulation. It is created using the program *RGFGRID* (created by Deltares). *RGFGRID* is used to 'create, modify and visualise orthogonal, curvilinear and unstructured grids' [40]. The program uses a M-axis and N-axis, which represent the x-axis and y-axis in XBeach. In XBeach, the x-axis has to be defined as pointing in positive direction towards the coastline. The positive direction of the y-axis is pointing perpendicular to the left of the x-axis. As described above, the dimensions of the XBeach grids have maximum dimensions in the order of kilometers. For this project, a grid of 620 m by 1100 m is created. The number of grid cells is 215 x 179. The grid can be seen in figure 0.1a. Cells do not have the same size. The largest cells are 20 x 20 m (top right corner) and the smallest cells are 2 x 2 m (in the mouth of the river). Most of the cells are 4 x 4 m (the area of the hotel and the lagoon and the nearshore area). A .grid file of the grid is made by *RGFGRID* and can be used as input for XBeach.

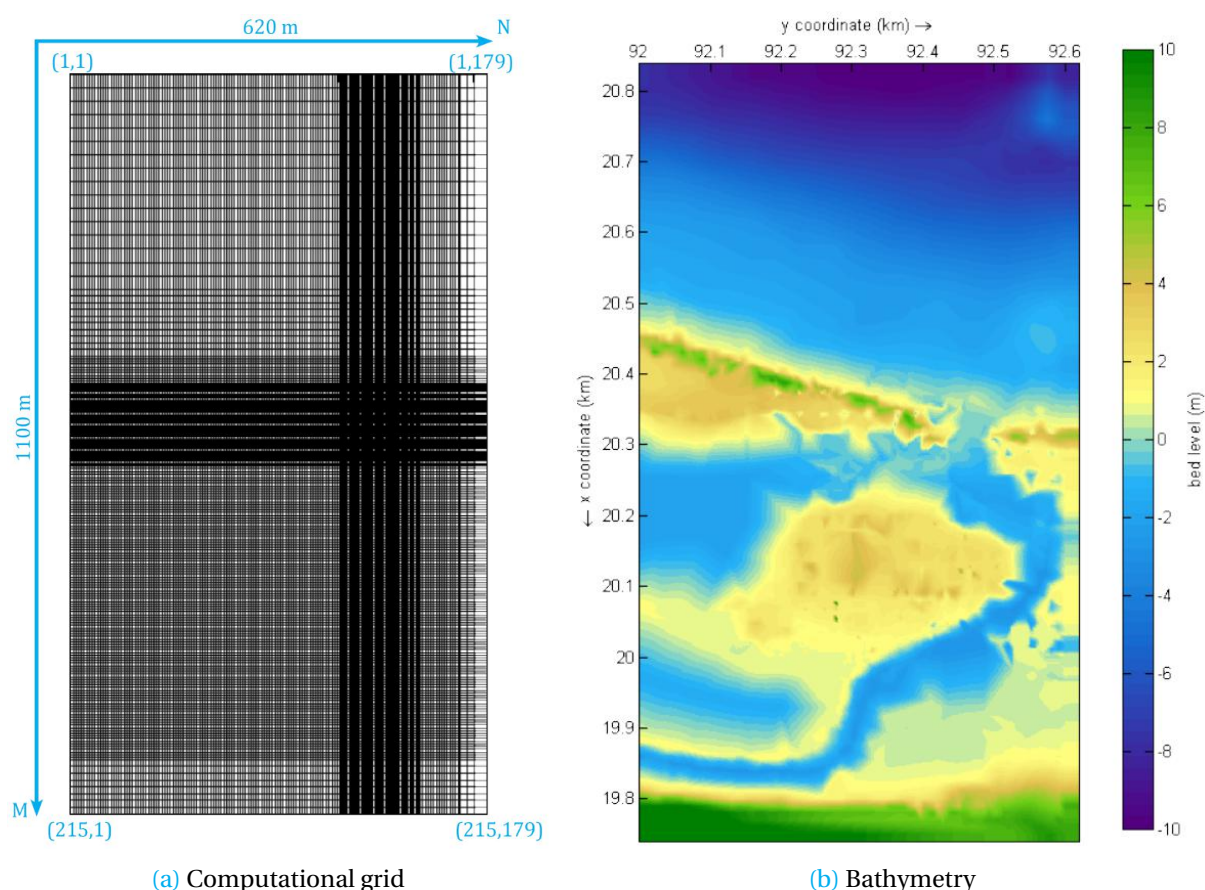


Figure 0.1: Input for XBeach model

### 0.1.3. BATHYMETRY

The bathymetry that is used in the model, is created using the data, measured by Geocuba [41], presented in section 2.4.3. The data is translated from the WGS84 coordinate system to meters. The (0,0) point is located in the lower left corner of the data. The resulting bathymetry can be seen in figure 0.1b. The Blau Arenal Hotel area is located between 92 km and 92.6 km in y-direction and

19.74 km and 20.84 km in x-direction. The deepest point offshore has a depth of approximately -10 m. All the values are with reference to mean sea level. A .dep file is created by the program *QUICKIN* (developed by Deltares). It contains a depth value at each grid point, obtained by triangular interpolation of the data points. The .dep file is the input file for the bathymetry in XBeach.

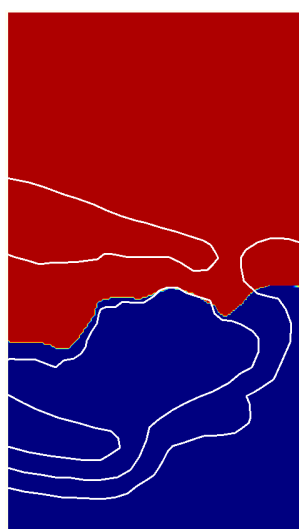
#### O.1.4. BOUNDARIES

The west and east boundaries are defined as Neumann boundaries, which state that there is no change in surface elevation and velocity locally [39]. The north and south boundaries are defined as flow boundaries of the type absorbing-generating (weakly-reflective). This means that waves and flow are able to pass through the boundary.

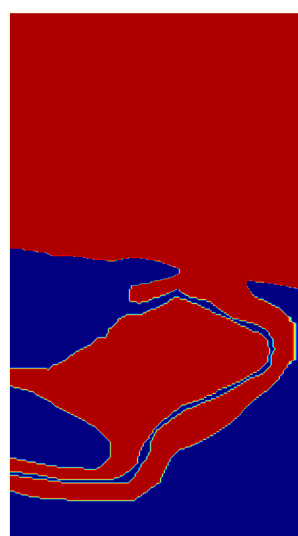
#### O.1.5. MORPHOLOGY

According to *Dr. Ing. Luis Fermín Córdova López* from *CUJAE*, the Itabo River has hardly any sediment. Therefore, only the coastal region and the area close to the inlet of the river are morphologically active. The rest of the region is assumed to have no sedimentation or erosion. In XBeach, this can be modelled by creating another .dep file, which contains the value of the thickness of the erodible layer for all grid points. The thickness of this layer in the erodible parts of the model is set to 2 meters, because the river is not assumed to be eroded any deeper. Figure O.2a shows the two areas.

A morphological factor (*morfac*) is used to speed up the morphological time scale relative to the hydrodynamic one. In this model, a *morfac* of 10 is used. This means that when 6 minutes of hydrodynamic time is simulated, one hour of morphological evolution is simulated effectively.



(a) Sediment layers: red indicates an erodible bed, blue is a fixed layer.



(b) Mangroves: blue areas contain mangroves

Figure O.2: Input for XBeach model, figures created with *QUICKIN*

### O.1.6. MANGROVES

XBeach has a parameter that is used to include vegetation in the model. A separate .dep file has to be created with *QUICKIN*, containing the information on the vegetation in all the grid points. Unfortunately, when using the vegetation mode and the river discharge input, the model gives a lot of errors that were not solvable. Therefore, it is chosen to use a spatially varying bed friction to represent the mangroves in the model. A value for the Chézy friction coefficient is used, because the Manning friction coefficient is not available in the current version of XBeach. Manning values are 0.02 for sand and 0.1 for mangrove forest [42]. When translating this values to Chézy values, a water depth has to be known. For the normal river bed, the water depth is assumed to be 2 m. For the mangroves, the water depth is assumed to be 0.5 m. The resulting Chézy values are:  $15 \text{ m}^{1/2}/\text{s}$  for the mangrove forest and  $55 \text{ m}^{1/2}/\text{s}$  for the river bed. The value for the river bed is a high value, due to the layer of organic material present at the bottom of the river.

### O.1.7. TIDE, SEA LEVEL RISE AND SURGE

The tide that is used in the model is derived in section 2.3.2. A tidal range of 0.5 m is used. Because of the use of a morphological factor, the tidal signal also has to be speeded up. Therefore, one tidal cycle takes 4,470 s instead of 44,700 s. The tide is put in the model at the offshore boundary, using separate file with time series of the water level.

The sea level rise is estimated to be 25 cm in 50 years in section 2.3.6. To be conservative, a value of 25 cm is used in the model. During normal sea conditions, no storm surge is put in the model. For severe- or extreme conditions, the storm surge level is derived in section 2.3.5. The value of the storm surge that is put in the model is 1.56 m. Therefore, the total water level elevation will be 1.71 m (combination of sea level rise and surge).

### O.1.8. WAVE CONDITIONS

The output of the SWAN model, described in appendix N is used as wave input for XBeach. The output is transformed to .sp2 files, which can be put in XBeach. The input in XBeach consists of wave spectra, defined at five locations. Three of them are located at the offshore boundary (one in the middle and two at the corners). The other two are located at the eastern- and western boundary. The spectra.txt file lists all the .sp2 files and their locations.

### O.1.9. RIVER DISCHARGE

In order to include the river in the model, a discharge point can be added. This point is added at the left boundary, where the river enters the domain (between x-coordinates 19.850 and 19.865). The hydrographs shown in section 2.11 are the time series that are put in the model. These time series have a length of 33 hours. Because of the morphological factor, the hydrograph will take 3 hours and 18 minutes in the model.

### O.1.10. SIMULATION TIME

The computational time is directly coupled to the simulation time. Therefore, the simulation time should be chosen carefully. A first important aspect to include, is the duration of discharging a peak rain event. The hydrographs contain a period of 33 hours, so the simulation time should be at least 33 hours to include this whole discharge. Furthermore, also the emptying of the system is desirable to compute. After some tests, this resulted in a simulation time of 45 hours. For sea storm conditions this is quite long. However, due to the shoal in front of the coast at Playas del Este (see appendix N), which ensures no waves larger than 3.5 m to occur at the beach, hurricane conditions can hold on for a long time. Not only the actual peak period of the storm is used in the model, but also the period before this peak of the storm and the period afterwards. All together this makes a simulation time of 45 hours reasonable.

Due to the morphological factor of ten, all the time durations are reduced to a factor ten smaller. Therefore, the simulation time of one run is 4.5 hours and the period of rainfall takes 3.3 hours.

## O.2. OUTPUT

The output that XBeach creates is a NetCDF file. This file contains all the data that is requested as output in the params.txt file. For this project the water- and bed levels are requested. Besides that, the velocities (both Eulerian and Lagrangian), sedimentation and erosion values and the significant wave height are in the .nc output file. Output can be visualised by using top view images with a colour bar at a certain point in time or by using a time versus value at a certain location (see figure O.3a). For this project, three locations are defined: the waste water treatment plant, the Blau Arenal Hotel and a point in the river. Besides that, cross-sections of the nearshore area and the dunes are made, to be able to see the changes of the coast (see figure O.3b).

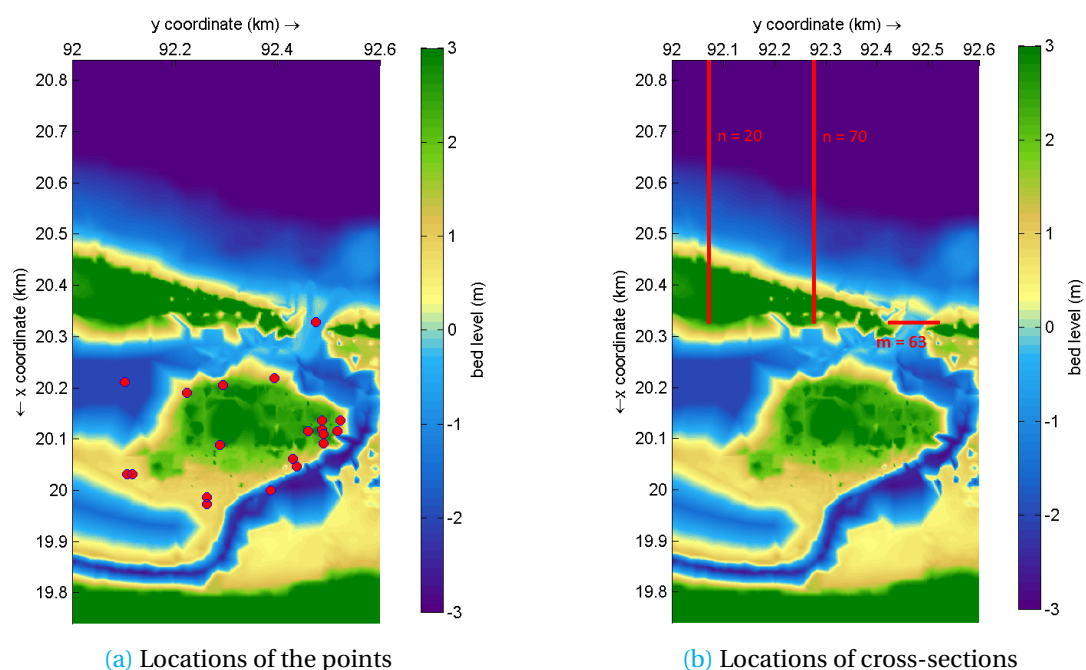


Figure O.3: Locations of output generation



# P

## BRAINSTORM SOLUTIONS

### P.1. FLOODING CAUSED BY WAVES

#### P.1.1. SHORE NOURISHMENT

Nourish the shore regularly with sand, so the shore nourishment will create a stable dune and beach profile that can protect the hinterland against waves. The shape of the dunes can be restored by filling the gaps and smoothing the seaside to get rid of the scarps. In this way, the natural function of the dune and beach profile to protect the shore against waves will be re-established. This could work well, however, the river mouth will always be an open connection with the hinterland, through which the waves can reach the mangrove forest and the Blau Arenal Hotel. A disadvantage for the Cuban government is that their own contractors do not have the dredging equipment for realising nourishments, so the external expertise of international contractors is needed. A schematisation of the shore nourishment is shown in figure [P.1a](#).

#### P.1.2. SUBMERGED BREAKWATER

Build a submerged breakwater to break the waves further offshore (see figure [P.1b](#)). The wave height at the coast line will be less, which reduces the impact. A submerged breakwater is preferred over an emerged one, because of the aesthetic value of the beach for tourists.

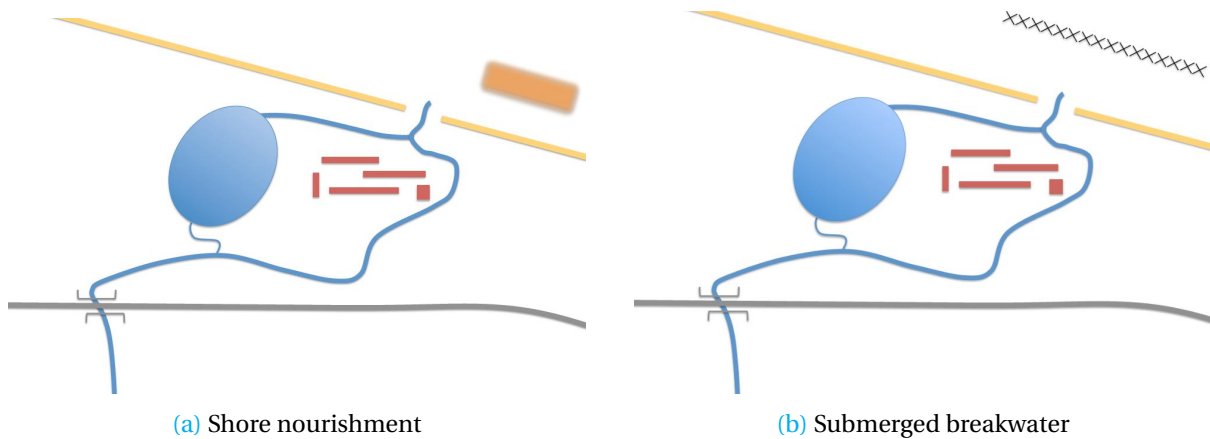


Figure P.1: Solutions for flooding caused by waves

## P.2. FLOODING CAUSED BY HIGH RIVER DISCHARGE

### P.2.1. UPSTREAM DAM

Build a dam upstream to create extra storage of water in case of a high river discharge due to heavy rainfall. This is visualised in figure P.2a. This storage can be used by the local residents living close to the dam. Furthermore, electricity could be generated via the dam, which could be beneficial for the local residents. The realisation of a dam is an expensive investment. Additionally, people living in the area where the dam will be built, need to give up their houses and move to another place.

### P.2.2. RETENTION BASIN

Use retention basins upstream (see figure P.2b), west (see figure P.3a) or east (see figure P.3b) to lower the river discharge that goes downstream to the area of the Blau Arenal Hotel. In this way, the retention basins can function as designated flooding areas that will create storage in case of heavy rainfall. This solution needs a large area situated below the level of the Itabo River. Possibly, excavation is needed. Besides, the local residents living in the designated areas would not be pleased when they are forced to move.

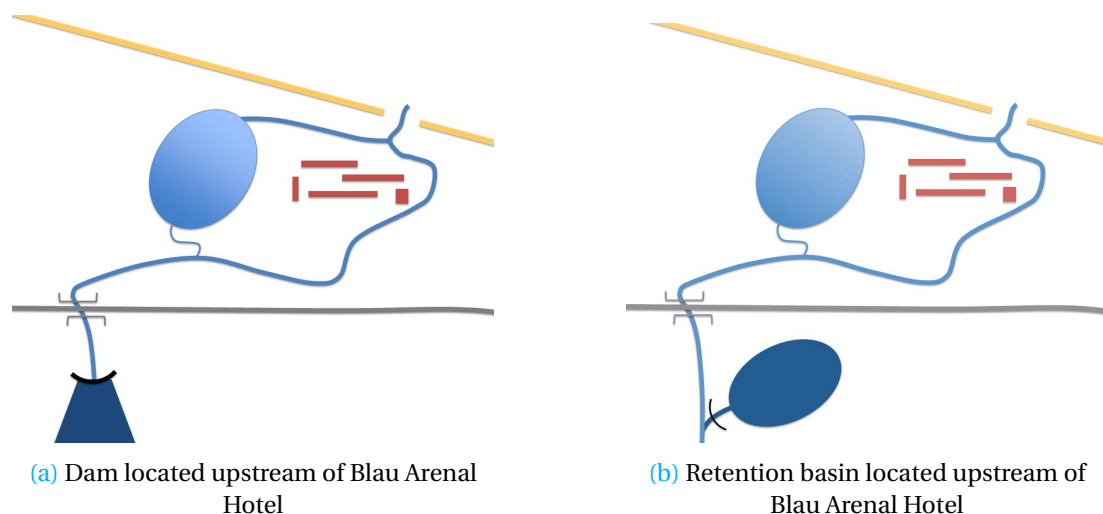


Figure P.2: Solutions for flooding caused by river discharge

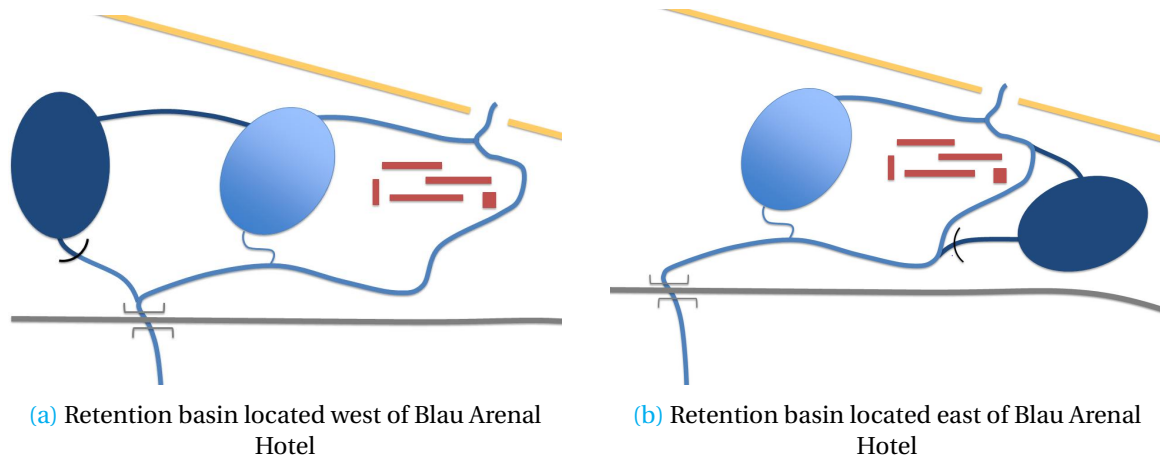


Figure P3: Solutions for flooding caused by river discharge

### P.2.3. EXTRA OUTFLOW POINT

Create an extra outflow point, like a culvert or pipeline, which will only be used in case of high river discharge. With normal weather conditions it will be closed, but when the river discharge is expected to increase significantly it should be opened. The extra outflow point will reduce the river discharge in the main branch. The outflow point can be located west of the Blau Arenal Hotel or north of the lagoon (see figure P4a and P4b).

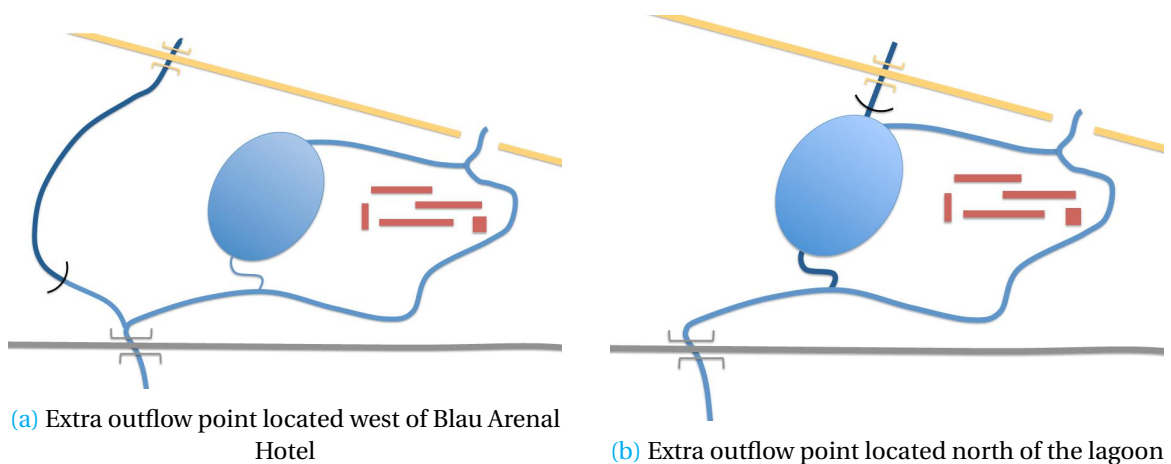


Figure P4: Solutions for flooding caused by river discharge

### P.2.4. WIDENING AND CHANNELLING THE RIVER MOUTH

By widening the end of the river and channelling the river mouth, the shape of the river mouth remains open at a fixed location and the river is able to discharge the amount of water without problems into the sea. This is schematised in figure P5.

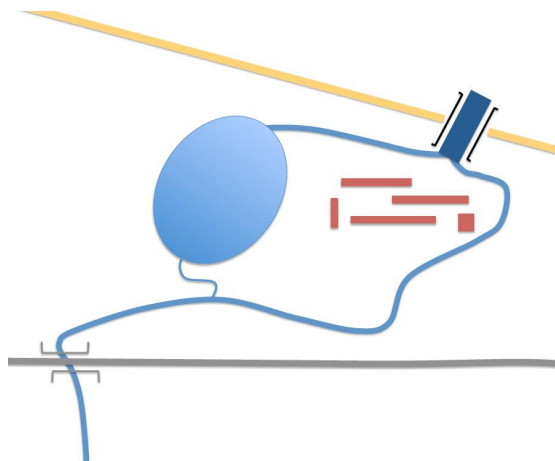


Figure P5: Widening and channelling of the river mouth

### P.3. FLOODING CAUSED BY BOTH WAVES AND RIVER DISCHARGE

#### P.3.1. STRUCTURE AROUND THE WASTE WATER TREATMENT PLANT

The waste water treatment plant can be protected against flooding by building a dike- or wall structure around it. In this way, the focus of the protection is on the prevention of contamination of the mangrove forest by the waste water and thus satisfying CITMA. The structure will need some space, so the tourists will see less of the waste water treatment plant. This is an extra advantage. Several variations can be chosen (see figure P6a, P6b and P6c), so the solution which can be integrated most in the area should be realised.

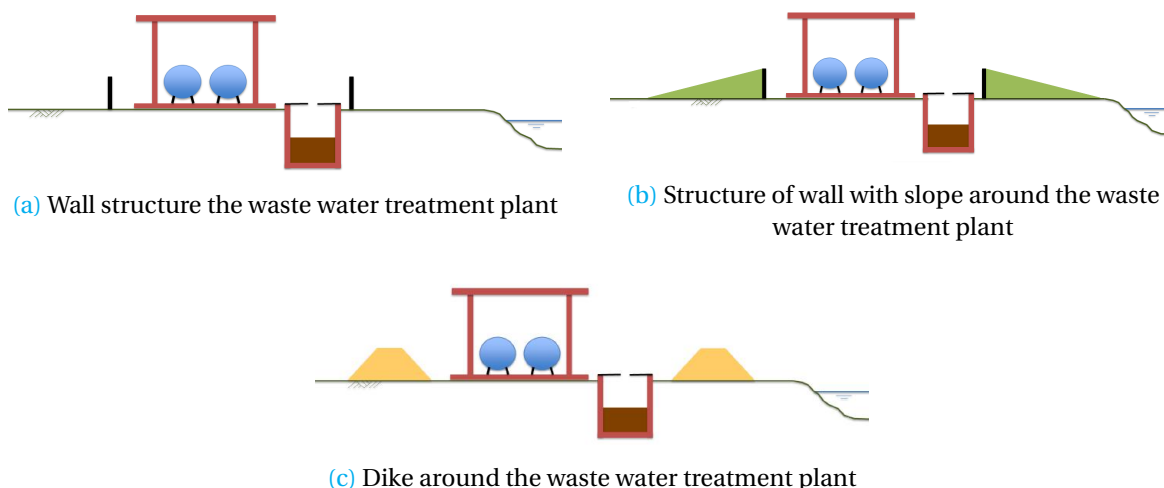


Figure P6: Solutions for flooding caused by both waves and river discharge

#### P.3.2. STRUCTURE AROUND THE BLAU ARENAL HOTEL

The Blau Arenal Hotel can also be protected against flooding by building a dike- or wall structure around it. With this solution, the entire area is protected against flooding, because the protection of both the tourists and the mangrove forest is taken into account. As can be seen in figure P7a, P7b and P7c, variations of this solution are possible.

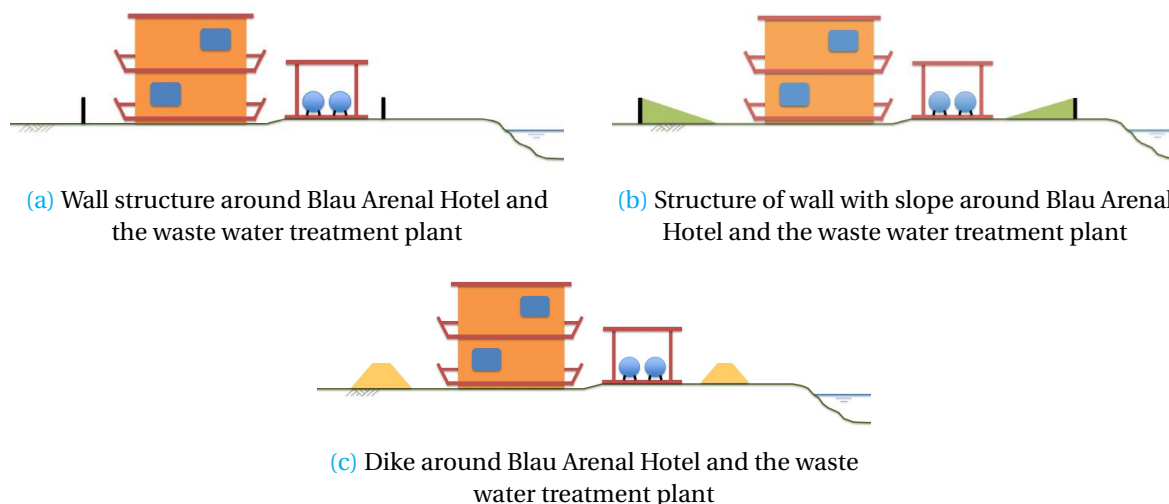


Figure P.7: Solutions for flooding caused by both waves and river discharge

### P.3.3. EXTENSION OF THE MANGROVE FOREST

Extend the mangrove forest by creating designated flooding areas close to the Blau Arenal Hotel. In this way, the excavated areas can be used to create an environment with favourable circumstances for new mangrove forest to develop in the future. This is a Building with Nature solution, where CITMA would be very interested in. The disadvantage of relocation of the local residents, where the flooding areas will come, should be taken into account.

### P.3.4. RELOCATION OF THE WASTE WATER TREATMENT PLANT

Relocating of the waste water treatment plant at a location safe from flooding, so the mangrove forest will not be contaminated in case of flooding due to waves or high river discharge. This option does not take into account the safety of the tourists in the Blau Arenal Hotel, but CITMA, with the power to close the hotel, is satisfied because of the protection of the unique ecosystem.

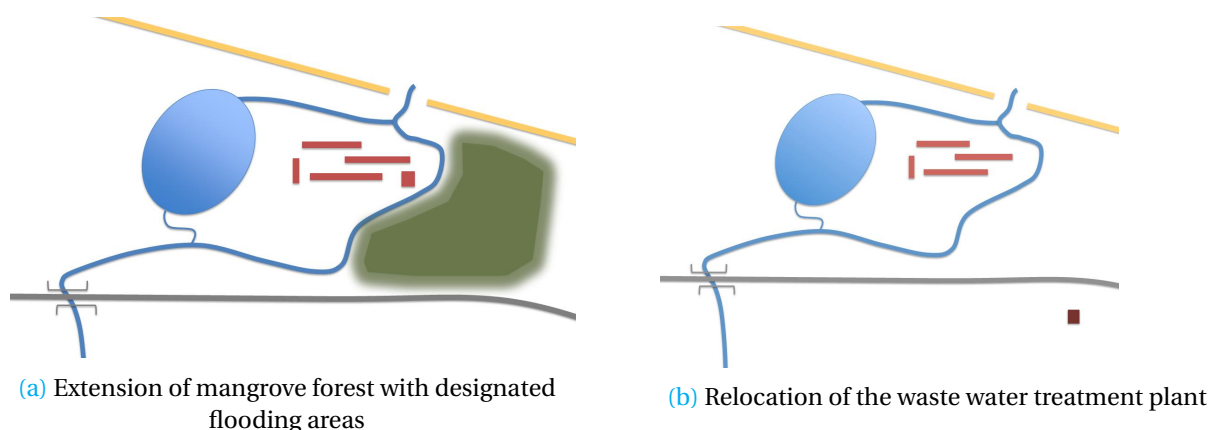


Figure P.8: Solutions for flooding caused by both waves and river discharge



# Q

## WALL STRUCTURE DESIGN

One of the solutions from the brainstorm is to create a wall or wall with slope structure around the Blau Arenal Hotel and the waste water treatment plant or around the waste water treatment plant solely. To design the first three wall structures, concrete and reinforcement steel will be used. The fourth option is the steel sheetpile wall. The main dimension that will function as a boundary condition is the height of the wall. To get an estimation of this value, an event with a return period of 225 years is chosen. For this situation the flood level is at 0.90 m above the ground (see figure Q.1, combined with a flooding value at the waste water treatment plant of 49 cm from table 3.1). For model uncertainties, possible wave interaction and safety, an extra 50 cm is added to this level. Therefore, the height of the wall needs to be 1.40 meter above the ground for a wall only around the waste water treatment plant (see figure Q.1).

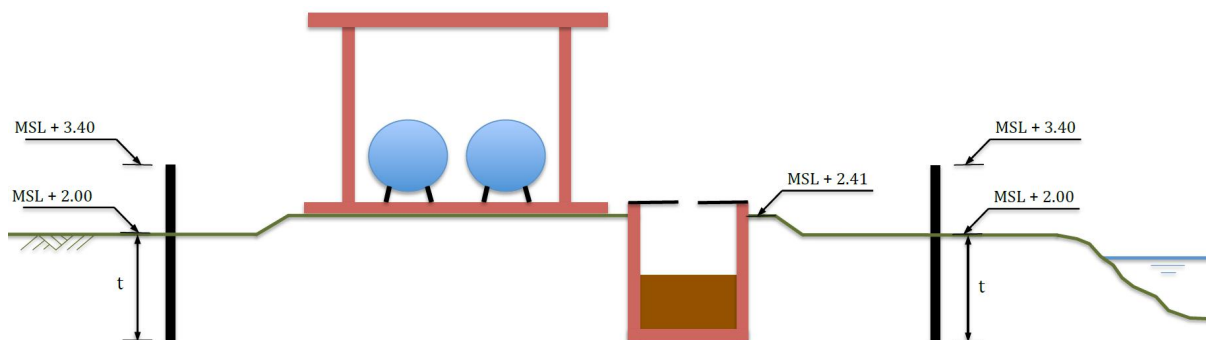


Figure Q.1: Schematisation of the cross-section of the wall structure

### Q.1. GRAVITY WALL

First, a design is made of a wall on top of the soil without embedment (see figure Q.2 for the schematisation). This solution is called the gravity wall, because the wall will have to withstand the hydrostatic pressure of the water with its own mass. The hydrostatic pressure is assumed to be the only force of the water, because the mangrove forest, which surrounds the whole area, will diminish the wave energy and only small negligible waves will hit the wall.



Figure Q.2: Schematisation of the cross-section of the gravity wall

The dimensions of the wall are checked for horizontal, rotational and vertical stability. For the density of the water, a value of  $\rho = 1,025 \text{ kg/m}^3$  of seawater has been used. The reason for this is that the area is close to the sea and there is a change of salt water intrusion. Therefore, the conservative value of unmixed seawater is chosen as the density of the water. According to a research of *USACE*, the value of the friction coefficient between concrete and the soil is 0.45 for clayey sand [43]. The parameter  $\alpha$  is 0.5, as the turning point will be in the middle of the wall structure. In table Q.1 the input of the variables, parameters and calculated dimensions of the gravity wall are given. By iteration of the equations below, the final value for the width of the wall of  $b = 1.0 \text{ m}$  is obtained.

Table Q.1: Different parameters, variables and calculated dimensions needed for the gravity wall

Parameter	Value
Height $x$ [m]	1.40
Width $b$ [m]	1.0
$g$ [ $\text{m/s}^2$ ]	9.81
$\rho_w$ [ $\text{kg/m}^3$ ]	1025
$\rho_b$ [ $\text{kg/m}^3$ ]	2400
$f$ [-]	0.45
$\alpha$ [-]	0.5
$\Sigma H$ [kN/m]	9.85
$\Sigma V$ [kN/m]	32.96
$\Sigma V \cdot f$ [kN/m]	14.83
$\Sigma M$ [kNm/m]	4.60

To check for horizontal stability equation Q.1 is used.

$$UC = \frac{\Sigma H}{\Sigma V \cdot f} < 1.0 \quad (\text{Q.1})$$

Where:  $\Sigma H$  = Summation of all the horizontally loaded forces [kN/m]  
 $\Sigma V$  = Summation of all the vertically loaded forces [kN/m]  
 $f$  = Friction coefficient between concrete and the soil [-]

$$UC = \frac{9.85}{14.83} = 0.66 < 1.0$$

So the wall is horizontally stable with these dimensions. The rotational stability is determined with equation Q.2.

$$UC = \frac{\Sigma M / \Sigma V}{1/6 \cdot b} < 1.0 \quad (Q.2)$$

Where:  $\Sigma M$  = Summation of the moments around the turning point [kNm/m]  
 $1/6 \cdot b$  = Half of the width of the core of the structure [m]

$$UC = \frac{4.60/32.96}{1/6 \cdot 1.0} = 0.837 < 1.0$$

Also the rotational stability is met. Finally, the vertical stability is checked. Equation Q.3 is used.

$$\frac{\Sigma V}{b} - \frac{\Sigma M}{1/6 \cdot b^2} = \min \sigma > 0.0 \quad (Q.3)$$

Where:  $\min \sigma$  = Minimal stress at one of the edges of the structure [kN/m<sup>2</sup>]  
 $1/6 \cdot b$  = Half of the width of the core of the structure [m]

$$\frac{32.96}{1.0} - \frac{4.60}{0.167} = 5.37 > 0.0$$

This last equation shows that no tensile forces occur at the bottom of the structure, making it possible to withstand the force of the water with these dimensions. However, it has to be taken into account that the soil is fully saturated. This could mean that water will flow through the soil underneath the wall. This seepage can cause flooding of the area behind.

## Q.2. EMBEDDED WALL

The second option is the embedded wall. In this design the seepage will not be a problem anymore, because the wall is partially embedded in the ground. To calculate the dimensions, like depth, thickness, reinforcement ratio and location, Blum's assumption for horizontal soil pressure is used. Blum assumed that the local displacement of embedded walls would result in immediate yielding of the soil at both the active and passive side, instead of a gradual development of shear stresses in the soil [44]. For convenience the symbols presented in figure Q.3 are used throughout all calculations. The same height ( $x$ ), from table Q.1, is used since the same flood has to be retained.

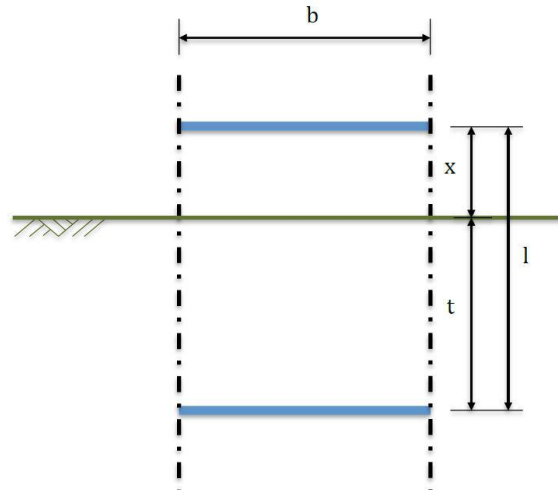


Figure Q.3: Front view wall with indications

The governing load situation for the embedded wall is when the water level is maximum at the outside. The soil is assumed to be fully saturated, because of the heavy rain during high discharge. The schematisation and symbols of the soil and wall can be seen in figure Q.4.

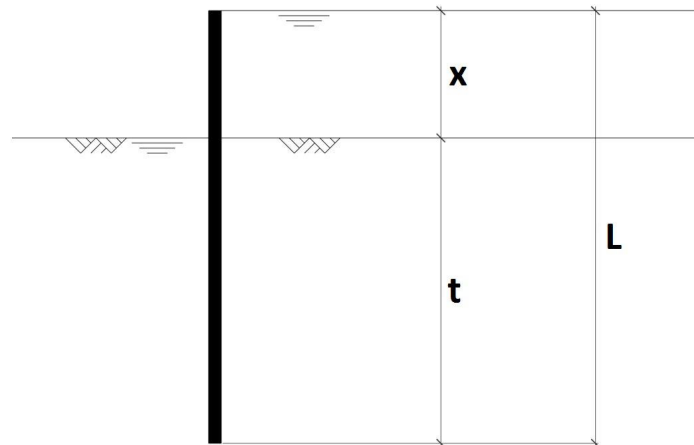


Figure Q.4: Overview soil embedded wall

First, the vertical and horizontal soil stresses on both sides are calculated as a function of the depth ( $t$ ) of the soil. The following soil parameters are shown in table Q.2 and have been taken from *Eurocode 7 NEN-EN1997-1* [45].

Table Q.2: Soil parameters [45]

Parameter	Value
$\Phi$ [°]	30
$K_a$ [-]	0.33
$K_p$ [-]	3
$\gamma_{\text{sat}}$ [kN/m <sup>3</sup> ]	18

The vertical water- and total stress diagram can be seen in figure Q.5a. The horizontal stress of water is equal to the vertical water stress. The horizontal soil pressure is equal to the vertical effective stress times the active or passive coefficient. The horizontal water- and soil stress can be seen in figure Q.5b.

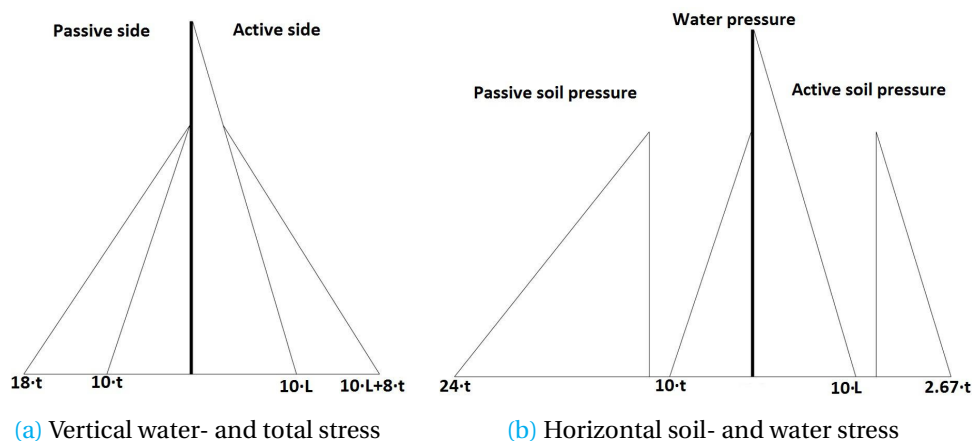


Figure Q.5: Horizontal and vertical soil pressures embedded wall

The wall will only have to be calculated for saturated soil as major forcing only takes place when flooding occurs. The slope at the With these parameters the depth of the wall  $t$  can be determined with an iterative process. At a certain depth the moments around this specific depth of the horizontal forces will add up to zero. With this known depth, the shear and moment stress can be calculated over the length of the wall. The maximum values of these curves of the shear and moment are given in table Q.3.

Table Q.3: Depth of the wall, maximum shear and moment value acting on the wall

Parameter	Value
Depth of the wall $t$ [m]	3.1
Total height wall $l$ [m]	4.5
$V_{ed}$ [kN/m]	49.4
$M_{ed}$ [kNm/m]	126.7

The total length of the wall will add up to 3.0 meters. To make sure the wall can withstand the moment, reinforcement is needed. This is calculated using the parameters of the cross-section of the wall (see table Q.4). The schematisation of the cross-section is shown in figure Q.6. Concrete strength class C20/25 will be used to construct all the concrete parts of the wall. Although the fact that the wall is constructed close to the sea, the wall structure is not constantly in contact with salt water. Therefore, the cover of the wall is chosen to be in the XS1 class, according to the exposure class from the *Hydraulic Structures Manual* [44]. Because the structure is a wall, the cover needed is 30 mm. Including a finished surface, an extra 5 mm will be added.

Table Q.4: Parameters for dimensions of the embedded wall

Parameter	Value	Parameter	Value
$f_{cd}$ [N/mm <sup>2</sup> ]	16.67	$D_{\text{rebar}}$ [mm]	22
$f_{yd}$ [N/mm <sup>2</sup> ]	435	$N_{\text{rebar}}$ [-]	10
$\gamma_c$ [-]	1.5	$D_{\text{stirrups}}$ [mm]	8
$\gamma_s$ [-]	1.15	$s$ [mm]	450
$\beta$ [-]	0.39	$\theta$ [°]	21.8
Width $h$ [mm]	350	$C_{rdc}$ [-]	0.12
$b$ [mm]	1000	$k_1$ [-]	0.15
$c$ [mm]	35		

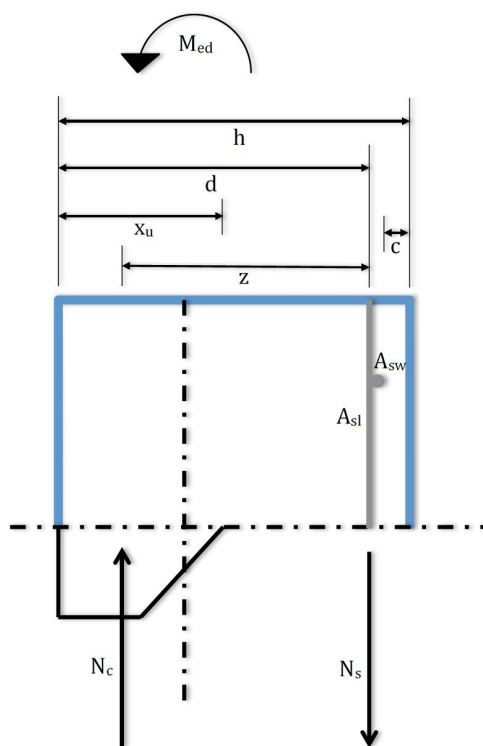


Figure Q.6: Schematisation of the cross-section of the embedded wall

These parameters make it possible to calculate the strength capabilities of the wall. Initially, certain imported values have to be calculated before performing the checks. These are listed in table Q.5.

Table Q.5: Calculated values following from the table Q.4

Parameter	Value
$d$ [mm]	296
$z$ [mm]	244.5
$X_u$ [mm]	132.2
$A_{sl}$ [mm <sup>2</sup> ]	3799
$\rho_l$ [%]	1.28
$A_{sw}$ [mm <sup>2</sup> ]	50.24

Then, the checks can be done to see if the wall can cope with the forces acting on the structure. For the moment, the equation Q.4 is needed.

$$UC = \frac{M_{ed}}{A_{sl} \cdot z \cdot f_{yd} / 10^6} = \frac{M_{ed}}{M_{rd}} < 1.0 \quad (\text{Q.4})$$

Where:  $A_{sl}$  = Surface area of the longitudinal reinforcement bars in the cross-section [mm<sup>2</sup>]  
 $z$  = Distance between the reinforcement and the centre of the concrete push section [mm]  
 $f_{yd}$  = Design strength of the steel [N/mm<sup>2</sup>]  
 $M_{ed}$  = Moment acting on the structure [kNm]  
 $M_{rd}$  = Possible moment that can be resisted by the structure [kNm]

If the values are inserted in the equation, the following answer is the result:

$$\frac{126.7}{403.83} = 0.31 < 1.0$$

With these dimensions and reinforcement, the wall structure can resist the maximum moment. The same calculation is executed for the shear force. The following calculation is used:

$$UC = \frac{V_{ed}}{C_{rdc} \cdot k \cdot (100 \cdot \rho_l \cdot f_{ck})^{1/3} \cdot b \cdot d} = \frac{V_{ed}}{V_{rd}} < 1.0 \quad (\text{Q.5})$$

Where:  $C_{rdc}, k$  = Coefficients [-]  
 $\rho_l$  = Reinforcement ratio for longitudinal reinforcement [-]  
 $f_{ck}$  = Characteristic compressive cylinder strength of concrete [N/mm<sup>2</sup>]  
 $b$  = Width of the cross-section [mm]  
 $d$  = Distance between the longitudinal reinforcement and the farthest edge of the cross-section [mm]  
 $V_{ed}$  = Shear force acting on the structure [N]  
 $V_{rd}$  = Possible shear force that can be resisted by the structure [N]

The result of this equation is:

$$\frac{49.4}{259.1} = 0.19 < 1.0$$

Again the requirement is fulfilled. Both checks result in a positive outcome. In figures Q.7a en Q.7b, the final dimensions of the embedded wall structure are shown.

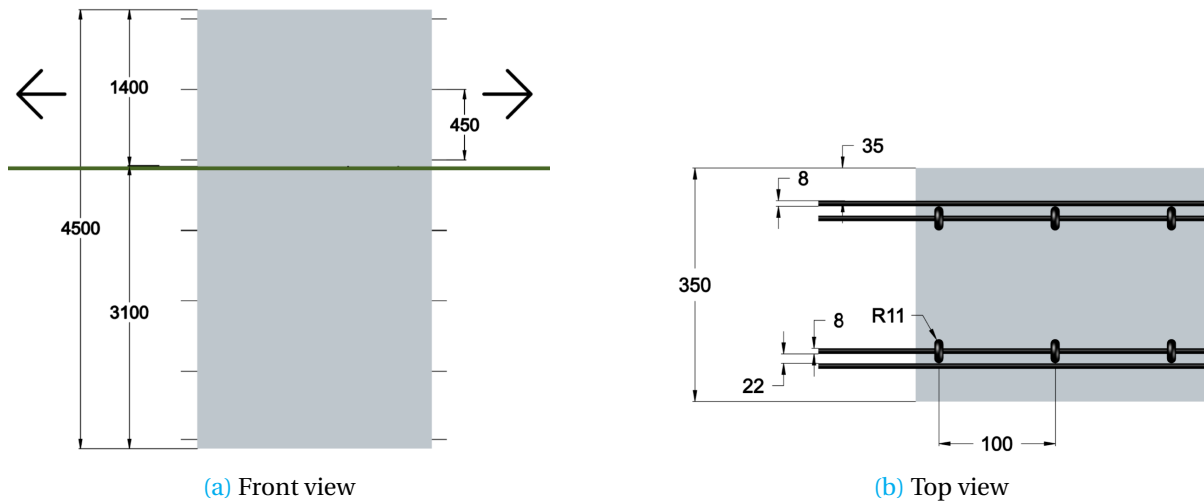


Figure Q.7: Different views of the wall. All values are in mm

Some final checks are executed to ensure that the dimensions are in the correct order of magnitude. For C20/25 concrete, the reinforcement ratio has to be between 0.15% and 1.38%. This is just met with 1.28%, which is present in the wall. Furthermore, stirrups are placed in the wall although it was calculated that they were not needed. They will function as guidance for the longitudinal reinforcement and make it easier to place the entire reinforcement cage. The stirrups will keep the reinforcement bars together before the concrete is poured. Because the stirrups are not needed for structural purposes but only during construction, they are placed at every 450 mm. In figure Q.8 a three dimensional overview of the wall is visualised.

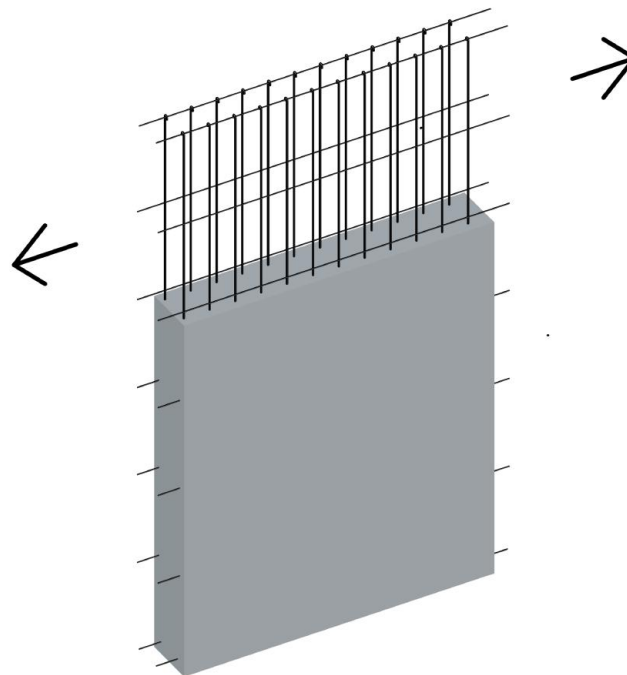


Figure Q.8: 3D overview of a cross-section of the wall. Top part of the wall is shown without concrete

### Q.3. WALL WITH SLOPE

For a more aesthetic view, the wall can also be built with a slope on the inside. This slope can be covered with vegetation. Because of the slope, the wall has other dimensions to cope with the extra soil pressure. The governing load situation is no water at the outside and fully saturated soil at the inside slope. The schematisation of the soil and wall can be seen in figure Q.9. Figure Q.9a shows the slope at the inside, in the calculations the schematisation of figure Q.9b will be used. This will simplify the calculations, the simplification is allowed since it is more conservative, the soil stresses are higher than in reality.

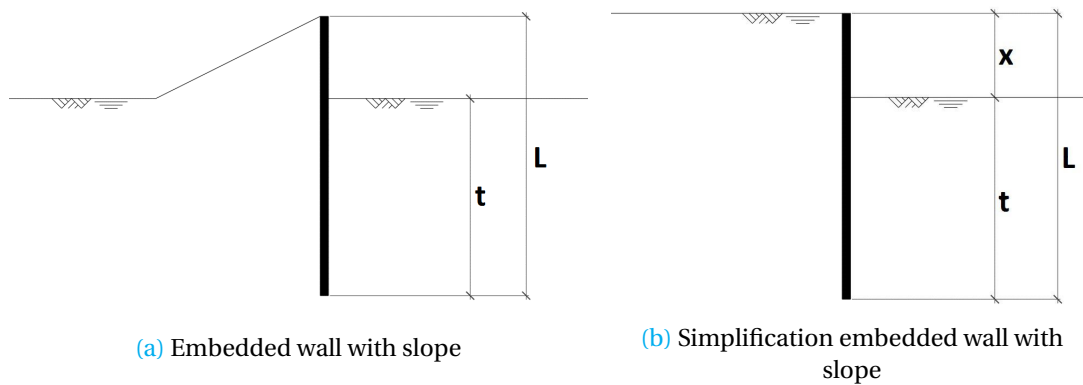


Figure Q.9: Soil schematisation

The vertical water- and total stress diagram can be seen in figure Q.10a. The horizontal stress of water is equal to the vertical water stress. The horizontal soil pressure is equal to the vertical effective stress times the active or passive coefficient. The horizontal water- and soil stress can be seen in figure Q.10b.

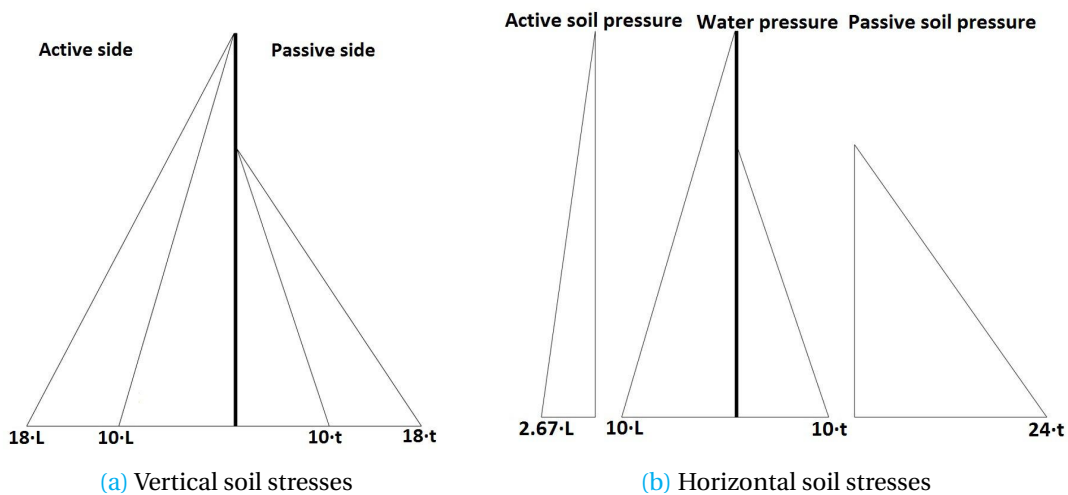


Figure Q.10: Soil stresses

The structure of the wall with slope has been calculated by iteration. The resulting moment around the tip of the structure should be zero. The technical characteristics of this variant are listed in table Q.6.

Table Q.6: Characteristics wall with slope

Parameter	Value
Depth of the wall $t$ [m]	3.6
Total height wall $L$ [m]	5.0
Width of the wall $b$ [mm]	350

The depth of the wall increases from 3.1 m to 3.6 m, so the wall needs to go further into the ground. With this adapted value and all other parameters the unaltered, both unity checks still come out positive.

#### Q.4. SHEETPILE WALL

The sheetpile wall has other material properties than the concrete walls described above. Because of the low aesthetic value of a steel wall, a slope is added on the inside to decrease the view on the structure. In this way, the sheetpile wall will have the same height calculation as that of the concrete wall with slope. The sheetpile wall is made of steel S235 and the type of sheetpile is HOESCH 2305 (finger-and-socket interlock). The characteristics of this sheetpile type are given in table Q.7 and shown in figure Q.11 [44].

Table Q.7: Characteristics of sheetpile profile, type HOESCH 2305 BRON HSM

	Section modulus $W_y$ [cm <sup>3</sup> /m]	Weight [kg/m <sup>2</sup> ]	Second moment of inertia $I_y$ [cm <sup>4</sup> /m]	Section width $b$ [mm]	Wall height $h$ [mm]	Back thickness $t$ [mm]	Web thickness $s$ [mm]
HOESCH 2305	2,320	142.3	40,600	575	350	11.5	8.4

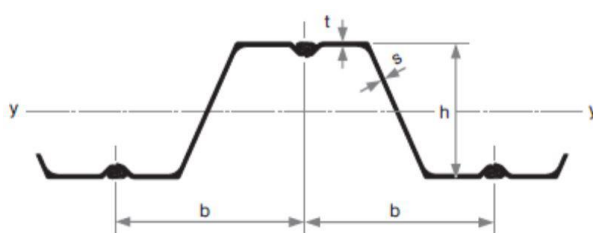


Figure Q.11: Schematisation of the sheetpile profile, type HOESCH 2305 [44]

The dimensions of the sheetpile wall are listed in table Q.8. The depth and the total height of the sheetpile wall are 3.6 m and 5.0 m, like the concrete wall with slope. The width of these walls differs significantly, 11.5 mm and 350 mm respectively.

Table Q.8: Characteristics sheetpile wall

Parameter	Value
Depth of the wall $t$ [m]	3.6
Total height wall $L$ [m]	5.0
Width of the wall $b$ [mm]	11.5

# R

## FLOOD RETENTION

### R.1. GENERAL PRINCIPLE

The flood retention principle is explained in figure R.1 and R.2. Controlled flooding of the flood retention basin should start at the right time. This time depends on on the available storage capacity. A bigger area can store more water and hence can start earlier with water storage. At the pre-flooding stage (see figure R.1 and R.2), all the water is discharged through the main river, as can be seen in figure R.2. At a certain water depth, controlled flooding of the retention basin starts. The discharge in the main branch will not follow the original hydrograph curve. A certain portion ( $\alpha$ ) will go through the main channel and the other part ( $1 - \alpha$ ) will go to the flood retention area. The development of the discharge in the main branch, downstream of the area, will depend on the amount of discharge upstream of the area and the discharge to the flood retention area. After a certain time, the discharge and water depth, upstream of the area, is decreased in such a way that all the discharge will go through the main channel again, the past-flooding stage of figure R.1 and R.2. The total storage of water in the flood retention area is equal to the area between the original and reduced hydrograph. This is the area between the orange and blue line from figure R.1.

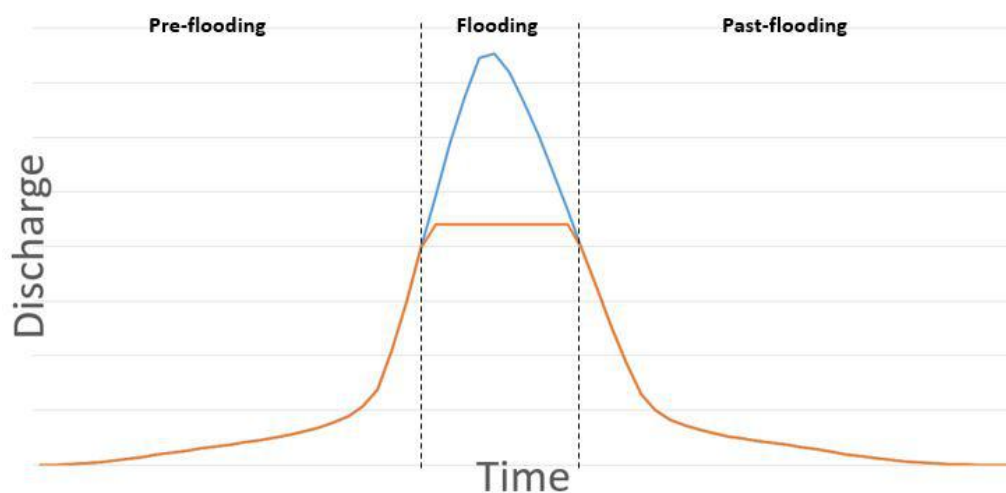


Figure R.1: Flood retention principle: hydrograph

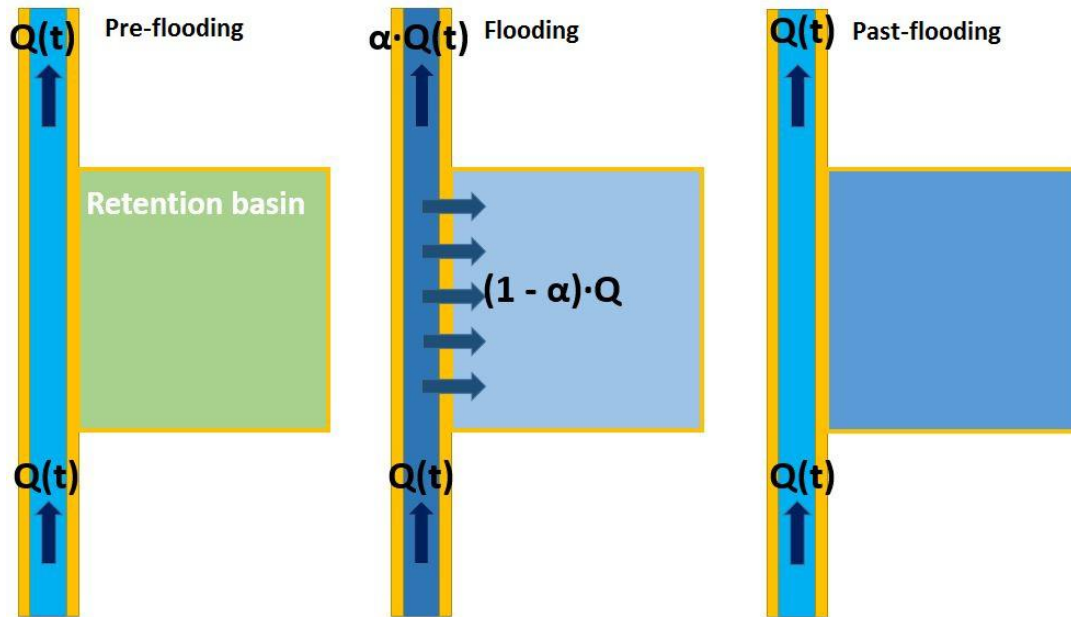


Figure R.2: Flood retention principle: river

## R.2. ASSUMPTIONS AND LIMITATIONS DESIGN

A lot of data is needed in order to design the flood retention basin. Unfortunately, much information is missing. Therefore, the design will be made, based on the available data. The reader should take in mind that further research is needed in order to make a more detailed design and a more reliable feasibility study. The following assumptions are made:

- The soil can easily be excavated. This means that in the upper layer of the surface no rocks are present. Deep excavations will lead to high costs. As a first design starting point an excavation depth of three meter is assumed to be feasible.
- The phreatic surface level is assumed to be low enough that excavating will lead to a dry surface. When the phreatic surface is high, excavation might lead to the creation of a pond, which reduces the effective storage capacity. The bottom of the flood retention area is still 7 to 8 meter above Mean Sea Level [2], which might imply that this is not a big issue. The location of the flood retention area is described in section 4.3.2.
- The hydrographs, calculated for the river mouth (see section 2.6), is assumed to be equal to the hydrograph at the start of water extraction. A small error is made because the part of the catchment area downstream of the flood retention basin does not contribute to the runoff upstream of this area. The discharge of the correct hydrograph is therefore a little lower.
- No flooding at other parts of the river is assumed. It is not unlikely that the river floods at other locations upstream in case of extreme river discharge. However, this assumption is conservative, since flooding upstream reduces the river discharge downstream.
- The discharge and water depth relationship is not known. This information is vital in order to design the flood retention basin. It is strongly recommended to investigate this relationship for

the part of the river close to the flood retention basin.

- The flood retention basin is optimised based on the hydrographs of the 100 and 225 year conditions, determined in section 2.6.

### R.3. ELEVATION FLOOD RETENTION AREA

An important factor is the height of the area. No detailed elevation map of the area is available. But a rough estimation is made with the Google Earth elevation measuring tool. The boundary of the area is divided into seven different sections, see figure R.3. The elevation of the area is roughly:

- Flood retention area, height between 7 and 8 meter above Mean Sea Level (MSL).
- Section A, height varies between 8 and 9 meter above MSL.
- Section B, height between 18 and 25 meter above MSL. Further south of section B, the height increases.
- Section C, height between 11 and 12 meter above MSL. This height is especially relevant because of the house in that corner.
- Section D, height approximately 8 meter above MSL.
- Section E, height approximately 9 meter above MSL.
- Section F, not included in the flood retention area. Height varies between 7 and 8 meter above MSL.
- Section G, also not included in the flood retention area. Height varies between 7 and 8 meter above MSL.

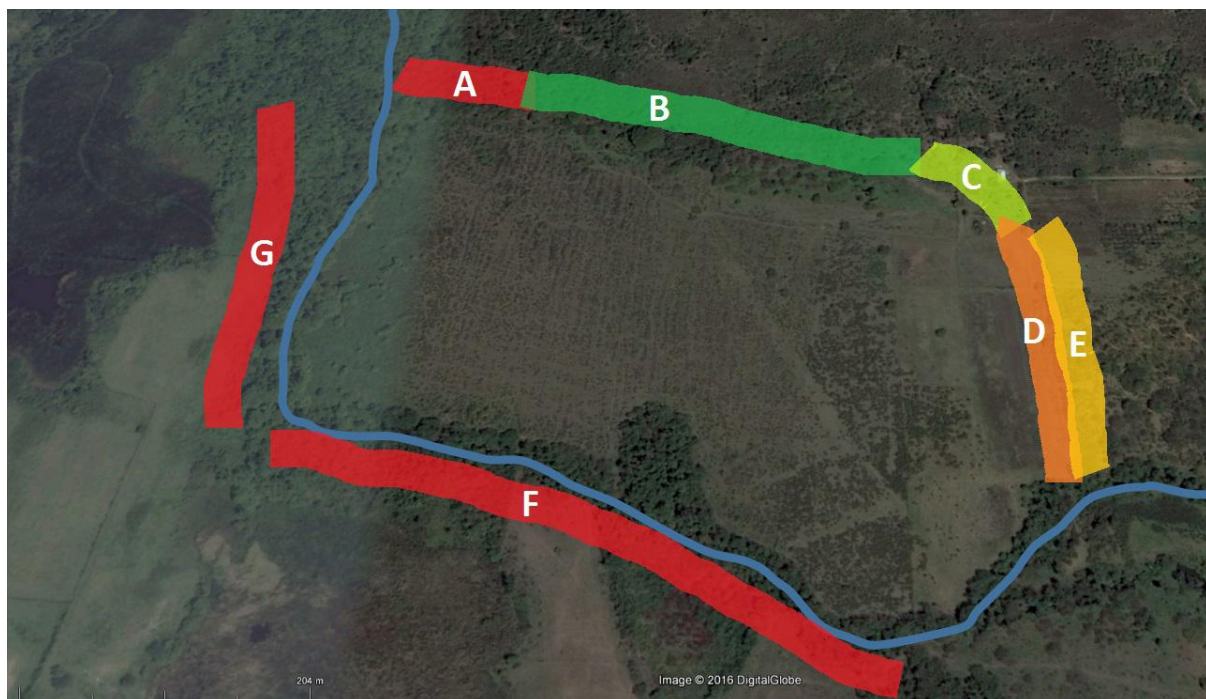


Figure R.3: Flood retention area, heights described [2]

## R.4. INLET STRUCTURE

### R.4.1. VARIANTS

Several variants of inlet structures are possible, for example:

- Culverts through the river bank that need to be opened manually.
- Gate structure, the gate should be opened in order to flood the flood retention area.
- Initiate river bank breach, the river can be breached on purpose in order to initiate flooding at the right location.

Structures that need to be opened manually are not preferred, because the discharges at which the flood retention should be used, are very rare. The management of the operation of the structure can fail due to lack of knowledge. Furthermore, the flood retention basin will not reduce the peak discharge if the inlet is not opened at the right time. In the worst case, this will lead to a basin that is already filled when the peak arrives. The probability of failure of operation is high. For these reasons a structure is designed that works naturally, without human interference. The design is presented in figure R.4. The main idea is that the bank at the flood retention basin side of the river floods at a certain water level (hence at a certain discharge).

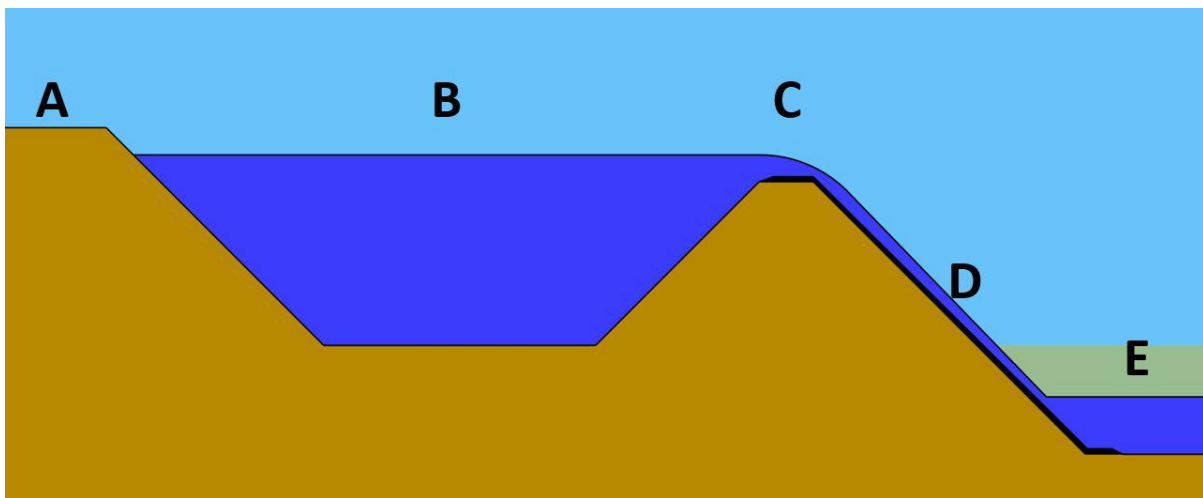


Figure R.4: Design inlet structure

### R.4.2. NATURAL INLET STRUCTURE

The idea of the structure is presented in figure R.4. Above a certain discharge the water depth should exceed the river bank next to the flood retention basin. The discharge and water depth relationship is not known, so further investigation with respect into the exact elevation of the river bank is needed. In this way, controlled flooding at the preferred side of the river is created.

The characters of figure R.4 are:

- **A.** River bank opposite to the inlet structure. The elevation of this bank should be high enough to prevent flooding of this side of the land.

- **B. River.** The water level in the river exceeds the bank on the right side, so the water level will decrease until it reaches the level of the right bank.
- **C. Inlet structure.** The length of the inlet structure should be long enough to guarantee that all the water, that is needed to restore the water level at the height of the right bank, can flow to the flood retention area.
- **D. Protection layer.** Water will flow over the dike to the flood retention area. This flow should not damage the dike itself, so a protection layer to prevent erosion will be designed. Failure of this dike is not a big problem, provided that the secondary flood defences (the boundaries of the flood retention area) are strong enough to prevent flooding of the hinterland.
- **E. Flood retention area.** The flood retention area is excavated to accommodate more water.

## R.5. TWO SCENARIOS

The two different scenarios are visualised in figure R.5. The height of the dike is higher for the one in 225 year condition, since the water depth at  $300 \text{ m}^3/\text{s}$  is higher than at  $265 \text{ m}^3/\text{s}$ . The additional dike height, dark brown part figure R.5b can be determined based on the discharge and water depth relation, which is not known yet. The difference in water depth between 265 and  $300 \text{ m}^3/\text{s}$  is equal to the difference in dike height. The height between the crest level and the bottom level of the storage area is equal to three meter in both cases, which results in a larger excavation depth for the 1/100 year condition.

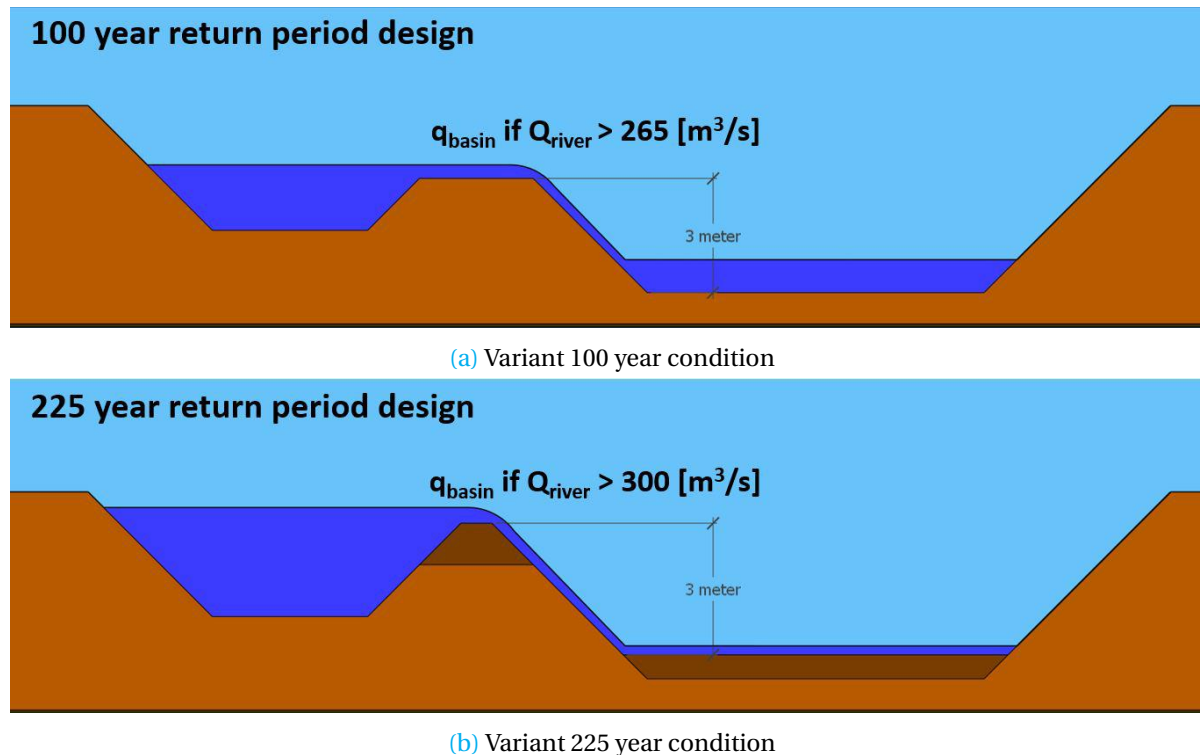


Figure R.5: Different variants inlet structure

In this design, the height of the dike will determine at which water level the area will be flooded. If the area is optimised for reduction of the 225 year condition river discharge, the lower return period

discharges will not be reduced as much as it would with a lower dike.

The discharge at flooding, for the 100 and 225 year return period, is determined based on the available storage, given the retention basin area of 176,700 m<sup>2</sup> and storage depth of 3 m. The procedure is explained by figure R.6. The orange area is the total storage of water. The discharge, which is cut off by the black line, is called the flooding discharge. This flooding discharge is determined such that the orange area is equal to the available storage, in the flood retention basin. In this way the discharge in the river will not exceed this value.

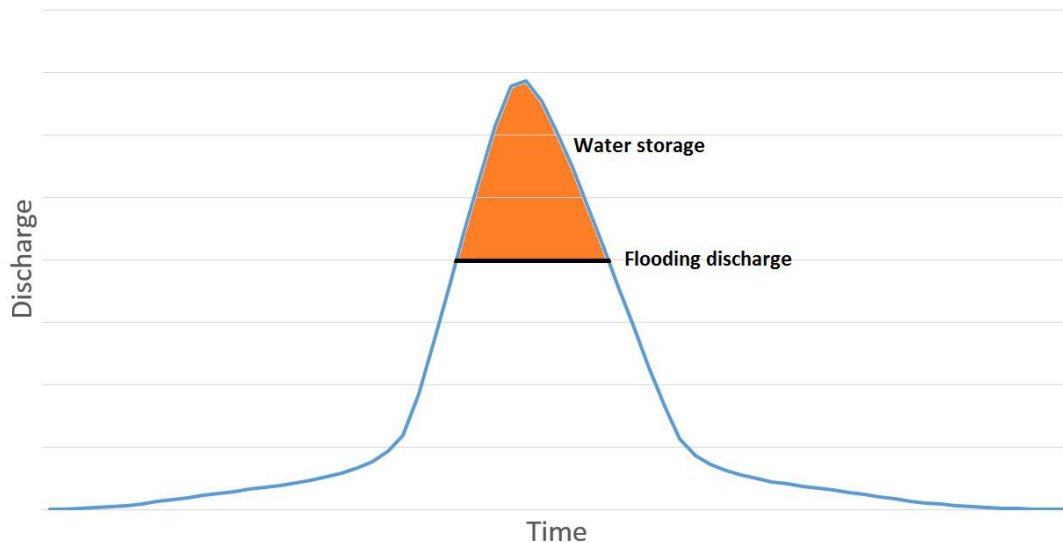


Figure R.6: Explanation discharge reduction

The above described procedure leads to the following scenarios:

- **Optimisation 100 year return period**

Design of dike such that the area floods given a river discharge of 265 m<sup>3</sup>/s. This flooding is ensured by the height of the dike. Given the discharge and water depth relationship, this height can be determined. The height of the dike is fixed, so a discharge with a return period of 225 year will give less peak reduction. This will be explained section R.6.

- **Optimisation 225 year return period**

Design of dike such that the area floods given a river discharge of 300 m<sup>3</sup>/s. The 100 year return period river discharge will not be reduced as much as it would with the 265 m<sup>3</sup>/s limit.

## R.6. REDUCTION DISCHARGE

The two scenarios are optimised for the two design conditions, one in 100 and 225 years. The design is such that in case of one in 100 years the discharge will not exceed 265 m<sup>3</sup>/s, the limit for the 225 years condition is 300 m<sup>3</sup>/s. The total discharge reduction is equal to the available storage in the flood retention area.

### R.6.1. SCENARIO 1: 100 YEAR MEASURE

The results of scenario 1 (100 year measure), in case of one in 100 and 225 year return period discharge can be seen in table R.1. The original and reduced hydrograph for both conditions can be found in figures R.7 and R.8. The flooding of the flood retention basin starts at a discharge of 265 m<sup>3</sup>/s. The reduction is optimal for the one in 100 year condition, the reduction is 22.7%. In case of a one in 225 year discharge the reduction is far from optimal, 4.6%. This is due to the fact that the flood retention basin is filled before the peak arrives. This can be seen in figure R.8.

Table R.1: Variant 1: 100 year measure, discharge 100 and 225 year condition

	100 year discharge	225 year discharge
<b>Unreduced peak discharge (m<sup>3</sup>/s)</b>	342.8	376.9
<b>Reduced peak discharge (m<sup>3</sup>/s)</b>	265	359.7
<b>Peak reduction (%)</b>	22.7	4.6
<b>Total storage (m<sup>3</sup>)</b>	547192	535221
<b>Nett storage depth (m)</b>	3.1	3.0

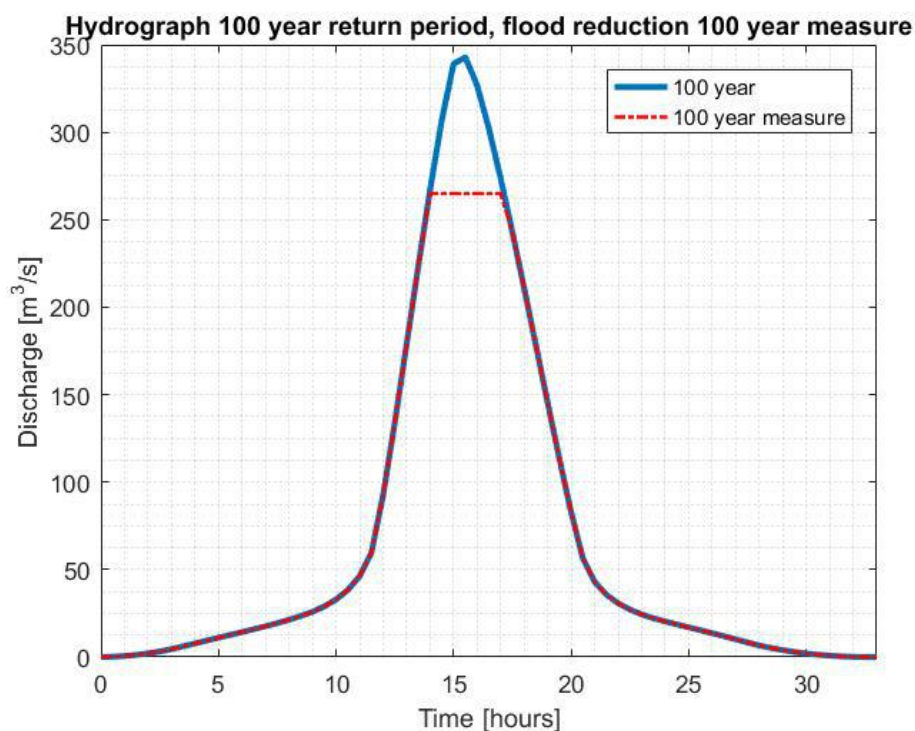


Figure R.7: 100 year measure, 100 year discharge

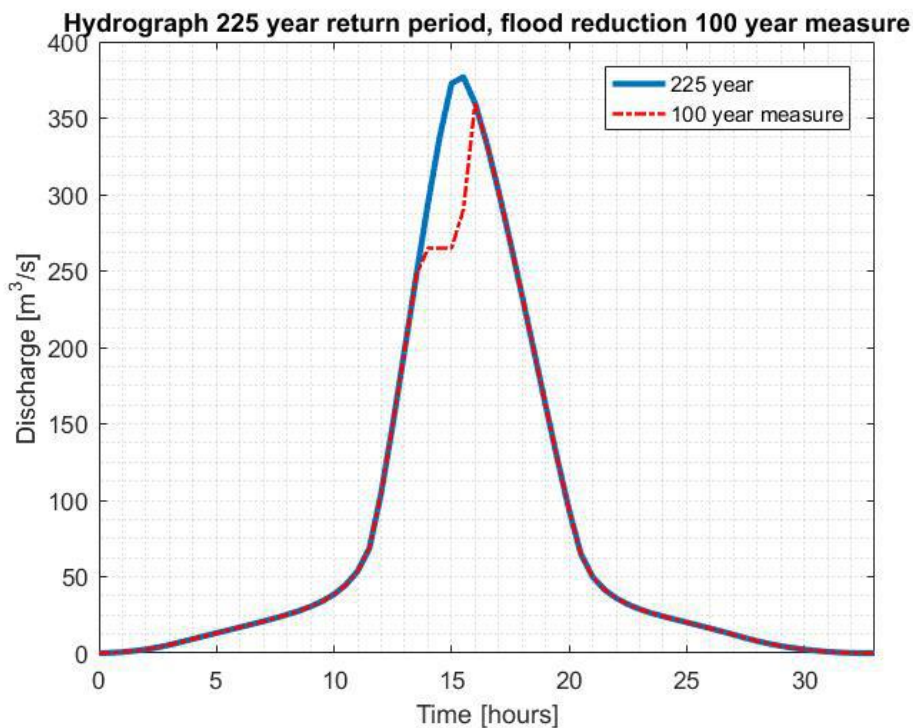


Figure R.8: 100 year measure, 225 year discharge

### R.6.2. SCENARIO 2: 225 YEAR MEASURE

The results of scenario 2 (225 year measure), in case of one in 100 and 225 year return period discharge can be seen in table R.2. The original and reduced hydrograph for both conditions can be found in figures R.9 and R.10. Flooding of the flood retention basin takes place above a discharge of 300 m<sup>3</sup>/s. This is optimal for the 225 year condition. The basin will not be used to its full capacity, since flooding of the basin starts at a discharge of 300 m<sup>3</sup>/s.

Table R.2: Variant 2: 225 year measure, discharge one in 100 and one in 225 year condition

	100 year discharge	225 year discharge
<b>Unreduced peak discharge (m<sup>3</sup>/s)</b>	342.8	367.9
<b>Reduced peak discharge (m<sup>3</sup>/s)</b>	300	300
<b>Peak reduction (%)</b>	12.5	20.4
<b>Total storage (m<sup>3</sup>)</b>	212680	509045
<b>Nett storage depth (m)</b>	1.2	2.9

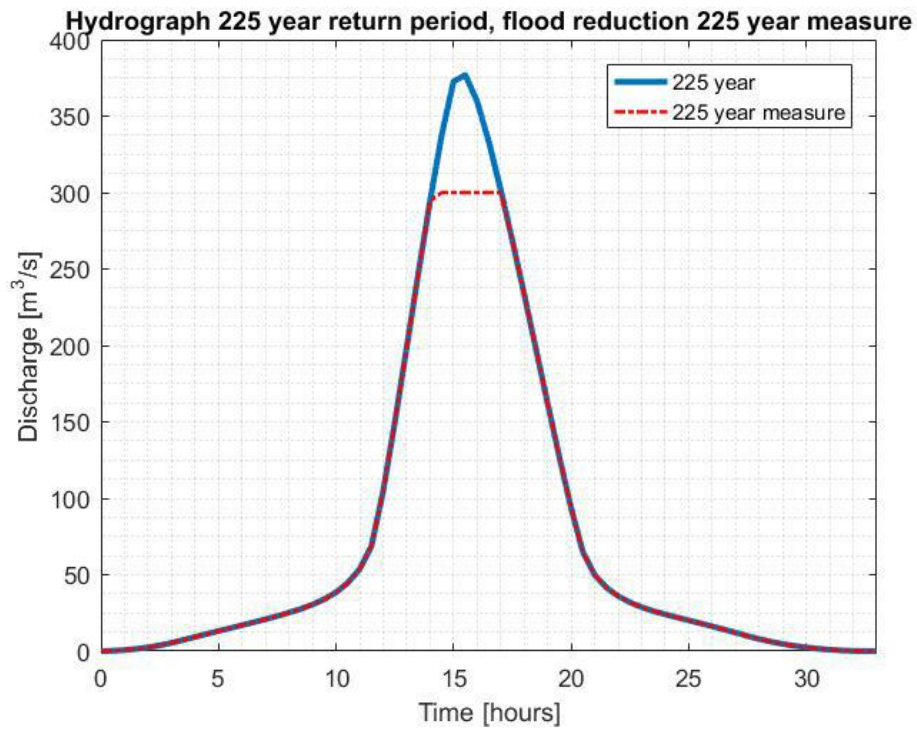


Figure R.9: 100 year measure, 100 year discharge

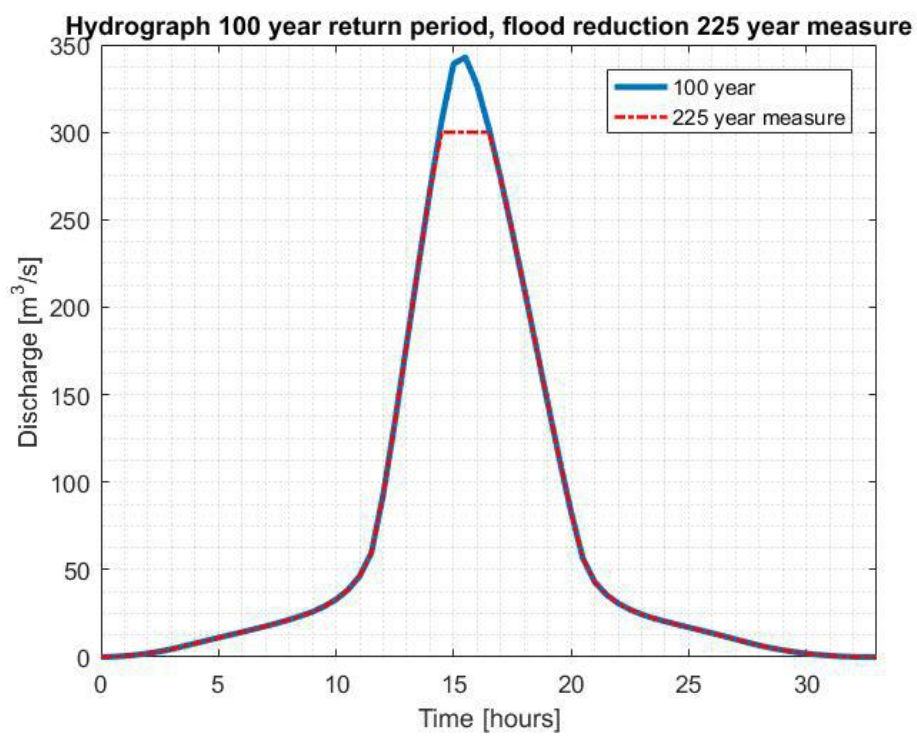


Figure R.10: 225 year measure, 100 year discharge

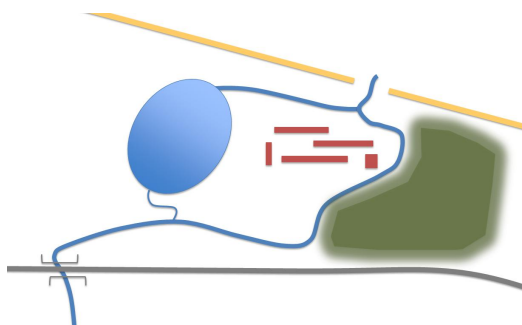
## R.7. DISCUSSION

- Rain in the flood retention basin is not taken into account in this preliminary design. The extreme rain conditions (1/100 and 1/225 year) do reduce a certain amount of rain, in the order of 20 to 50 cm. This height should be added to the storage depth.
- After flooding of the area, in very rare conditions, the water should be removed with pumps or by infiltration in the bottom. Because of the low frequency of the event and the low consequences of the flooding no expensive de-watering solution is designed.

# S

## SOLUTION: MANGROVE FOREST EXTENSION

Figure S.1a shows a Building with Nature solution that improves the presence of mangrove forest by extending the already existing forest. The mangrove forest houses a unique ecosystem with a lot of flora and fauna. The extension of mangrove forest is therefore a sustainable solution, which can be created by excavating a large area next to the downstream part of the Itabo River. In this designated flooding area, water is already present, which is needed for the growth of the mangroves. The idea is that extra water can be stored in the excavated lagoon in case of high river discharge. In this way, the river discharge further downstream is lowered to prevent flooding at the east side of the study area, where the waste water treatment plant is located.



(a) Schematisation of the solution



(b) Planned area

Figure S.1: Mangrove forest extension

### S.1. ADVANTAGES

- The main goal of the solution is the extra storage of water, to prevent flooding in case of high river discharge.
- This Building with Nature concept extends the unique ecosystem of mangrove forest by creating ideal conditions for the environment to develop into mangrove forest.

- This solution has an aesthetic value that will attract nature loving tourists, as mangrove forests are protected nature that needs to be preserved.
- CITMA will be intrigued to invest in a solution that favours nature.
- Part of the ecosystem lost by the construction of the Blau Arenal Hotel will be restored.

## S.2. DISADVANTAGES

- A large area is needed next to the existing mangrove forest. The local residents, living in this area for mangrove extension, need to move to another place. Therefore, their attitude towards the project will be negative. The scheduled area for the mangrove extension is shown in red, in figure S.1b, and consists of 15 blocks of houses. These houses need to be removed and the owners need to be relocated. The government has to arrange proper housing and the relocation of all these people. This will be an expensive part of the solution.
- The location of the mangrove forest is planned at the downstream end of the Itabo River and east of the Blau Arenal Hotel. Flooding of the river will mainly happen more upstream, so it is uncertain if this designated flooding area will function properly.
- It is uncertain if the development of mangrove forest will succeed as it is difficult to create the favourable circumstances. The process needs extensive monitoring to observe the succession of the vegetation. This will bring additional costs.
- The time it takes to develop a fully grown mangrove forest is not known. This option could possibly take several years or even decades to realise. CITMA, which demands to have a solution for the contamination problem now, does not want to wait that long.
- A temporary structure, like a small breakwater or brushwood dams (cheaper option) should be built, because the pioneer vegetation will need a sheltered environment against waves. This will bring additional costs.

## S.3. CONCLUSION

The special flooding area with mangrove forest extension will not be a good solution for the flooding problem, despite the environmental advantages. This is concluded, because of the large costs due to the removal of people living in the designated flooding area and the excavation to prepare the area for the creation of mangroves. Additionally, there are the costs of the temporary structure to shelter the pioneer vegetation. Furthermore, the flooding problem due to high river discharge begins more upstream of the Itabo River. This causes flooding at the west side of the study area and the functionality of the water storage eastwards will be less. Moreover, the amount of water, which is already present in the retention basin for the growth of the mangroves, will make the solution less effective. Because of these disadvantages and the uncertainties, no further elaboration will be done on this ecofriendly solution.

# T

## SOLUTION: EXTRA OUTFLOW POINT

From the brainstorm, two possible locations for an extra outflow point have been determined. The extra outflow point will only be used in case of high discharge events. The reason for this is that during normal river conditions, the water level in the main branch needs to be sufficient to prevent the river to change its course. If the river changes its course, it could eventually lead to closure of the river mouth, which would have a large impact on the environment. In figure T.1, the two possible locations for an extra outflow point are highlighted in the blue and red coloured boxes.



Figure T.1: Satellite image of the study area with visualisation of the extra outflow points [2]

The western extra outflow point (blue) will connect the large west branch of the Itabo River downstream of the bridge with the sea. This branch houses a dense mangrove forest, that lives in submerged areas. Therefore, this is an easy option to connect the river with the sea, as only the dunes are in between the river and the sea. A pipe will be used to cut through the dune, because excavation of the dunes will decrease the natural function of the dunes to protect against flooding from the sea. A path, where no residences are situated, has been chosen for the pipeline. This pipe will only be used if a predetermined water level of the river is exceeded. When this water level is reached, a weir, located in front of the pipe, will overflow and water will be discharged to the sea through the pipe.

The northern location for an extra outflow point (red) is connected to the river via the lagoon. The lagoon is linked with the river via a culvert. This outflow point will also function with a weir and only in case of high river discharge. The shortest trajectory of the pipeline is chosen for economic reasons. Furthermore, the location is without buildings in the neighbourhood.

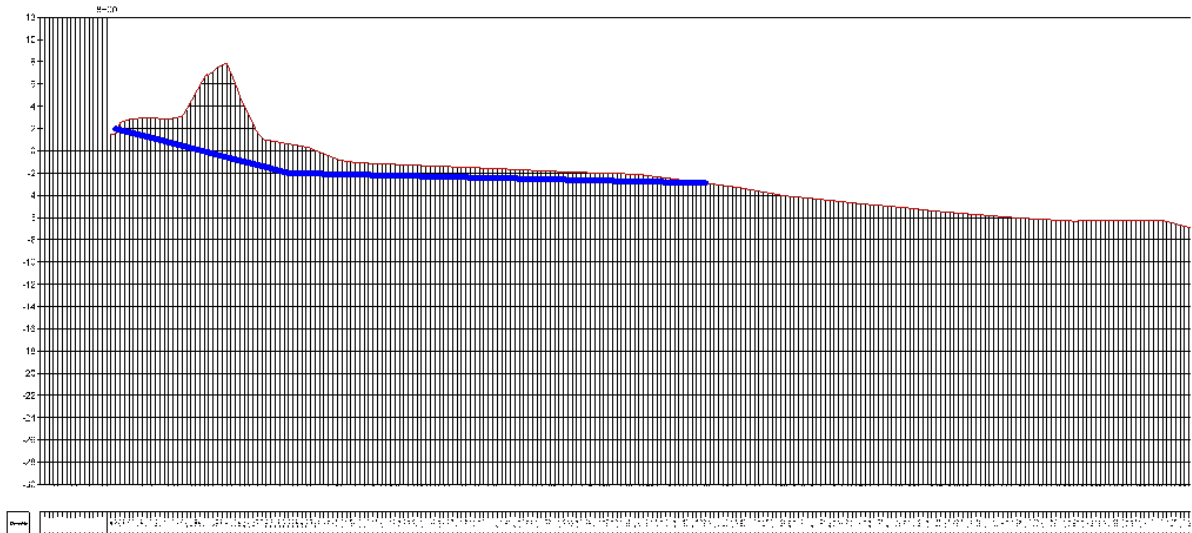


Figure T.2: Schematisation of the pipeline, connecting the lagoon to the sea [41]

As can be seen in figure T.2, the trajectory of the pipeline goes a relatively large distance into the sea to keep the beach, which is a popular destination for recreation and leisure, free from harm due to a visible pipeline. The pipeline will go from the predetermined water level to about MSL -3 m. A pump will be installed to secure the outflow into the sea. Because the area is prone to storms with a high storm surge, the pipe needs to be equipped with a single way closure system.

## T.1. ADVANTAGES

- The flooding due to high river discharge is mitigated or even prevented due to the extra outflow point.
- The environment is preserved after the construction of the pipeline.
- The solution has aesthetic value, as no one can see the hidden pipeline.

### T.1.1. DISADVANTAGES

- Both possible trajectories of the pipeline will go underneath the protected mangrove forest. The construction of these pipelines will lead to a damaged ecosystem. CITMA will never approve a solution that does not take into account the value of the unique ecosystem of mangrove forest.
- The pipeline will also go through the dunes. This is not preferred, because the dunes are already in a bad condition (see figure A.8 in appendix A). The construction of a pipeline will decrease the state of the dunes even more.

- Extensive maintenance of the inlet and outlet of the pipeline is needed, as no garbage or sediment, on the sea side, may block the pipeline.
- Additional maintenance of the pump and the single way closure system is needed.
- The high costs of the construction of the solution.

## T.2. CONCLUSION

The extra outflow point is a solution that mitigates or prevents the flooding of the area. Besides, the solution has aesthetic value. The solution is not chosen, because damage is done to the unique ecosystem of mangrove forest and the dunes during construction of the pipeline. The high costs of the construction of the pipeline and the extensive maintenance of inlet and outlet are also disadvantages that are taken into account in this conclusion.





## MULTI CRITERIA ANALYSIS

### U.1. SCORES

The solutions are evaluated by means of the criteria. Each of the 14 solutions will get a value that lies between zero (very poor) and five (excellent). The criterion is mentioned in the caption above the table and the height of the score of the solution is explained in the final column of the table.

Table U.1: Criterion: Prevention of contamination of the mangrove forest

Nr.	Solution	Score	Explanation	
1	Wall around WWTP 1/225	Gravity wall	4	Structure fulfils pollution criterion
2		Embedded wall	4	Structure fulfils pollution criterion
3		Sheetpile wall	4	Structure fulfils pollution criterion
4	Wall around WWTP 1/225 and hotel 1/225	Gravity wall	4	Structure fulfils pollution criterion
5		Embedded wall	4	Structure fulfils pollution criterion
6		Sheetpile wall	4	Structure fulfils pollution criterion
7		Wall with slope	4	Structure fulfils pollution criterion
8	Wall around WWTP 1/225 and hotel 1/100	Gravity wall	4	Structure fulfils pollution criterion
9		Embedded wall	4	Structure fulfils pollution criterion
10		Sheetpile wall	4	Structure fulfils pollution criterion
11		Wall with slope	4	Structure fulfils pollution criterion
12	Wall around WWTP 1/225 and retention basin 1/100	Gravity wall	5	Basin slightly reduces 1/225 water level
13		Embedded wall	5	Basin slightly reduces 1/225 water level
14		Sheetpile wall	5	Basin slightly reduces 1/225 water level

Table U.2: Criterion: Water damage hotel

Nr.	Solution	Score	Explanation	
1	Wall around WWTP 1/225	Gravity wall	1	1/100: flooding hotel (low inundation depth)
2		Embedded wall	1	1/100: flooding hotel (low inundation depth)
3		Sheetpile wall	1	1/100: flooding hotel (low inundation depth)
4	Wall around WWTP 1/225 and hotel 1/225	Gravity wall	5	Safety level hotel above standard
5		Embedded wall	5	Safety level hotel above standard
6		Sheetpile wall	5	Safety level hotel above standard
7		Wall with slope	5	Safety level hotel above standard
8	Wall around WWTP 1/225 and hotel 1/100	Gravity wall	4	Structure fulfils safety requirement
9		Embedded wall	4	Structure fulfils safety requirement
10		Sheetpile wall	4	Structure fulfils safety requirement
11		Wall with slope	4	Structure fulfils safety requirement
12	Wall around WWTP 1/225 and retention basin 1/100	Gravity wall	2	1/100: flooding hotel (very low inundation depth)
13		Embedded wall	2	1/100: flooding hotel (very low inundation depth)
14		Sheetpile wall	2	1/100: flooding hotel (very low inundation depth)

Table U.3: Criterion: Aesthetic value

Nr.	Solution	Score	Explanation	
1	Wall around WWTP 1/225	Gravity wall	5	WWTP covered
2		Embedded wall	5	WWTP covered
3		Sheetpile wall	4	Less aesthetic value of steel compared to concrete
4	Wall around WWTP 1/225 and hotel 1/225	Gravity wall	2	Landscape pollution hotel area
5		Embedded wall	2	Landscape pollution hotel area
6		Sheetpile wall	1	Less aesthetic value of steel compared to concrete
7		Wall with slope	3	Covering of one side of wall structure
8	Wall around WWTP 1/225 and hotel 1/100	Gravity wall	3	Landscape pollution hotel area, height less compared to 1/225
9		Embedded wall	3	Landscape pollution hotel area, height less compared to 1/225
10		Sheetpile wall	2	Less aesthetic value of steel compared to concrete
11		Wall with slope	4	Covering of one side of wall structure
12	Wall around WWTP 1/225 and retention basin 1/100	Gravity wall	2	WWTP covered, loss of aesthetic value basin
13		Embedded wall	2	WWTP covered, loss of aesthetic value basin
14		Sheetpile wall	1	Less aesthetic value of steel compared to concrete

Table U.4: Criterion: Constructability

Nr.	Solution	Score	Explanation	
1	Wall around WWTP 1/225	Gravity wall	3	Logistics difficult, much hardening time
2		Embedded wall	2	Very difficult construction method
3		Sheetpile wall	4	Easy construction method
4	Wall around WWTP 1/225 and hotel 1/225	Gravity wall	2	Logistics difficult, much hardening time, length wall greater
5		Embedded wall	1	Very difficult construction method, length wall greater
6		Sheetpile wall	3	Easy construction method, length wall greater
7		Wall with slope	1	Very difficult construction method
8	Wall around WWTP 1/225 and hotel 1/100	Gravity wall	2	Logistics difficult, much hardening time
9		Embedded wall	1	Very difficult construction method
10		Sheetpile wall	3	Easy construction method
11		Wall with slope	1	Very difficult construction method
12	Wall around WWTP 1/225 and retention basin 1/100	Gravity wall	1	Logistics difficult, much hardening time + excavation work basin
13		Embedded wall	1	Very difficult construction method + excavation work basin
14		Sheetpile wall	2	Easy construction method + excavation work basin

Table U.5: Criterion: Maintenance

Nr.	Solution	Score	Explanation	
1	Wall around WWTP 1/225	Gravity wall	4	Regular checks concrete cracking and reinforcement corrosion
2		Embedded wall	4	Regular checks concrete cracking and reinforcement corrosion
3		Sheetpile wall	5	Regular corrosion checks
4	Wall around WWTP 1/225 and hotel 1/225	Gravity wall	3	Regular checks concrete cracking and reinforcement corrosion, larger length wall compared to WWTP only
5		Embedded wall	3	Regular checks concrete cracking and reinforcement corrosion, larger length wall compared to WWTP only
6		Sheetpile wall	4	Regular corrosion checks, larger length wall compared to WWTP only
7		Wall with slope	3	Regular checks concrete cracking and reinforcement corrosion, larger length wall compared to WWTP only
8	Wall around WWTP 1/225 and hotel 1/100	Gravity wall	3	Regular checks concrete cracking and reinforcement corrosion, larger length wall compared to WWTP only
9		Embedded wall	3	Regular checks concrete cracking and reinforcement corrosion, larger length wall compared to WWTP only
10		Sheetpile wall	4	Regular corrosion checks, larger length wall compared to WWTP only
11		Wall with slope	3	Regular checks concrete cracking and reinforcement corrosion, larger length wall compared to WWTP only
12	Wall around WWTP 1/225 and retention basin 1/100	Gravity wall	2	Often maintenance inlet structure, regular checks concrete cracking and reinforcement corrosion
13		Embedded wall	2	Often maintenance inlet structure, regular checks concrete cracking and reinforcement corrosion
14		Sheetpile wall	3	Often maintenance inlet structure, regular corrosion checks

Table U.6: Criterion: Social acceptance

Nr.	Solution	Score	Explanation	
1	Wall around WWTP 1/225	Gravity wall	5	Wall covers WWTP, positive influence on hotel area
2		Embedded wall	5	Wall covers WWTP, positive influence on hotel area
3		Sheetpile wall	5	Wall covers WWTP, positive influence on hotel area
4	Wall around WWTP 1/225 and hotel 1/225	Gravity wall	4	Solution at hotel area, no negative influence on neighbourhood
5		Embedded wall	4	Solution at hotel area, no negative influence on neighbourhood
6		Sheetpile wall	4	Solution at hotel area, no negative influence on neighbourhood
7		Wall with slope	4	Solution at hotel area, no negative influence on neighbourhood
8	Wall around WWTP 1/225 and hotel 1/100	Gravity wall	4	Solution at hotel area, no negative influence on neighbourhood
9		Embedded wall	4	Solution at hotel area, no negative influence on neighbourhood
10		Sheetpile wall	4	Solution at hotel area, no negative influence on neighbourhood
11		Wall with slope	4	Solution at hotel area, no negative influence on neighbourhood
12	Wall around WWTP 1/225 and retention basin 1/100	Gravity wall	1	Basin will destroy landscape and cause controlled flooding in catchment area
13		Embedded wall	1	Basin will destroy landscape and cause controlled flooding in catchment area
14		Sheetpile wall	1	Basin will destroy landscape and cause controlled flooding in catchment area

Table U.7: Criterion: Sustainability

Nr.	Solution	Score	Explanation	
1	Wall around WWTP 1/225	Gravity wall	5	Relatively easy construction method (less environmental pollution), short wall length
2		Embedded wall	3	More difficult construction method, short wall length
3		Sheetpile wall	4	Transportation of steel, short wall length
4	Wall around WWTP 1/225 and hotel 1/225	Gravity wall	3	Relatively easy construction method (less environmental pollution), longer length wall
5		Embedded wall	2	Difficult construction method, pollution due to concrete usage
6		Sheetpile wall	3	Easy construction method, long wall length
7		Wall with slope	2	Difficult construction method, pollution due to concrete usage
8	Wall around WWTP 1/225 and hotel 1/100	Gravity wall	3	Relatively easy construction method (less environmental pollution), longer length wall
9		Embedded wall	2	Difficult construction method, pollution due to concrete usage
10		Sheetpile wall	3	Easy construction method, long wall length
11		Wall with slope	2	Difficult construction method, pollution due to concrete usage
12	Wall around WWTP 1/225 and retention basin 1/100	Gravity wall	2	Easy construction method, much construction work at basin
13		Embedded wall	1	Difficult construction method, much construction work at basin
14		Sheetpile wall	3	Easy construction method, much construction work at basin



# V

## COSTS

Two categories are used to divide the total costs. All direct related costs to the construction are called primary costs and all indirect related costs are called secondary costs. Furthermore, these main categories have been subdivided in sections, which are explained below.

### V.1. PRIMARY COSTS

Direct costs of material (C1)

- Construction material, which forms an integral part of the construction (concrete, concrete elements, steel, reinforcement, cables, pipes etc)
- Supporting materials, which are used during the work (wood, molds etc.)
- Semi-manufactured parts (the elements that arrive at the construction site in a partial state)
- Prefabricated materials (construction of concrete, construction of wooden sections)
- Costs of the use of water during the fabrication of concrete

Direct costs of work by hand (C2)

- Design
- Technical preparations (office, calculations, communication)
- Salaries
- Water (not used for concrete)

Direct costs of equipment (C3)

- Fuel, lubricant (oil), electrical energy
- Salaries for the permanent operators of the material

- Reparation and maintenance of the material
- Security for the material
- Tires
- Interest of the use of the capital
- Taxes

Direct costs of means of support and small material (C4)

- 3% of  $C1 + C2 + C3$

Total direct costs (C5)

- Sum of C1 to C4

Indirect costs (C6)

- 29% of C5

Total costs (C7)

- $C5 + C6$

Profit (C8)

- 20% of the preparation costs

Total primary costs (C9)

- $C7 + C8$

## V.2. SECONDARY COSTS

Temporary facilities (P1)

- Toilets, material warehouses etc.

Transport (P2)

- Trucks etc.

Other additional costs (P3)

- Proof of good quality of the used materials for the client
- Transport of not used materials at the finish of the work
- Cleaning

Banking (P4)

- Risk of cost estimation (5% of  $C9 + P1 + P2 + P3$ )

- Risk of time estimation (5% of C2 (components with hours) + C3 (components with hours))
- Risk of price-changes during the project (10% of C1)

Security (P5)

Unpredictable costs (P6)

Total secondary costs (P7)

- Sum of P1 to P6

### V.3. RISK

To give a more accurate estimation of the costs several risks have to be taken into account. This has been done in section banking (P4) for the secondary costs. As can be seen, the risk of cost, time and price-changes are valued. The costs are obtained by estimation, so they are not specific. This can possibly result in underestimation. Therefore, the risk for cost has been valued by adding 5% to the total primary costs and to the first three components of the secondary costs (P1 up to P3). These combine all major costs, giving a weighted estimation of the risk for each specific alternative. For time, all components that contain hours as a quantity in the primary costs, will be used to estimate the risk. Also 5% of the summation of all these values will be added to the total costs. These values have been taken as they are a vital part of the construction and delay of these actions will cause the project to be more expensive. Finally, the price of materials can change during the construction or even before starting. To evaluate this, the material costs from C1 are used and 10% of these costs will be added to the final costs.

## V.4. COSTS ESTIMATION OF EACH SOLUTION

Primary costs				Secondary costs					
	Quantity	Unit price [€]	Subtotal [€]	Total		Quantity	Unit price [€]	Subtotal [€]	Total
<b>C1 - Direct costs of material</b>					<b>P1 - Temporary facilities</b>				
	Concrete in situ [m³]	357,00	230	82,110		Toilets, material warehouses etc.		1,000	1,000
									1,000
<b>C2 - Direct costs of Labour</b>				82,110	<b>P2 - Transport</b>				
	Design (5 people; 8 weeks) [hrs]	1,600	4	6,400		Concrete trucks (15 m³) [hrs]	80	24,28	1,942
	Technical preparations [hrs]	500	3,5	1,750		Transport of elements [hrs]	20	35	700
	Salaries (10 people; 5 weeks) [hrs]	2,000	3,5	7,000					2,642
				15,150	<b>P3 - Other additional costs</b>				
<b>C3 - Direct costs of equipment</b>						Proof of good quality		10,000	
	Fuel, lubricant, oil [gallons]	1,000	0,64	640		Transport of unused materials	5	23,56	118
	Concrete mill [hrs]	200	24,28	4,856					10,118
	Security for material and equipment			5,000	<b>P4 - Banking</b>				
				10,496		Risk of cost estimation		7,928	
<b>C4 - Direct costs of means of support and small material</b>				3,233		Risk of time estimation		1,000	
						Risk of price-changes during the project		8,211	
<b>C5 - Total direct costs</b>				110,989	<b>P5 - Security</b>				5,000
<b>C6 - Indirect costs</b>				32,187	<b>P6 - Unpredictable costs</b>				50,000
<b>C7 - Total costs</b>				143,175	<b>P7 - Total secondary costs</b>				50,000
<b>C8 - Profit</b>				1,630					85,900
<b>C9 - Total primary costs</b>				144,805					

Figure V.1: Gravity wall around the waste water treatment plant only for a 225 year condition

	Primary costs				Total	Secondary costs				Total
	Quantity	Unit price [€]	Subtotal [€]			Quantity	Unit price [€]	Subtotal [€]		
C1 - Direct costs of material	Concrete in situ [m³]	386,968,448	230	89,003	P1 - Temporary facilities Toilets, material warehouses etc.			1,000	1,000	
	Steel reinforcement [m²]	5,031,552	600	3,019						
92,022					P2 - Transport					
C2 - Direct costs of Labour	Design (5 people; 8 weeks) [hrs]	1,600	4	6,400	Concrete trucks (15 m³) [hrs]	100	24,28	2,428	3,128	
	Technical preparations [hrs]	500	3,5	1,750	Transport of elements [hrs]	20	35	700		
	Salaries (10 people; 5 weeks) [hrs]	2,000	3,5	7,000	P3 - Other additional costs					
					Proof of good quality			10,000		
15,150					Transport of unused materials	6	23,56	141	10,141	
C3 - Direct costs of equipment	Fuel, lubricant, oil [gallons]	1,000	0,64	640	P4 - Banking					
	Concrete mill [hrs]	200	24,28	4,856	Risk of cost estimation			9,068		
	Excavator [hrs]	200	34,33	6,866	Risk of time estimation			1,344		
	Security for material and equipment			5,000	Risk of price-changes during the project			9,202		
17,362								19,614		
C4 - Direct costs of means of support and small material				3,736	P5 - Security			5,000	5,000	
C5 - Total direct costs				128,270						
C6 - Indirect costs				37,198	P6 - Unpredictable costs			50,000	50,000	
C7 - Total costs				165,468						
C8 - Profit				1,630					50,000	
<b>C9 - Total primary costs</b>					<b>P7 - Total secondary costs</b>					
<b>167,098</b>					<b>88,883</b>					

Figure V.2: Embedded wall around the waste water treatment plant only for a 225 year condition

Primary costs				Secondary costs				
	Quantity	Unit price [€]	Subtotal [€]		Quantity	Unit price [€]	Subtotal [€]	
C1 - Direct costs of material	Sand [m³]	525	10	5,250	P1 - Temporary facilities	Toilets, material warehouses etc.	1,000	
	Steel [m³]	15,65	600	9,390				1,000
14,640				P2 - Transport	Dumpttruck [hrs]	400	24,28	
C2 - Direct costs of Labour	Design (5 people; 8 weeks) [hrs]	1,600	4					6,400
	Technical preparations [hrs]	2,000	3,5					7,000
	Salaries (10 people; 10 weeks) [hrs]	4,000	3,5					14,000
27,400				P3 - Other additional costs	Proof of good quality	400	10,000	
C3 - Direct costs of equipment	Fuel, lubricant, oil [gallons]	2,000	0,64					1,280
	Sheepile driver [hrs]	400	80	32,000	942			
	Excavator [hrs]	400	34,33	13,732	P4 - Banking	Risk of cost estimation	8,497	
	Security for material and equipment			10,000				Risk of time estimation
57,012				Risk of price-changes during the project				1,464
2,972				P5 - Security				5,000
102,024				P6 - Unpredictable costs				100,000
29,587				P7 - Total secondary costs				154,272
131,610								100,000
2,680								
134,290								

Figure V.3: Sheetpile wall around the waste water treatment plant only for a 225 year condition

	Primary costs			Total	Secondary costs			Total
	Quantity	Unit price [€]	Subtotal [€]		Quantity	Unit price [€]	Subtotal [€]	
C1 - Direct costs of material	Concrete in situ [m <sup>3</sup> ]	6,000.00	230	1,380,000	P1 - Temporary facilities Toilets, material warehouses etc.		1,000	1,000
				1,380,000	P2 - Transport Concrete trucks (15 m <sup>3</sup> ) [hrs] Transport of elements [hrs]	400 50	24.28 35	9,712 1,750
C2 - Direct costs of Labour	Design (5 people; 8 weeks) [hrs] Technical preparations [hrs] Salaries (10 people; 20 weeks) [hrs]	1,600 1,000 8,000	4 3.5 3.5	6,400 3,500 28,000	P3 - Other additional costs Proof of good quality Transport of unused materials			10,000 530
				37,900	P4 - Banking Risk of cost estimation Risk of time estimation Risk of price-changes during the project			97,154 2,866 138,000
C3 - Direct costs of equipment	Fuel, lubricant, oil [gallons] Concrete mill [hrs] Security for material and equipment	2,000 800	0.64 24.28	1,280 19,424 5,000	P5 - Security Risk of price-changes during the project			238,021
C4 - Direct costs of means of support and small material				43,308				
C5 - Total direct costs				1,486,912				5,000
C6 - Indirect costs				431,205				5,000
C7 - Total costs				1,918,117	P6 - Unpredictable costs			100,000
C8 - Profit				1,980				100,000
C9 - Total primary costs				1,920,097	P7 - Total secondary costs			366,013

Figure V.4: Gravity wall around the hotel and the waste water treatment plant for a 225 year condition

Primary costs				Secondary costs					
	Quantity	Unit price [€]	Subtotal [€]		Quantity	Unit price [€]	Subtotal [€]		
C1 - Direct costs of material	Concrete in situ [m³]	8,511.50	230	1,957,645	P1 - Temporary facilities	Toilets, material warehouses etc.	1,000		
	Steel reinforcement [m³]	38.5	600	23,100				1,000	
				1,980,745	P2 - Transport	Concrete trucks (15 m³) [hrs]	600	24.28	14,568
C2 - Direct costs of Labour	Design (5 people; 8 weeks) [hrs]	1,600	4	6,400		Transport of elements [hrs]	50	35	1,750
	Technical preparations [hrs]	1,000	3.5	3,500	P3 - Other additional costs	Proof of good quality		10,000	
	Salaries (10 people; 20 weeks) [hrs]	8,000	3.5	28,000			Transport of unused materials	32.5	23.56
				37,900				10,766	
C3 - Direct costs of equipment	Fuel, lubricant, oil [gallons]	2,000	0.64	1,280	P4 - Banking	Risk of cost estimation		139,144	
	Concrete mill [hrs]	800	24.28	19,424			Risk of time estimation		4,239
	Excavator [hrs]	800	34.33	27,464	P5 - Security	Risk of price-changes during the project		198,075	
	Security for material and equipment			5,000					341,458
C4 - Direct costs of means of support and small material			62,154				5,000		
C5 - Total direct costs			2,133,967				5,000		
C6 - Indirect costs			618,851				5,000		
C7 - Total costs			2,752,818	P6 - Unpredictable costs			100,000		
C8 - Profit			1,980				100,000		
C9 - Total primary costs			2,754,798	P7 - Total secondary costs			474,542		

Figure V.5: Embedded wall around the hotel and the waste water treatment plant for a 225 year condition

	Primary costs			Subtotal [\$]	Total	Secondary costs			Subtotal [\$]	Total	
	Quantity	Unit price [\$]				Quantity	Unit price [\$]				
C1 - Direct costs of material	Sand [m <sup>3</sup> ]	4,500	10	45,000	P1 - Temporary facilities Toilets, material warehouses etc.			1,000	1,000		
	Steel [m <sup>3</sup> ]	132.91	600	79,746							
				124,746							
C2 - Direct costs of Labour	Design (5 people; 8 weeks) [hrs]	1,600	4	6,400	P2 - Transport Dumptruck [hrs] Transport of elements [hrs]			29,136	71,136		
	Technical preparations [hrs]	3,000	3.5	10,500				42,000			
	Salaries (10 people; 30 weeks) [hrs]	12,000	3.5	42,000							
				58,900							
C3 - Direct costs of equipment	Fuel, lubricant, oil [gallons]	5,000	0.64	3,200	P3 - Other additional costs Proof of good quality Transport of unused materials			10,000	12,827		
	Sheepile driver [hrs]	1,200	80	96,000				2,827			
	Excavator [hrs]	1,200	34.33	41,196							
	Security for material and equipment			10,000							
C4 - Direct costs of means of support and small material				150,396	Risk of price-changes during the project Risk of cost estimation Risk of time estimation 12,475						48,889
C5 - Total direct costs				344,063	P5 - Security						5,000
C6 - Indirect costs				99,778	P6 - Unpredictable costs						100,000
C7 - Total costs				443,842	P7 - Total secondary costs						238,852
C8 - Profit				3,380							100,000
C9 - Total primary costs				447,222							238,852

Figure V.6: Sheetpile wall around the hotel and the waste water treatment plant for a 225 year condition

Primary costs				Secondary costs						
	Quantity	Unit price [\$]	Subtotal [\$]	Total		Quantity	Unit price [\$]	Subtotal [\$]	Total	
C1 - Direct costs of material	Concrete in situ [m³]	11,398.82	230	2,621,728	P1 - Temporary facilities	Toilets, material warehouses etc.		1,000	1,000	
	Steel reinforcement [m²]	41,194	600	24,710						
				2,646,438	P2 - Transport	Concrete trucks (15 m³) [hrs]	600	24.28	14,568	
C2 - Direct costs of Labour	Design (5 people; 8 weeks) [hrs]	1,600	4	6,400			Transport of elements [hrs]	50	35	1,750
	Technical preparations [hrs]	1,000	3.5	3,500		P3 - Other additional costs	Proof of good quality			10,000
	Salaries (10 people; 25 weeks) [hrs]	10,000	3.5	35,000			Transport of unused materials	32.5	23.56	766
				44,900					10,766	
C3 - Direct costs of equipment	Fuel, lubricant, oil [gallons]	2,000	0.64	1,280	P4 - Banking	Risk of cost estimation			184,613	
	Concrete mill [hrs]	1,000	24.28	24,280			Risk of time estimation			5,176
	Excavator [hrs]	1,000	34.33	34,330	Risk of price-changes during the project				264,644	
	Security for material and equipment			5,000						454,433
				64,890						
C4 - Direct costs of means of support and small material				82,687	P5 - Security			5,000	5,000	
C5 - Total direct costs				2,838,915						
C6 - Indirect costs				823,285	P6 - Unpredictable costs			100,000	100,000	
C7 - Total costs				3,662,200						
C8 - Profit				1,980						
C9 - Total primary costs				3,664,180	P7 - Total secondary costs				587,516	

Figure V.7: Wall with a slope around the hotel and the waste water treatment plant for a 225 year condition



	Primary costs			Subtotal [\$]	Total	Secondary costs			Subtotal [\$]	Total
	Quantity	Unit price [\$]				Quantity	Unit price [\$]			
C1 - Direct costs of material	Concrete in situ [m³]	5,773.02	230	1,327,794	P1 - Temporary facilities					
	Steel reinforcement [m²]	36,9838	600	22,190	Toilets, material warehouses etc.			1,000		1,000
				1,349,984	P2 - Transport					
C2 - Direct costs of Labour	Design (5 people; 8 weeks) [hrs]	1,600	4	6,400	Concrete trucks (15 m³) [hrs]	600	24.28	14,568		
	Technical preparations [hrs]	1,000	3.5	3,500	Transport of elements [hrs]	50	35	1,750		16,318
	Salaries (10 people; 25 weeks) [hrs]	10,000	3.5	35,000	P3 - Other additional costs					
				44,900	Proof of good quality			10,000		
C3 - Direct costs of equipment	Fuel, lubricant, oil [gallons]	2,000	0.64	1,280	Transport of unused materials	32.5	23.56	766		10,766
	Concrete mill [hrs]	1,000	24.28	24,280	P4 - Banking					
	Excavator [hrs]	1,000	34.33	34,330	Risk of cost estimation			98,483		
	Security for material and equipment			5,000	Risk of time estimation			5,176		
C4 - Direct costs of means of support and small material				64,890	Risk of price-changes during the project			134,998		238,657
C5 - Total direct costs				1,503,567	P5 - Security			5,000		5,000
C6 - Indirect costs				436,034	P6 - Unpredictable costs			100,000		100,000
C7 - Total costs				1,939,602						
C8 - Profit				1,980						
C9 - Total primary costs				1,941,582	P7 - Total secondary costs			371,741		371,741

Figure V.9: Embedded wall around the hotel with a 100 year condition and the waste water treatment plant with a 225 year condition

Primary costs				Secondary costs				
	Quantity	Unit price [\$]	Subtotal [\$]		Quantity	Unit price [\$]	Subtotal [\$]	
C1 - Direct costs of material	Sand [m <sup>3</sup> ]	4,305	10	43,050	P1 - Temporary facilities Toilets, material warehouses etc.		1,000	
	Steel [m <sup>3</sup> ]	121.4	600	72,840				1,000
					P2 - Transport			
C2 - Direct costs of Labour				115,890	Dumptruck [hrs]	1200	24.28	29,136
	Design (5 people; 8 weeks) [hrs]	1,600	4	6,400	Transport of elements [hrs]	1200	35	42,000
	Technical preparations [hrs]	3,000	3.5	10,500				71,136
	Salaries (10 people; 30 weeks) [hrs]	12,000	3.5	42,000	P3 - Other additional costs			
			58,900	Proof of good quality			10,000	
C3 - Direct costs of equipment					Transport of unused materials	120	23.56	2,827
	Fuel, lubricant, oil [gallons]	5,000	0.64	3,200				12,827
	Sheepile driver [hrs]	1,200	80	96,000	P4 - Banking			
	Excavator [hrs]	1,200	34.33	41,196	Risk of cost estimation			26,021
			150,396	Risk of time estimation			9,805	
C4 - Direct costs of means of support and small material			9,756	Risk of price-changes during the project			11,589	
C5 - Total direct costs			334,942	P5 - Security			5,000	
C6 - Indirect costs			97,133				5,000	
C7 - Total costs			432,075	P6 - Unpredictable costs			100,000	
C8 - Profit			3,380				100,000	
C9 - Total primary costs			435,455	P7 - Total secondary costs			237,378	

Figure V.10: Sheetpile wall around the hotel with a 100 year condition and the waste water treatment plant with a 225 year condition

Primary costs				Secondary costs					
	Quantity	Unit price [€]	Subtotal [€]		Quantity	Unit price [€]	Subtotal [€]		
C1 - Direct costs of material	Concrete in situ [m³]	7,579.75	230	1,743,341	P1 - Temporary facilities	Toilets, material warehouses etc.	1,000		
	Steel reinforcement [m²]	40,004.8	600	24,003		1,000			
				1,767,344					
C2 - Direct costs of Labour	Design (5 people; 8 weeks) [hrs]	1,600	4	6,400	P2 - Transport	Concrete trucks (15 m³) [hrs]	550	24.28	13,354
	Technical preparations [hrs]	1,000	3.5	3,500		Transport of elements [hrs]	50	35	1,750
	Salaries (10 people; 25 weeks) [hrs]	10,000	3.5	35,000	P3 - Other additional costs				
					44,900	Proof of good quality		10,000	
C3 - Direct costs of equipment	Fuel, lubricant, oil [gallons]	2,000	0.64	1,280	Transport of unused materials	30	23.56	707	10,707
	Concrete mill [hrs]	1,000	24.28	24,280	P4 - Banking				
	Excavator [hrs]	1,000	34.33	34,330	Risk of cost estimation			126,147	
	Security for material and equipment			5,000	Risk of time estimation			5,176	
				64,890	Risk of price-changes during the project		176,734		
C4 - Direct costs of means of support and small material				56,314	P5 - Security				308,057
C5 - Total direct costs				1,933,448	P6 - Unpredictable costs				5,000
C6 - Indirect costs				560,700	P7 - Total secondary costs				439,868
C7 - Total costs				2,494,148					
C8 - Profit				1,980					
C9 - Total primary costs				2,496,128					

Figure V.11: Wall with a slope around the hotel with a 100 year condition and the waste water treatment plant with a 225 year condition





# W

## FINAL SOLUTION

### W.1. BEARING CAPACITY OF THE SOIL

In this section the bearing capacity of the soil is examined, to see whether the soil will be able to bear the weight of the gravity wall around the waste water treatment plant. To analyse this, the Brinch Hansen method is used [44]. First, the method is described and after that the calculation is shown.

#### W.1.1. METHOD

To analyse the bearing capacity of the soil around the waste water treatment plant, the Brinch Hansen method is used [44]. The bearing capacity is calculated using equations W.1 to W.5.

$$F_{\max} = p'_{\max} \cdot A \quad (\text{W.1})$$

$$p'_{\max} = c' \cdot N_c \cdot s_c \cdot i_c + q' \cdot N_q \cdot s_q \cdot i_q + 0.5 \cdot \gamma' \cdot B \cdot N_\gamma \cdot s_\gamma \cdot i_\gamma \quad (\text{W.2})$$

$$N_c = (N_q - 1) \cot \phi' \quad N_q = \frac{1 + \sin \phi'}{1 - \sin \phi'} e^{\pi \tan \phi'} \quad N_\gamma = 2(N_q - 1) \tan \phi' \quad (\text{W.3})$$

$$s_c = 1 + 0.2 \frac{B}{L} \quad s_q = 1 + \frac{B}{L} \sin \phi' \quad s_\gamma = 1 - 0.3 \frac{B}{L} \quad (\text{W.4})$$

$$i_c = \frac{i_q N_q - 1}{N_q - 1} \quad i_q = \left(1 - \frac{0.70H}{F + A \cdot c' \cot \phi'}\right)^3 \quad i_\gamma = \left(1 - \frac{H}{F + A \cdot c' \cot \phi'}\right)^3 \quad (\text{W.5})$$

Where:	$F_{max}$	=	Maximal bearing capacity	[kN]
	$p'_{max}$	=	Maximal average effective stress on the effective foundation area	[kPa]
	$A$	=	Effective foundation area	[m <sup>2</sup> ]
	$c'$	=	Cohesion (weighted, design value)	[kPa]
	$N_x, s_x, i_x$	=	Factors	[-]
	$q'$	=	Effective stress at the depth of, but next to foundation surface	[kPa]
	$\gamma'$	=	Effective volumetric weight of the soil below construction depth (weighted, design value)	[kN/m <sup>3</sup> ]
	$B$	=	Width of the effective foundation area	[m]
	$\phi'$	=	Effective angle of internal friction (weighted, design value)	[°]
	$L$	=	Length of the effective foundation area	[m]
	$H$	=	Shear force, i.e.: component of the force in the plane of the foundation surface (design value)	[kN]
	$F$	=	Component of the exerted force perpendicular to the foundation surface (design value)	[kN]

In equation W.3 the calculation of the bearing capacity factors is shown. The shape factors, based on the shape of the foundation, can be calculated with equation W.4.

The water is imposing an inclined load on the structure. This has to be taken into account with inclination factors, shown in equation W.5. These are the equations to be used when drained conditions are present during the loading. Since the soil is loaded slowly, drained conditions will occur.

All these factors have a component for cohesion forces (subscript  $c$ ), surcharge (subscript  $q$ ) and capacity of the soil below the foundation (subscript  $\gamma$ ). No surcharge is present. The calculation of the bearing capacity pressure is shown in equation W.2, and the final calculation of the bearing capacity is shown in equation W.1.

## W.2. CALCULATION

The dimensions of the wall used in this calculation can be seen in table 7.1. The soil consists of a combination of clay and sand [5]. The effective volumetric weight ( $\gamma'$ ) is set to 8 kN/m<sup>3</sup>. Because the soil properties are not known exactly, the bearing capacity is calculated for different soils: clean clay (without any sand), slightly sandy clay, greatly sandy clay and organic clay. The results can be seen in table W.1.

Table W.1: Results of the Brinch Hansen calculation

Clay category	$c'$ [kPa]	$\phi'$ [°]	$R/S$ [-]
Clean	5	17.5	1.23
Slightly sandy	5	22.5	1.89
Greatly sandy	0-1	27.5-32.5	0.57-2.62
Organic	0-1	15	0.07-0.31

In this table the last column ( $R/S$ ) shows the resistance compared to the solicitation. Based on the observations made at the hotel the clay seems to be slightly sandy, which means that no soil improvement is needed. However, only the top layer was observed at a limited area. At some places the clay can be greatly sandy. This results in the need for soil improvements, as the lowest  $R/S$ -value is 0.57. However, this value is obtained by choosing the value for cohesion of 0 kPa and an internal friction angle of  $27.5^\circ$  which results in an unrealistically conservative value. If a lot of sand is present in the clay, this will give a larger internal friction angle, while less sand will result in a larger value for the cohesion. By taking  $32.5^\circ$  instead of  $27.5^\circ$  for the friction angle, the resistance is already bigger than the solicitation ( $R/S = 1.27$ ). The same holds for changing the value for cohesion from 0 kPa to 1 kPa ( $R/S = 1.35$ ). For this reason, soil improvement is not needed for the sandy clay soil with the gravity wall around the waste water treatment plant.

### W.3. PIPING

In order to get piping, three mechanisms are needed [29]: heave, seepage and uplift. Mitigation of one of these mechanisms will prevent piping. As the bottom consists of sandy clay, seepage is unlikely to occur. The top layer is a clay layer which prevents seepage. Besides that, sandy clay is not very permeable. Despite the fact that sand is present in this clay, the permeability is low and seepage does not have time to become a problem. The difference in water head is only present during flooding, and this period is around 17.5 hours (see appendix J).

### W.4. DRAINAGE OF PRECIPITATION

The upper clay layer prevents an easy drainage of precipitation. This is a problem, because the wall encloses the waste water treatment plant. The one in 225 year river discharge has been determined with an IDF curve, exponentially interpolated using the IDF curves of a one in 100 year event and a one in 1000 year event. In appendix J the amount of rainfall can be observed for a one in 100 year event and a one in 1000 year event. With the same exponential interpolation a 1/225 year event gives a rainfall of 30 cm, with a peak intensity of 8 mm in half an hour. This amount of water will cause flooding itself if the water cannot be discharged. Also, for rain events with a smaller return period the water should be removed. As the wall surrounds an area of  $40 \text{ m} \cdot 47.5 \text{ m} = 1900 \text{ m}^2$ , this means the total water falling in this area during the 1/225 year event equals  $570 \text{ m}^3$ . This is too much to store in this area.

As can be seen in figure 7.1, the wall around the waste water treatment plant is at a ground level which is 41 cm lower than the lowest point of the waste water treatment plant, ensuring the water flows from the waste water treatment plant towards the walls. However, the storage capacity is not large enough to keep the total waste water treatment plant dry. As was discussed in appendix C, the pump providing the large cylindrical tanks with air (see figure C.7a) is 30 cm above the ground level. In combination with a maximum rainfall of 30 cm, of which a part can flow to the lower area directly next to the wall, this pump will not be flooded. However, the total volume of  $570 \text{ m}^3$  is too much to keep within this area. The tanks underground are flooded with this amount of water. This can lead to the spreading of waste water, resulting in contamination. Also the drink water reservoir could be

intruded by the rainwater, resulting in polluted freshwater. Therefore, the rain water should be removed from the area enclosed by the walls.

The drainage solution must not create any weak spots in the wall. Closure of the openings (copures) might be forgotten when flooding is coming. If they are not closed in time, the wall has no use. As the ground level is lowest next to the southern wall, a good solution is to place a pump over there. To create an automatic system, implementation of a submersible pump is proposed. This pump works automatically when a water depth of more than 10 cm is reached, to ensure no layer of water at the several components of the waste water treatment plant. It works automatically in order to avoid malfunctioning caused by man made errors when flooding occurs. This pump has a capacity of 8.5 L/s to work properly during the peak intensity. The height of pumping is equal to the height of the wall: 1.7 meter. An axial pump is recommended, because this pump with a high specific rpm is able to deliver a large discharge over a relatively small height [46]. Assuming a hydraulic efficiency of 80%, which is conservative for an axial pump [46], this gives a power need of 100 Watt. Since a cut-off of electricity might occur in case of flooding, the submersible pump works on fuel.

## W.5. FRENCH DRAINAGE

The French drainage system, discussed in appendix C, will not function during flooding. This causes a problem when the waste water storage is completely filled, because, in case no more storage is possible, the waste water will flow into the soil and to the river, causing contamination to the mangrove forest. Therefore, a check should be done to guarantee that sufficient storage of produced waste water is available during a flooding event. In order to do that, the water usage of the Blau Arenal Hotel and the maximum waste water production of 148.5 m<sup>3</sup>/day (from section C.3) is used to determine if the storage capacity of the waste water is sufficient.

The duration of flooding of the French drainage system is chosen to be the same as that of the Blau Arenal Hotel, because the location of the French drainage system is situated inside the Blau Arenal Hotel area. Furthermore, the freshwater is consumed and the waste water is produced by the people present in the hotel. Therefore, the durations of flooding of the 1/100 year and 1/225 year river discharge conditions for the Blau Arenal Hotel can be used from section 3.2.2.

- The duration of flooding is 14.2 hours for the 1/100 year river discharge conditions.
- The duration of flooding is 17.5 hours for the 1/225 year river discharge conditions.

For both durations of flooding two capacities need to be checked: the capacity of the freshwater storage and the capacity of the waste water storage. In case of flooding, freshwater cannot be supplied to the freshwater tanks, while there should be enough to consume. With the maximum daily waste water production of 148.5 m<sup>3</sup> and the flooding duration, the freshwater and waste water volumes can be calculated for both river discharge conditions. These volumes are shown in table W.2.

Table W.2: The water usage during a flooding event in m<sup>3</sup>

Return period [1/year]	Duration of flooding [hours]	Freshwater volume [m <sup>3</sup> ]	Waste water volume [m <sup>3</sup> ]
1/100	14.2	98	88
1/225	17.5	120	108

The underground freshwater storage has a capacity of 320 m<sup>3</sup> [5]. This means that the freshwater reservoir should be at least 40% filled with freshwater in order to make sure enough is available for the tourists and employees present in the Blau Arenal Hotel in case of a flooding event.

The waste water can be stored underground in two basins with a total capacity of 30 m<sup>3</sup>. Besides, two cylinders above ground have a storage capacity of 20 m<sup>3</sup> [47]. This gives a total storage of 50 m<sup>3</sup>. Because only 47% of the 108 m<sup>3</sup> waste water can be stored during a flooding event, the mangrove forest will be contaminated. For the final solution, an extra waste water storage of 60 m<sup>3</sup> should be created to make sure that all waste water produced during the flooding is stored and pollution of the mangrove forest is prevented.

Of course it is more likely that during a period of flooding the available evacuation plan will make sure people left the Blau Arenal Hotel before the flooding arrives. In this case no waste water would be produced and there would be no need for freshwater. However, in order to guarantee that contamination of the mangrove forest is prevented and to ensure that sufficient freshwater is available for trapped people in the hotel, the calculation is performed in the above explained way.

## W.6. ACCESSIBILITY

Besides the drainage problem that is caused by the wall, also limited accessibility is a result of the wall. Equipment and personnel do not have an easy access to this area anymore. However, the centre of this area and the southern side was already not accessible for large equipment, because the spaces between the different components of the waste water treatment plant are small (see appendix C). The wall is located directly next to the freshwater tank, so trucks which supply freshwater to this tank only need to have a flexible tube, which is long enough to pass the wall with a maximum height of 1.7 meter. The area directly next to the wall is still accessible, so equipment can still be placed within the walls using cranes. Two stairs are placed for accessibility of workers and personnel.

The main reason for this solution, is that no weak spots in the wall are created. A gate to allow for equipment could also solve the drainage problem when built in the southern wall, but if flooding occurs and the gate malfunctions, the whole waste water treatment plant floods. The probability of failure would become larger than allowed for a 1/225 year event due to the gate, which is not desirable.



# X

## CONSTRUCTION METHOD

### X.1. STAGES

#### X.1.1. STAGE 1 - PREPARATION OF SITE

##### CONSTRUCTION SITE SET-UP

During the construction set-up, the workers will arrive on site and construct a small temporary building in which the workers can meet, discuss, eat, have a break and store small equipment. This building does not need to contain all these features, as the hotel is only 100 meters away. An agreement with the hotel is preferred, as it saves costs. The workers will bring small equipment needed for the preparation stage.

##### REMOVING VEGETATION

For a clean workspace, the vegetation needs to be removed at the location of the wall. The workers need to remove all vegetation.

##### SURVEYING AND MAPPING

The specific location of the wall will have to be inspected. Some specialised workers will map the area in detail. The exact heights of the soil are needed to be able to build the wall to the correct height. Also, the soil has to be examined, because it could have effect on the settlements of the wall. In section [W.1](#), the importance of the soil strength is acknowledged. Finally, a clear overview of all (pipe)lines going through the site needs to be made. This is desired, because they should not be harmed during the construction. If the structure would interfere with some of these lines, relocation has to be performed in advance.

##### PREPARATION OF SUBLAYER

If weak spots are found during the inspection of the soil, they need to be strengthened. This is done by removing the weak soil and refilling it with better soil.

### LEVELLING SUBLAYER

For construction, a levelled work plane is easier to handle. The entire subsoil does not need to be at the same height, but a smoother subsurface is preferred for the casting of the concrete. With small digging tools this can be accomplished, as the height differences are relatively small, in the order of 0.5 meter.

### X.1.2. STAGE 2 - CONSTRUCTION OF THE WALL

The steps of the construction, explained below, are shown in section appendix X.2.

#### PLACING BOTTOM LAYER

To be sure that the concrete does not flow into the soil, a small sheet will be placed on top of the soil. The sheet is made from geotextile and has approximately the same roughness as the soil, because the horizontal stability should be maintained. The sheet layer extends beyond the dimensions of each concrete section (2m x 11m). The layer will function as permanent formwork. As can be seen in figure X.1, it will be the first material placed for construction.

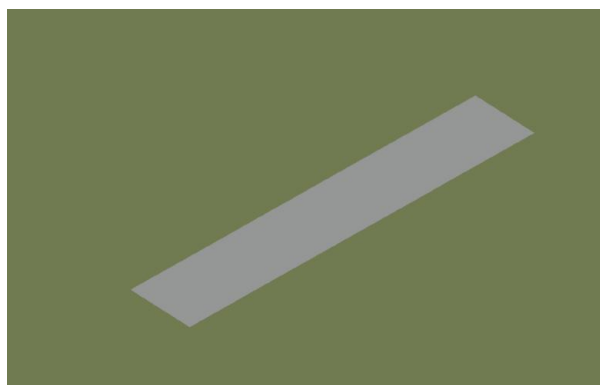


Figure X.1: Schematisation of the bottom layer

#### ERECTING FORM- AND FALSEWORK

Formwork needs to be erected on all four sides. This formwork is held on its place by struts, called falsework. The form- and falsework is made of wood and bolts. Four sections will have to be built in order to keep up with the described time schedule. The sections consist of two walls of 2.0 meter high and 1.2 meter wide and two walls of 2.0 meter high and 10 meters wide, as can be seen in figure X.2. When the concrete is strong enough to stand on its own, the formwork will be taken away and reused in the next section.

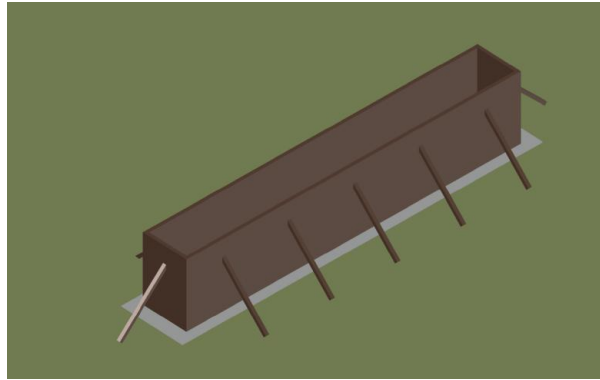


Figure X.2: Schematisation of the form- and falsework

### CASTING CONCRETE

Concrete will be cast in the section of ten meters at once. The casting process will start from two sides and will continue towards each other until the final section is filled up. Concrete trucks will have to arrive quickly at the day of casting, as the concrete needs to be poured at the same rate in each section. An amount of  $20.4 \text{ m}^3$  of concrete is needed for each section.

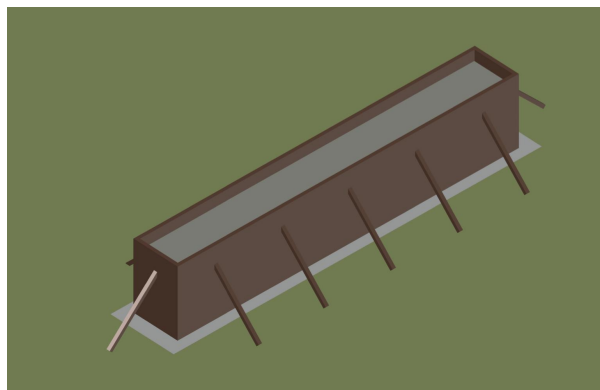


Figure X.3: Schematisation of the concrete, just after casting

### HARDENING OF THE CONCRETE

The concrete elements need time for hardening before they are finished in a later stage. A time of 28 days is needed for the concrete to harden and get strength. For this project a time of 18 days is taken, because the concrete will not be loaded heavily in the first 28 days after construction.

### CONSTRUCTING ENTRANCE STAIRS

The wall will be 1.7 meters high at the highest location. For easy access to the waste water treatment plant stairs are constructed. These will be constructed at two locations and can be built from concrete. In figure X.4, a design of the stairs is shown.

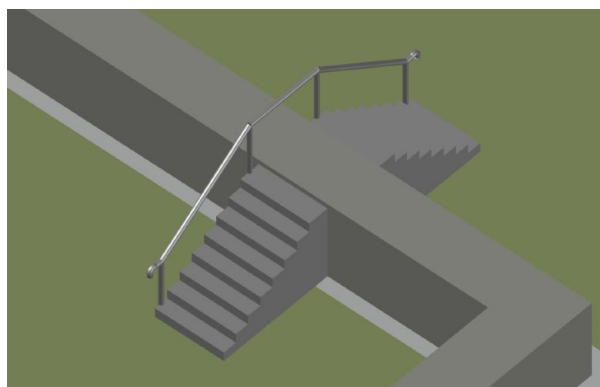


Figure X.4: Schematisation of the staircase over the wall

### X.1.3. STAGE 3 - FINISHING

#### PAINTING CONCRETE (IF DESIRED)

The wall will be standing close to the hotel and can be painted for a higher aesthetic value, if desired by the hotel owners. If this is desired, the paint should be ordered in advance, because a large amount is required.

#### REMOVING FORM- AND FALSEWORK FROM SITE

Finally the form- and falsework needs to be dismantled and removed. This can only be done after the concrete is hard enough that it can stand on its own, which is about 3 days.

### X.1.4. STAGE 4 - MAINTENANCE

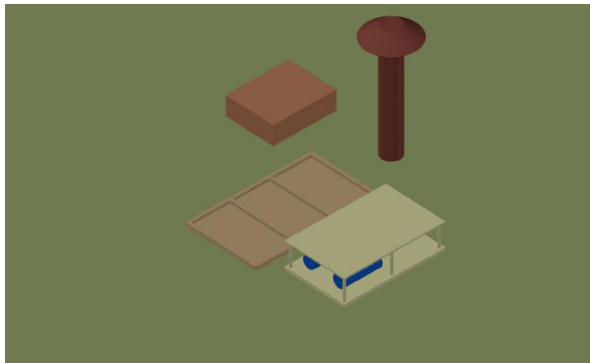
#### CONDITION-BASED

The wall and soil around the wall should be inspected in a condition-based way. The condition prior to inspection is flooding. It is called flooding when the water from the Itabo River flows over its banks, even if it happens slightly. After flooding occurred, the wall should be checked for seepage, settlements, cracks and whether soil around the structure has been washed away. This soil is part of the foundation of the structure and should never be removed. If the wall is damaged, reparation should be executed. This maintenance strategy should be enough for the wall, as the service life is 50 years.

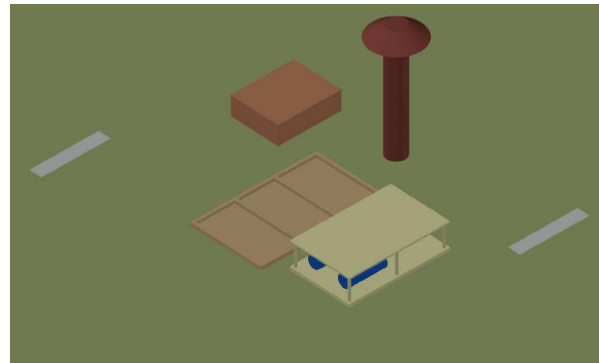
#### TIME-BASED

The axial pump, which is used to remove the rainwater from the enclosed area, should be inspected in a time-based manner. The pump should be inspected twice a year. The first time is in April, a month before the wet season starts (see section 1.1.3). This is done, because the highest probability of large rainfall is during the wet season and the pump should function at maximum capacity. The second time of inspection is at the end of October, when the wet season has just ended. If the pump does not fully function at this time, a new pump can easily be installed before the wet season starts again.

## X.2. STEPS



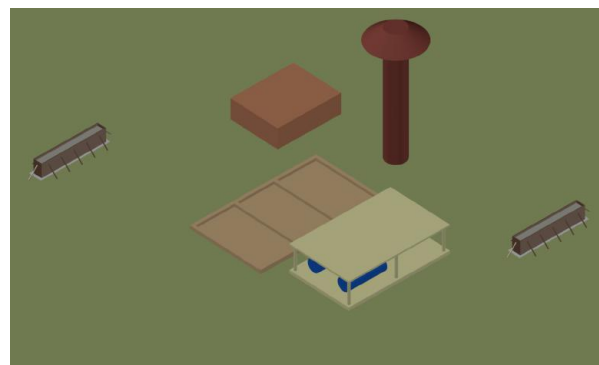
(a) Initial situation



(b) Step 1



(c) Step 2



(d) Step 3



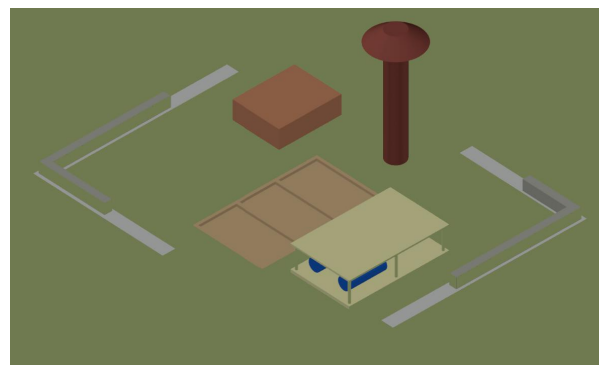
(e) Step 4



(f) Step 5

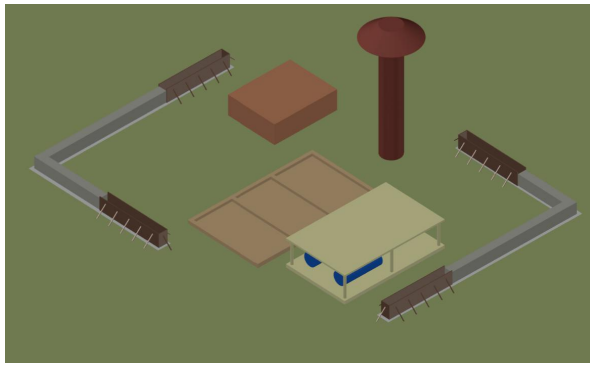


(g) Step 6

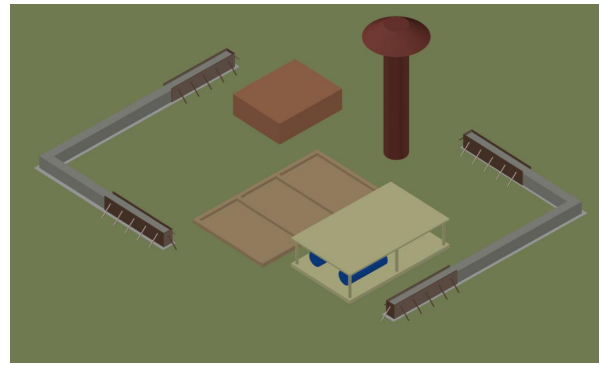


(h) Step 7

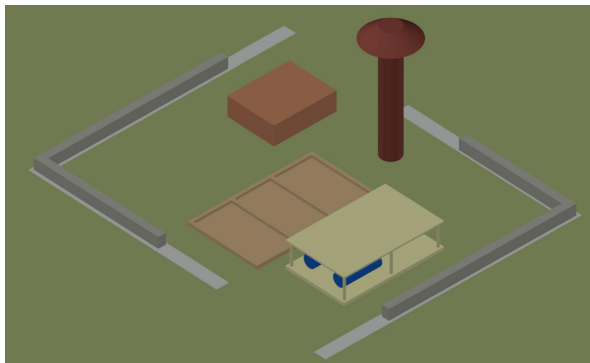
Figure X.5: Steps for the construction of the wall



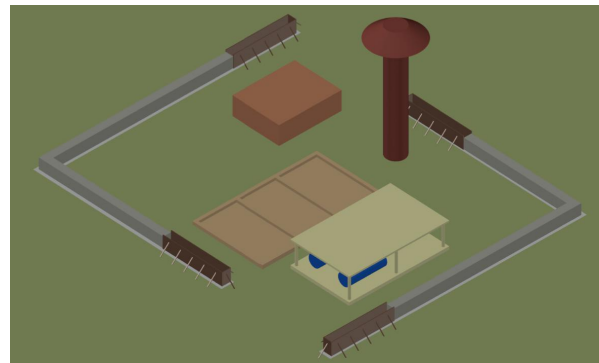
(a) Step 8



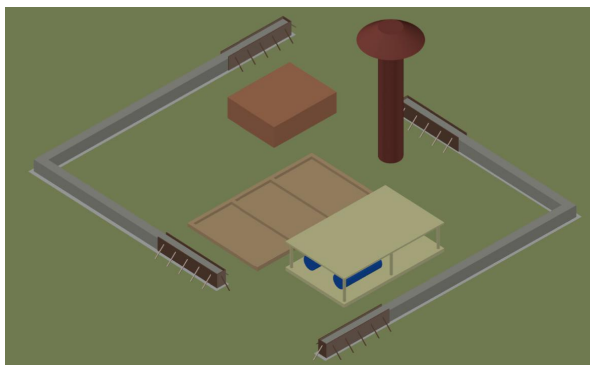
(b) Step 9



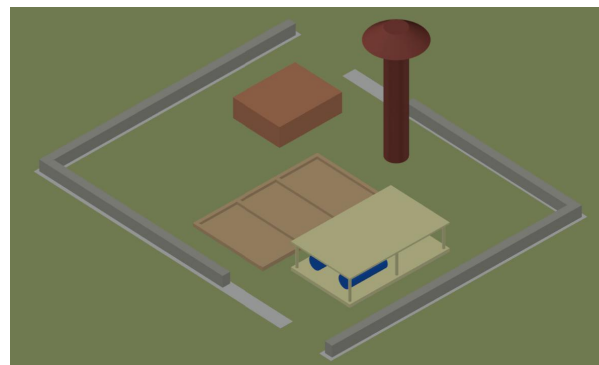
(c) Step 10



(d) Step 11



(e) Step 12



(f) Step 13

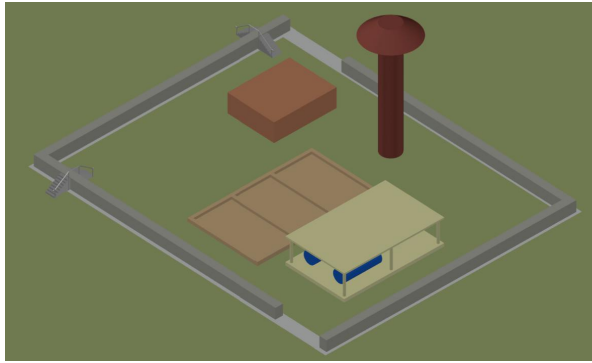


(g) Step 14



(h) Step 15

Figure X.6: Steps for the construction of the wall



(a) Step 16



(b) Step 17



(c) Step 18



(d) Final situation

Figure X.7: Steps for the construction of the wall



# BIBLIOGRAPHY

- [1] Cubanacan Grupo, **Hotel Arenal: High resolution photos**, <http://www.cubanacan.cu/en/images?slug=arenaname=Arenal>, (Website visited on 22nd August 2016).
- [2] Google, **Google Earth**, (2016), (Program used on 11th August 2016).
- [3] L.F. Córdova López et. al., **Informe final de la visita técnica realizara al hotel Arenal**, (2016).
- [4] Emproy-2 Arquitectura Eingenieria, **Plano de Hotel Blau Arenal - Drenaje de los puntos de inundacion**, (2013).
- [5] Projectgroup 199, **Interview with David, Head of Investment Office of Playas del Este** (2016).
- [6] Centro Nacional del Clima del Instituto de Meteorología, **Informe**, (2015).
- [7] BMT ARGOSS, **Waveclimate data**, <http://www.waveclimate.com/cgi-bin/query>, (Website visited on 5th September 2016).
- [8] H. J. Verhagen, K. d'Angremond, and F. van Roode, **Breakwaters and Closure Dams** (VSSD, 2009).
- [9] Church, J.A., P.U. Clark, A. Cazenave, J.M. Gregory, S. Jevrejeva, A. Levermann, M.A. Merrifield, G.A. Milne, R.S. Nerem, P.D. Nunn, A.J. Payne, W.T. Pfeffer, D. Stammer and A.S. Unnikrishnan, **Sea Level Change. In: Climate Change 2013: The Physical Science Basis. Contribution of Working Group I to the Fifth Assessment Report of the Intergovernmental Panel on Climate Change**, Cambridge University Press, Cambridge, United Kingdom and New York, NY, USA (2013).
- [10] Institute of Meteorology (INSMET), **The coastal floods in the Cuban territory, the most sensitive areas and the possible impact of the climate change**, (2000).
- [11] R.F. Guerra García et. al., **Evolution of the texture and composition of beach sand in playas del Este, Havana, Cuba**, Serie Oceanológica. No. 6, ISSN 2072-800x (2009).
- [12] G. Anfuso et. al., **Sand colour at Cuba and its influence on beach nourishment and management**, Ocean & Coastal Management 126 51e60, Elsevier (2016).
- [13] P. Dayaxny Hernández et. al., **Análisis de los peligros naturales y antrópicos que inciden en el turismo de Playas del Este** (Instituto Superior de Tecnologías Ciencias Aplicadas (InSTEC)).
- [14] S. Solomon et al., **IPCC, Climate Change 2007: The Physical Science Basis, Contribution of Working Group I to the Fourth Assessment Report of the Intergovernmental Panel on Climate Change**, Cambridge (2007).

- [15] P. Bruun, *Stability of tidal inlets - theory and engineering. Developments in Geotechnical Engineering* (Elsevier, 1978).
- [16] T.M. Duong, *Climate change impance STI* (Unesco IHE, 2015).
- [17] J. Bosboom and M. J. F. Stive, *Coastal Dynamics I* (DAP, 2015).
- [18] R. Ranasinghe et. al., *A morphodynamic model to simulate the seasonal closure of tidal inlets* (Coastal Engineering, 1999).
- [19] F.F. Escoffier, *The stability of tidal inlets* (Shore and Beach, 1940).
- [20] NOAA, *Tide Predictions, Havana 2016*, (2016).
- [21] M.P. O'Brien, *Estuary and tidal prisms related to entrance areas* (Civil Engineering, 1931).
- [22] H. H. G. Savenije, *Hydrology of Catchments, Rivers and Deltas* (Lecture notes CT5450, TU Delft, 2007).
- [23] D. M. Gray, *Handbook om the Principles of Hydrology with special emphasis on Canadian conditions* (Water Information Center, New York, 1973).
- [24] V. te Chow et. al., *Hidrologia Aplicada*, Tiempo de Gestión (1994).
- [25] M. Villón Béjar, *Hidrologia* (Instituto Tecnológico de Costa Rica, 2002).
- [26] J. D. Ruiz Sinoga et. al., *Estudio geoambiental de la cuenca de guanabo. Cuba. Aproximacion a la problematica del agua*, (2010).
- [27] L. Gonzáles Spíndola et. al., *Hydrologia superficial para ingenieros*, (2007).
- [28] Y. Martinez, *Discharge calculations Itabo catchment area - Excel sheet* (Instituto Superior de Tecnologías Ciencias Aplicadas (InSTEC), 2016).
- [29] S.N. Jonkman and T. Schweckendiek, *Flood defences Lecture notes CIE5314* (TU Delft, 2016).
- [30] S.N. Jonkman et. al., *Probabilistic Design: Risk and Reliability Analysis in Civil Engineering* (TU Delft, 2015).
- [31] GeoCuba and Grupo Empresarial, *Levantamiento Hotel Arenal* (2016).
- [32] Grupo de Evaluación de Riesgo de la Agencia de Medio Ambiente (AMA), *Metodologías para la determinación de riesgos de desastres a nivel territorial, parte 1* (PNUD Cuba, 2014).
- [33] L.H. Holthuijsen, *Waves in Oceanic and Coastal Waters* (Cambridge University Press, 2007).
- [34] SWAN team, *SWAN User Manual* (TU Delft, 2016).
- [35] N. Booij, R. C. Ris and L. H. Holthuijsen, *A third-generation wave model for coastal regions, Part I, Model description and validation* (J. Geophys. Res., 104, C4, 7649–7666, 1999).

- [36] J.R. Shewchuk, *Triangle: Engineering a 2D Quality Mesh Generator and Delaunay Triangulator* (Applied Computational Geometry: Towards Geometric Engineering, volume 1148 of Lecture Notes in Computer Science, pages 203-222, 1996).
- [37] A. Bilgili, K.W. Smith, D.R. Lynch, *BatTri: A two-dimensional bathymetry-based unstructured triangular grid generator for finite element circulation modeling* (Journal Computers & Geosciences, Volume 32 Issue 5, pages 632-642, 2006).
- [38] J.W. Kamphuis, *BatTri: A two-dimensional bathymetry-based unstructured triangular grid generator for finite element circulation modeling* (Introduction to coastal engineering and management, Advances Series on Ocean Engineering -vol 16, 2000).
- [39] Deltares, *XBeach Manual* (Deltares, 2015).
- [40] Deltares, *RGFGRID, User Manual* (Deltares, 2016).
- [41] GeoCuba, *Levantamiento Hotel Arenal* (2016).
- [42] H. H. G. Savenije, *Hydrologie lecture notes*, TU Delft .
- [43] USACE, (Engineering Technical Letter 1110-3-446, 1992).
- [44] W.F. Molenaar and M.Z. Voorendt, *Manual Hydraulic Structures* (TU Delft, 2016).
- [45] Nederlands Normalisatie Instituut, *Eurocode 7: "Geotechnical design - Part 1: General rules" (NEN-EN1997-1)* (Nederlands Normalisatie Instituut, 2005).
- [46] L. Rietveld, *Dictaat CTB2120 Gezondheidstechniek* (TU Delft, 2013).
- [47] Instituto Nacional de Recursos Hidráulicos, *P.I.D. Solución residuales Hotel Blau Arenal* (CIH, 2013).